

SECONDA UNIVERSITÀ DEGLI STUDI DI NAPOLI  
FACOLTÀ DI INGEGNERIA  
DIPARTIMENTO DI INGEGNERIA DELL'INFORMAZIONE

DOTTORATO DI RICERCA IN CONVERSIONE  
DELL'ENERGIA ELETTRICA - XV CICLO

TESI DI DOTTORATO

# MODELS AND METHODS FOR THE OPTIMAL DESIGN OF SUPERCONDUCTING POWER DEVICES

CANDIDATO:      ING.      MARCO CIOFFI

TUTOR:            PROF.   RAFFAELE MARTONE

COORDINATORE:   PROF.   RAFFAELE MARTONE

ANNO ACCADEMICO 2001-02

## Abstract

High field superconducting magnets are used in different power applications, such as nuclear magnetic resonance systems, thermonuclear fusion technologies and energy storage. These magnets have to fulfill high quality standards in terms of field uniformity and stability, by keeping construction costs and size as low as possible while respecting superconducting critical state constraints.

The subject of this Thesis is the statement of models and resolution strategies for the optimal engineering design of such superconducting power devices. It is shown here that the design of such magnets can have a great benefit by the adoption of the multi-objectives optimisation techniques, in particular the evolutionary approaches such as the Genetic Algorithms. State-of-the-art models and methods of multi-objective optimisation are presented and discussed and new strategies are proposed, able to be applied to industrial relevant problems. Beside the classical approach based on the definition of a scalar weighted-sum objective function to minimise, another strategy exploiting the concept of *Pareto optimality* is adopted in addition.

A *parallel optimisation* environment is exploited to increase the computing performances of the proposed algorithms and to implement a distributed multi-populations Genetic Algorithm with migration and aggression genetic operators using new population indices.

The concept of *solution robustness* in the design process is introduced to deal with the effect of manufacturing and assembling tolerances and suitable corrective strategies are proposed by adopting a new expression of the objective function and Monte Carlo analysis.

The resolution strategy of inverse problems is similar to multi-objectives optimisation problems by properly defining an error functional: the attention is focused on non-destructive testing, where the task is to identify flaws in critical structural parts by using external measures of physical parameters. A benchmark for the eddy current testing problem is solved with the use of the concept of evolution by *biological diversity*.

The previous methodologies are exploited with the development of two *prototypes*, a software tool (**Marides**) and a cluster computing environment (**Beosun**). The presented strategies have been then applied to test cases and real world industrial problems. In particular, to the design of an energy storage system and of both low and high critical temperature superconducting magnets used for magnetic resonance imaging.

## Riassunto

Magneti superconduttori ad elevato campo sono usati in diverse applicazioni elettriche di potenza, quali sistemi per la risonanza magnetica nucleare, tecnologie della fusione termonucleare e per l'immagazzinamento di energia. Tali magneti devono soddisfare elevati standard qualitativi, relativamente all'uniformità ed alla stabilità del campo prodotto, mantenendo al contempo costi costruttivi e ingombri quanto più bassi possibile e rispettando oltresi' i vincoli legati alle condizioni critiche superconduttive.

L'argomento di questa Tesi è la presentazione di modelli e di strategie di risoluzione per il progetto ottimo ingegneristico di tali sistemi superconduttori di potenza. È qui mostrato che il progetto di tali magneti può trarre un grande beneficio dall'adozione di tecniche di ottimizzazione multi-obiettivo, in particolare di approcci evolutivi quali gli Algoritmi Genetici.

Modelli e metodi che rappresentano lo stato dell'arte dell'ottimizzazione multi-obiettivo sono presentati e discussi, e sono proposte nuove strategie da applicare a problemi di interesse industriale. Oltre il classico approccio basato sulla definizione di una funzione obiettivo scalare come media pesata da minimizzare, si adotta inoltre un'altra strategia che sfrutta il concetto di *ottimo secondo Pareto*.

È stato sviluppato un ambiente di *ottimizzazione parallela* per incrementare le prestazioni di calcolo degli algoritmi proposti e per implementare un Algoritmo Genetico distribuito e multi-popolazione con operatori genetici di migrazione e aggressione, che utilizzano nuovi indici di popolazione.

Il concetto di *robustezza della soluzione* è introdotto nella fase di progetto per tener conto degli effetti delle tolleranze costruttive e di assemblaggio e sono quindi proposte adatte strategie correttive che utilizzano una nuova espressione della funzione obiettivo e analisi alla Monte Carlo.

La strategia di risoluzione di problemi inversi è simile a quella adottata per problemi di ottimizzazione multi-obiettivo con la definizione corretta di un funzionale di errore: l'attenzione è focalizzata sulle prove non distruttive, nelle quali il compito è l'identificazione di difetti di parti strutturali critiche, utilizzando misure esterne di parametri fisici. Un problema test per prove alle correnti indotte (eddy current) è risolto con l'utilizzo del concetto di evoluzione per *diversità biologica*.

Le precedenti metodologie sono messe in opera con lo sviluppo di due *prototipi*, un pacchetto software (**Marides**) ed un ambiente di calcolo di tipo cluster (**Beosun**). Le strategie presentate sono state poi applicate a casi di

prova e problemi di effettivo interesse industriale. In particolare al progetto di un sistema per l'immagazzinamento di energia ed a magneti superconduttori, sia ad alta che a bassa temperatura critica, utilizzati per diagnostica a risonanza magnetica.

## Acknowledgements and Reminds

*I wish to thank Professor Raffaele Martone and Professor Alessandro Formisano, who have given me the possibility to fulfill this Dottorato di Ricerca and to investigate new research fields and for their continuous assistance in my work.*

*Part of this work has been shared with Ing. Vincenzo Cavaliere of CRIS-Ansaldo, who also suggested the exploration of many natural and evolutionary concepts.*

*And now, at the end in writing this Thesis, my memories go to my last years working in a number of different research communities.*

*For a strange fortune chain (actually it started with a leaflet I picked up in Capri), I arrived to Electromagnetic Optimal Design coming from Computational Fluid Dynamics, passing through the High Performance Computing world in Edinburgh.*

*Indeed, this is not my first Doctoral Thesis: some years ago I was writing my final thesis for a Dottorato in Aerospace Engineering about a quite different topic, microgravity. And I want to remember here that microgravity was the main field of interest of the unforgettable Professor Luigi G. Napolitano.*



Figure 1: *M.C. Escher: Metamorphosis II*

# Contents

|          |  |           |
|----------|--|-----------|
| <b>1</b> | <b>Introduction - The Design</b>                     | <b>1</b>  |
| 1.1      | Definition of Design . . . . .                       | 1         |
| 1.2      | Research objectives . . . . .                        | 2         |
| 1.3      | Overview of the Thesis . . . . .                     | 3         |
| 1.4      | Appendix: Design and Nature . . . . .                | 4         |
| <b>2</b> | <b>The Optimal Design in Electromagnetics</b>        | <b>5</b>  |
| 2.1      | Electromagnetic devices . . . . .                    | 5         |
| 2.2      | Basic problems in engineering design . . . . .       | 6         |
| 2.3      | Superconducting magnets . . . . .                    | 7         |
| 2.3.1    | Design of fusion magnets . . . . .                   | 8         |
| 2.3.2    | Design of MRI superconducting magnets . . . . .      | 8         |
| <b>3</b> | <b>Optimisation Problems and Objective Functions</b> | <b>11</b> |
| 3.1      | The optimisation problems . . . . .                  | 11        |
| 3.2      | Definition of the problem . . . . .                  | 12        |
| 3.3      | Partial and total order . . . . .                    | 13        |
| 3.4      | Mathematical background . . . . .                    | 15        |
| 3.4.1    | Pareto dominance . . . . .                           | 15        |
| 3.4.2    | Statistical definitions . . . . .                    | 16        |
| 3.5      | Definition of the Objective Function . . . . .       | 18        |
| 3.6      | Constraints handling: penalty functions . . . . .    | 19        |
| 3.7      | Test problems . . . . .                              | 20        |
| 3.7.1    | Rastrigin function . . . . .                         | 20        |

|          |   |           |
|----------|---|-----------|
| 3.7.2    | TEAM 22 Problem . . . . .                                       | 22        |
| <b>4</b> | <b>Search Algorithms</b>  | <b>26</b> |
| 4.1      | Pareto optimality and $OF$ minimisation . . . . .               | 26        |
| 4.1.1    | Pareto front: analytical test case . . . . .                    | 28        |
| 4.2      | Stochastic and deterministic methods . . . . .                  | 30        |
| 4.2.1    | Deterministic methods . . . . .                                 | 33        |
| 4.3      | Evolutionary computation . . . . .                              | 34        |
| 4.3.1    | Biological basis . . . . .                                      | 34        |
| 4.4      | Genetic Algorithms . . . . .                                    | 35        |
| 4.4.1    | Constraints handling in GAs . . . . .                           | 38        |
| 4.4.2    | Initial population selection . . . . .                          | 40        |
| 4.4.3    | Evolutionary stall . . . . .                                    | 40        |
| 4.4.4    | Meta-optimisation of GAs . . . . .                              | 41        |
| 4.5      | Proposed and implemented strategies . . . . .                   | 41        |
| 4.5.1    | Operators adaptation and hybrid GA . . . . .                    | 41        |
| 4.5.2    | Optimal design and uncertainties . . . . .                      | 42        |
| 4.5.3    | Increasing the robustness of the design solution . . . . .      | 43        |
| 4.5.4    | Sensitivity analysis . . . . .                                  | 47        |
| 4.5.5    | Monte Carlo analysis and Pareto Front . . . . .                 | 49        |
| 4.6      | Appendix: the Nash equilibrium . . . . .                        | 51        |
| <b>5</b> | <b>Parallel Genetic Algorithms</b>                              | <b>55</b> |
| 5.1      | Computational Electromagnetics and Parallel Computing . . . . . | 55        |
| 5.1.1    | Present trends in parallel computing . . . . .                  | 56        |
| 5.2      | Parallel Genetic Algorithms . . . . .                           | 56        |
| 5.3      | Population moments . . . . .                                    | 58        |
| 5.4      | Population operators . . . . .                                  | 59        |
| 5.4.1    | Migration policy . . . . .                                      | 60        |
| 5.4.2    | Resources allocation and aggression policy . . . . .            | 61        |
| 5.5      | Implementation of Island GA . . . . .                           | 61        |
| 5.5.1    | Load balancing issues: Master-Slave approach . . . . .          | 62        |

|          |   |           |
|----------|---|-----------|
| 5.5.2    | Implementation details . . . . .                                  | 63        |
| 5.6      | Exploring the Biodiversity . . . . .                              | 68        |
| <b>6</b> | <b>Inverse problems: minimisation of error functionals in ECT</b> | <b>70</b> |
| 6.1      | Eddy Current Testing . . . . .                                    | 70        |
| 6.1.1    | Problem formulation . . . . .                                     | 71        |
| 6.1.2    | Direct problem resolution . . . . .                               | 72        |
| 6.1.3    | Inverse problem model . . . . .                                   | 74        |
| 6.1.4    | Parallel computing environment . . . . .                          | 78        |
| 6.1.5    | Results . . . . .   | 78        |
| 6.1.6    | Section summary . . . . .   | 80        |
| <b>7</b> | <b>Computing environment</b>                                      | <b>81</b> |
| 7.1      | Beowulf Clusters . . . . .  | 81        |
| 7.2      | Beosun . . . . .  | 82        |
| 7.3      | Software . . . . .  | 85        |
| 7.3.1    | Libraries . . . . .   | 85        |
| 7.3.2    | Graphical user interfaces . . . . .                               | 86        |
| 7.3.3    | Parallel Matlab . . . . .   | 86        |
| <b>8</b> | <b>Results</b>  | <b>87</b> |
| 8.1      | Island GA for the TEAM 22 Problem . . . . .                       | 87        |
| 8.1.1    | Migrations without aggression . . . . .                           | 87        |
| 8.1.2    | Aggression strategy . . . . .                                     | 89        |
| 8.2      | Design of high $T_c$ superconducting magnets . . . . .            | 90        |
| 8.2.1    | Optimisation strategy . . . . .                                   | 96        |
| 8.2.2    | Results . . . . .   | 97        |
| 8.3      | Sensitivity analysis on tolerances . . . . .                      | 98        |
| 8.3.1    | Sensibility analysis in MRI magnet design . . . . .               | 101       |
| 8.3.2    | Assessment of performance for the proposed algorithm              | 104       |
| 8.3.3    | Section summary . . . . .   | 107       |
| 8.4      | Marides: an industrial tool . . . . .                             | 110       |



|   |            |
|---|------------|
| <i>CONTENTS</i>   | viii       |
| 8.5 Solution robustness in optimal MRI magnets design . . . . . | 112        |
| 8.6 Robust design and Biodiversity . . . . .                    | 115        |
| 8.6.1 Section summary . . . . .                                 | 120        |
| <b>9 Conclusions</b>  | <b>121</b> |
| <b>A Code Fragments</b>   | <b>123</b> |
| A.1 Weights for robust $OF$ . . . . .                           | 123        |
| A.2 IGA Aggression: create new MPI communicators . . . . .      | 125        |

# List of Figures

|     |   |    |
|-----|---|----|
| 1   | <i>M.C. Escher: Metamorphosis II</i> . . . . .  | iv |
| 2.1 | ITER project: toroidal field model coil (TFMC). . . . .   | 9  |
| 3.1 | Section of the Rastrigin function on the plane $x_2=0$ for $n = 2$ . . . . .  | 21 |
| 3.2 | Section of the Rastrigin function on the plane $x_1=0$ for $n = 2$ . . . . .  | 21 |
| 3.3 | TEAM 22 problem: SMES geometry. . . . .   | 24 |
| 4.1 | Pareto Front and $OF$ . . . . .   | 28 |
| 4.2 | Pareto Front analytical test case: partial objectives plots and $OF$ s for different weight sets (the minima of each $OF$ s are plotted with marks). . . . .                | 29 |
| 4.3 | Pareto Front analytical test case: Pareto Front with MC worst cases bars in dashed lines for partial objectives. . . . .  | 31 |
| 4.4 | Continuous (continuous line) and discrete (dashed line) probabilistic density functions. . . . .  | 45 |
| 4.5 | Robust Objective Function for the demonstration example. . . . .  | 47 |
| 4.6 | Pareto Front analytical test case: PDF of objective $F_1$ for $w_1 = 1/3$ and the Gaussian distribution with the same mean and standard deviation (in dashed line). . . . . | 51 |
| 4.7 | Pareto Front analytical test case: PDF of objective $F_2$ for $w_1 = 2/3$ and the Gaussian distribution with the same mean and standard deviation (in dashed line). . . . . | 52 |
| 4.8 | Pareto Front analytical test case: plot of standard deviation $\sigma$ of objectives $F_1$ (continuous line) and $F_2$ (dashed line) versus weight $w_1$ . . . . .          | 53 |

|     |   |     |
|-----|---|-----|
| 5.1 | Proposed IGA flow chart. . . . .  | 64  |
| 5.2 | Hybrid multilevel IGA model structure. . . . .  | 65  |
| 5.3 | IGA: master process flow chart. . . . .   | 66  |
| 5.4 | IGA: slave processes flow chart. . . . .  | 67  |
| 5.5 | IGA aggression: Phase A. . . . .  | 67  |
| 5.6 | IGA aggression: Phase B. . . . .  | 68  |
| 5.7 | IGA: biodiversity model structure. . . . .  | 69  |
| 6.1 | Schematics for JSAEM benchmark problem #2. . . . .  | 73  |
| 6.2 | ECT analysis: top view of the plate mesh. The dashed circle<br>indicate the region zoomed in Figure 6.3 . . . . .   | 75  |
| 6.3 | ECT analysis: zoom plot of the fine mesh region. . . . .  | 76  |
| 6.4 | ECT: master-slaves IGA structure. . . . .   | 78  |
| 7.1 | The Beosun Beowulf machine . . . . .  | 84  |
| 8.1 | Best SMES configuration for migration IGA with magnetic<br>field map on a radial plane sector. . . . .  | 88  |
| 8.2 | Axial section of the best computed SMES geometry by aggres-<br>sion IGA (filled boxes) and present TEAM solution (empty<br>boxes). . . . .                                    | 91  |
| 8.3 | HTS magnet: critical current densities versus $f_1(B_{//})$ and<br>$f_2(B_{\perp})$ for a commercial HTS tape. . . . .  | 93  |
| 8.4 | HTS magnet poloidal cross section describing the geometrical<br>parameters. . . . .   | 95  |
| 8.5 | HTS magnet: sketch of the computational approach for the<br>fast field map evaluation scheme (just one fictitious coil is<br>reported). . . . .                               | 97  |
| 8.6 | Proposed HTS magnet configuration. . . . .  | 99  |
| 8.7 | Optimised HTS magnet: field distribution in the terminal part<br>of the windings, in the cases of presence (solid) and absence<br>(dashed) of the compensation coils. . . . . | 100 |
| 8.8 | Typical MRI field contour plot in the VOI. . . . .  | 103 |
| 8.9 | MRI magnet poloidal cross section with eight coils. . . . .   | 105 |

|      |   |     |
|------|---|-----|
| 8.10 | MC analysis of MRI magnets: the means of the first three field harmonic expansion coefficients against the number of runs. . . . .  | 106 |
| 8.11 | MC analysis of MRI magnets: PDF plot of coefficient $A_{30}$ (mean=0.7, standard deviation=9.3) and the normal PDF with same mean and standard deviation, in continuous line. . . . . | 108 |
| 8.12 | MC analysis of MRI magnets: PDF plot of uniformity in ppm: mean=41, standard deviation=24, maximum value=162, minimum value=5. . . . .  | 109 |
| 8.13 | MC analysis of MRI magnets: histogram of covariance coefficients of input variables with $A_{30}$ for each coil. . . . .  | 110 |
| 8.14 | Marides GUI. . . . .  | 111 |
| 8.15 | MRI magnet poloidal cross section with six coils. . . . .   | 113 |
| 8.16 | Different MRI magnet solution layouts: coils 1, 2 and 3. . . . .  | 114 |
| 8.17 | Pareto Front for the TEAM 22 problem. . . . .   | 117 |
| 8.18 | TEAM 22: PDF of objective $F_1$ for $w_1 = 0.245$ and the Gaussian distribution with the same mean and standard deviation (in dashed line). . . . .                                   | 118 |
| 8.19 | TEAM 22: PDF of objective $F_2$ for $w_1 = 0.245$ and the Gaussian distribution with the same mean and standard deviation (in dashed line). . . . .                                   | 119 |

# List of Tables

|     |   |     |
|-----|---|-----|
| 3.1 | Geometrical constraints and fixed parameters of the SMES design parameters: three parameters problem. . . . .     | 24  |
| 3.2 | Allowable ranges for the SMES design parameters: eight parameters problem. . . . .                                | 25  |
| 4.1 | Pareto Front analytical test case: minima $OF$ s for different weight sets. . . . .                               | 30  |
| 4.2 | Comparison between SVD computed (with 500 samples) and analytical derivatives for the Rastrigin function. . . . . | 50  |
| 6.1 | Skin depths for different frequencies in the INCONEL 600 MA alloy. . . . .  | 73  |
| 6.2 | Results of the ECT numerical experiments: percentage of the success on localising the crack. . . . .              | 79  |
| 8.1 | Best $OF$ values for different migration IGA parameters, with populations of 1000 individuals. . . . .            | 88  |
| 8.2 | Best TEAM 22 results with migration IGA. . . . .  | 89  |
| 8.3 | IGA parameters for aggression. . . . .  | 90  |
| 8.4 | Best results for IGA with aggression, compared to the TEAM 22 results. . . . .                                    | 91  |
| 8.5 | Aggression IGA solutions ranking. . . . .   | 91  |
| 8.6 | HTS magnet geometrical limits. . . . .  | 98  |
| 8.7 | HTS magnet best configuration. . . . .  | 98  |
| 8.8 | MRI magnets: standard deviation of geometric tolerances in mm (mean=0). . . . .                                   | 105 |

|      |  |     |
|------|--|-----|
| 8.9  | MRI magnets: coils dimensions (in meters) for the different magnets and $OF$ values. . . . .   | 114 |
| 8.10 | MRI magnets: robustness for different magnets. . . . .   | 115 |
| 8.11 | MRI magnets: most robust solution found. . . . .   | 116 |
| 8.12 | TEAM 22 problem: difference between mean value and reference one and standard deviation of partial objectives for different Pareto points. . . . . | 117 |

# List of Acronyms

|             |   |
|-------------|---|
| CDF         | Cumulative Distribution Function                        |
| CEM         | Computational Electromagnetics                          |
| COTS        | Commodity Off-The-Shelf                                 |
| <i>e.g.</i> | exempli gratia  |
| ECT         | Eddy Current Testing                                    |
| DM          | Decision Maker  |
| DOF         | Degrees of Freedom                                      |
| ES          | Evolutionary Strategies                                 |
| GA          | Genetic Algorithm                                       |
| GUI         | Graphical User Interface                                |
| HPC         | High Performance Computing                              |
| HTS         | High Temperature Superconductors                        |
| <i>i.e.</i> | id est  |
| IGA         | Island Genetic Algorithm                                |
| ITER        | International Thermonuclear Experimental Reactor        |
| JSAEM       | Japan Society of Applied Electromagnetics and Mechanics |
| LM          | Linearisation Methods                                   |
| MC          | Monte Carlo   |
| MOP         | Multi Objective Problem                                 |
| MPI         | Message Passing Interface                               |
| MRI         | Magnetic Resonance Imaging                              |
| NDT         | Non Destructive Testing                                 |
| NIC         | Network Interface Card                                  |
| <i>OF</i>   | Objective Function                                      |
| PDF         | Probabilistic Distribution Function                     |
| PMF         | Probabilistic Mass Function                             |
| PVM         | Parallel Virtual Machine                                |
| SA          | Sensitivity Analysis                                    |
| SM          | Statistical Methods                                     |
| SMES        | Superconducting Magnetic Energy Storage                 |
| SOP         | Single Objective Problem                                |
| SPMD        | Single Program, Multiple Data                           |
| SVD         | Singular Value Decomposition                            |
| TEAM        | Testing Electromagnetic Analysis Methods                |
| VOI         | Volume of Interest                                      |
| WCA         | Worst Case Analysis                                     |

# Table of Symbols and Notations

|                |   |
|----------------|---|
| $\exists$      | there exists                            |
| $\forall$      | for all                                 |
| $\subset$      | subset, set inclusion                   |
| $\in$          | included, element in set                |
| $\wedge$       | and                                     |
| $\neg$         | not                                     |
| $\Phi$         | "penalised" objective function          |
| $\preceq$      | Pareto dominate                         |
| $\mathcal{P}$  | Pareto Set                              |
| $\mathcal{PF}$ | Pareto Front                            |
| $[a, b]$       | closed interval                         |
| $]a, b[$       | open interval                           |
| <b>A</b>       | matrix                                  |
| <b>x</b>       | vector                                  |
| $\  \quad \ $  | norm of a vector or a matrix            |
| $\mu$          | statistical mean (for a Gaussian PDF)   |
| $\sigma$       | standard deviation (for a Gaussian PDF) |
| $P_n^m$        | Legendre functions of the first kind    |
| <b>B</b>       | magnetic flux density                   |
| <b>H</b>       | magnetic field                          |
| <b>I</b>       | current                                 |
| <b>J</b>       | current density                         |
| $K$            | Kelvin degree                           |
| $T_c$          | critical temperature                    |



# Chapter 1

## Introduction - The Design

THIS THESIS IS about the Optimal Design (in Power Electromagnetics). I enclose "Power Electromagnetics" in brackets because many topics I will present are general and common to other engineering fields: the main attention will however be focused on the power applications, in particular on the superconducting magnets technologies used in nuclear fusion systems and in magnetic resonance devices.

Before talking about the Design, it is necessary to define the topic I am going to discuss. This Chapter proposes some definitions of engineering optimal Design.

### 1.1 Definition of Design

The Optimal Design is a multidisciplinary task and usually it is an iterative work performed by a team of skilled and experienced engineers. Actually for many people, and I agree with them, Design is, or should be, always *optimal* and therefore we could simply talk about Design. In other words, by definition a good designer always produces an optimal design.

During my University studies, I was taught to consider the "Engineer" (note the capital "E") as who is able to design and to build his goal with € 1 while "the others" need € 10 for it. In this statement the attention is clearly focused just on the economic optimisation of the design task. In general, several other aspects should be considered.

There are many wide-range works about engineering design: I recall the book of Sen & Yang [1] and the one of Pahl & Beitz [2] and the recent PhD thesis of Dragan Cvetković [3], Geoff Leyland [4] and Johan Andersson [5].

According to Pahl & Beitz [2]: *"the main task of engineers is to apply their scientific and engineering knowledge to the solution of the technical problems, and then to optimise those solutions within the requirements and constraints set by material, technological, economical, legal, environmental and human-related considerations. Problems become concrete tasks after the clarification and definition of the problems which engineers have to solve to create new technical products (artifacts)"*.

Another definition is given by the ABET (the US Accreditation Board for Engineering and Technology): *the "engineering design is the process of devising a system, component, or process to meet desired needs. It is a decision-making process (often iterative), in which the basic science and mathematics and engineering sciences are applied to convert resources optimally to meet a stated objective. Among the fundamental elements of the design process are the establishment of objectives and criteria, synthesis, analysis, construction, testing and evaluation"*.

It is possible to say that Design is the process to build *devices*: objects intended for desired purposes. These devices are naturally wanted as good as possible, and even better. I want to stress that the adjective "better" means different depending on the field of interest. For instance, in the space sector, better means generally *lighter*, while in the consumer arena, better means *cheaper*.

Solving a problem or achieving a purpose can be represented as finding a path to a goal. The path consists of a sequence of steps, where at each step a decision among alternative choices must be made. The plan is the sequence of decisions that leads from the starting state to the goal state. It is realised in the given domain, its "problem-space," which is set by the scientific models and technological procedures that constrain the realisation of the goal. The search for a plan to reach the goal applies these models and procedures as constraints on the possible alternatives at each step

## 1.2 Research objectives

The main objective of this Thesis is to direct the optimal design of superconducting power devices, in particular of high field magnets used in nuclear magnetic resonance systems and in fusion technologies. To fulfill this goal, state-of-the-art models and methods of multi-objective optimisation are presented and discussed in view of their application to specific problems of industrial interest. To increase the efficiency and to improve the quality of the

available algorithms, new techniques have been developed and implemented with the following aims:

- to introduce the concepts of *solution robustness* in the design process, both during optimisation phase and as a post-processing step.
- to increase the *computing performances* of the proposed algorithms by adopting a parallel optimisation environment and other high performance computing techniques.
- to develop two *pre-commercial prototypes*: a high-performance parallel cluster computer and a software for industrial optimal design.

### 1.3 Overview of the Thesis

This Thesis is organised in the following way:

Chapter 2 gives the general description of the problems in optimal design of electromagnetic devices

Chapter 3 introduces the multi-objective optimisation problem and the main topics about the Objective Function definition. In addition some mathematical background about the Pareto optimality concept and statistical definitions are given. Some test cases to be used in the following are then described.

In Chapter 4 the current and proposed search algorithms for multi-objective optimisation are illustrated. The main attention is focused on Genetic Algorithms and their meta-optimisation strategies. The concepts of solution robustness in the design process is then introduced together with the Monte Carlo analysis.

The topics of Chapter 5 are the main issues of parallel computing applied to electromagnetics, the parallel Island Genetic Algorithms and the new population genetic operators and indices.

In Chapter 6 the inverse problems resolution is introduced with its similarity to the optimisation problems and the concept of biological diversity is exploited.

Chapter 7 describes the developed parallel computing simulation environment (based on a Beowulf cluster) used to implement the previous models.

Chapter 8 gives some results of the proposed strategies with test cases and real world industrial problems. The discussed problems are the design

of an energy storage system and of both low and high critical temperature magnets used for magnetic resonance imaging.

The conclusion of the Thesis are given in Chapter 9, together with some further research pointers.

## 1.4 Appendix: Design and Nature

Many methodologies described in the following base themselves on concepts coming from the natural world.

Some biologists debate about design in nature and about the design of living organisms. But usually few biologists have experience designing anything intended to achieve a specified function subject to physical constraints [6].

On the other hand, engineering can be called the science of design. Engineers design devices or processes to achieve a function they have in mind. They apply physical and economic constraints to problem-solving.

The Darwinian "mechanism" of natural selection by an environment presented with alternative organisms through genetic mutation is claimed to have produced the present complexity from the simplest forms of life. If so, from an engineering viewpoint, this appears to be a highly empirical way to design more complex organisms. The search mechanism is the random selection of a given operator at each branch in the search tree of the problem space.

However, because the actual behaviour of the Darwinian "mechanism" are unidentified, it is not possible to conclude that the search is entirely unguided. Intelligent-design theorists postulate that it is guided in a top-down, model-driven or goal-driven way while theistic evolutionists postulate bottom-up, data-driven or environment-driven guidance.

The statistician Amir D. Aczel in his book *Probability 1* [7] recalled the famous sentence of Albert Einstein "God does not play dice" questioning about how Darwinian natural evolution could produce creatures capable of creating art, music, poetry, mathematics and philosophy, none of which seems to have much Darwinian survival value. Are they mere by products of a brain designed by nature only to increase its survival efficiency?

# Chapter 2

## The Optimal Design in Electromagnetics

This chapter introduces the main characteristics and problems in the optimal design of electromagnetic devices, in particular about the principal application topic of this Thesis, the design of high field superconducting magnets.

### 2.1 Electromagnetic devices

THE OPTIMAL DESIGN of an electromagnetic device is a complex process including the definition of the device layout and the selection of the design parameters, in such a way to perform "as well as possible" the assigned task with the satisfaction of the required performances and of the imposed physical and technological constraints due to the stringent and demanding requirements and quality standards [8].

Previously, the device, its performances and characteristics have to be properly modelled. Like other engineering activities, the design in electromagnetics involves unstructured, real-life features that are hard to model, since they require inclusion of unusual factors (from accident risk factors to aesthetics). In general, the final cost of the device is an important aspect: it includes the materials cost, the production and manufacturing cost and the maintenance cost. Factors like the physical life span of the device have often to be taken into account with the minimisation of the device probability of failure.

For industrial relevant problems, in particular in the power and energy field, the optimal design is usually a multi-objective task where different specifications, often in conflict among them, have to be pursued with several

design Degrees Of Freedom (DOF) [4]. The optimisation of the device looks for an equilibrium point of the different and non-homogeneous goals. Each generic admissible solution for the design problem represents one point in the multi-dimensional design space spanned by all admissible device parameters satisfying the requirements and the technological and physical constraints.

Therefore it is necessary the use of a multi-objective optimisation strategy based on a rigorous mathematical formulations and automatic design aids to help the engineer's technical sensibility and experience during the process.

Due to the presence of multiple quasi-optimal solutions and to the typical complexity of electromagnetic calculations, the automatic optimal design of electromagnetic devices is a very challenging task. In addition, as a further complexity element, the mathematical model of the design problem does not always include all the design goals and constraints: it could be too difficult to mathematically define some of the objectives or constraints or the inclusion of a particular objective could deeply increase the complexity of the problem resolution. For instance, some of these not usual constraints or "auxiliary" information about the problem come from the designer's experience and knowledge. For these cases, it is preferable to adopt an optimisation strategy able to find a set possible solution: in this way, the Decision Maker (DM) has the final duty of selecting the best solution among the set.

## 2.2 Basic problems in engineering design

Some of the basic problems of engineering design can be stated in the following way [3]:

- There are objectives and there are constraints. The difference between them is not always well established and some of them can move from objectives to constraints or vice-versa.
- Some constraints are strict and some are not and can be relaxed.
- The design parameters ranges can be also "fuzzy" and flexible: the real bounds are not always known at the beginning of the design process.
- The parameters and the objectives values can be effected by uncertainty due to measure or computing errors.
- The output should contain both optimal solutions and suggestions of extending ranges and/or inclusion/removals of constraints.

- It is useful for the engineer to have a set of results to post-analyse: for instance, those results can be processed by some other programs or tools or by consulting some knowledge databases or experts.

In engineering practice, the optimal design problem is usually formulated in terms of constrained optimisation of a multi-objective scalar function, typically constructed as a weighted sum of different cost functions, each one specialized to mathematically represent a partial objective. The overall Objective Function ( $OF$ ) is then minimised inside a suitable search domain defined by the admissible ranges for each parameter while taking into account the imposed constraints. In general, the  $OF$  presents multiple local minima scattered in the admissible solutions space: therefore its minimisation calls for global techniques able to explore the complete space without being trapped by local minima.

Stochastic evolutionary strategies are a family of well known global optimisation algorithms widely used in different research fields for their robustness and generality. In particular, the Genetic Algorithms (GAs) have achieved a particular relevance, both for their quite simple implementation and for the effectiveness of their action: recently performed numerical experiments confirmed the interest and documented the algorithm performances.

”Real world” design problem can be very demanding in terms of computing resources, by requiring the resolution of a complex electromagnetic problem for each  $OF$  evaluation: High Performance Computing (HPC) techniques are therefore necessary to low down the development time of a new device configuration when the complexity of the adopted models increases. In such a context, the present growing diffusion of parallel computing architectures pushes towards the development of innovative versions of the minimisation algorithms able to take maximum advantage of the performances and specific technical characteristics of the new computing resources.

## 2.3 Superconducting magnets

Superconductors are a class of materials which show no Ohmic resistance to direct current when cooled below a critical cryogenic temperature  $T_c$ , also called the *transition temperature*. In addition, superconduction state requires that the current density passing through the material must be below a characteristic level known as the critical current density ( $J_c$ ) and the magnetic field, to which the material is exposed, must be below a characteristic value

(critical magnetic field  $H_c$ ). These critical conditions are interdependent and define the environmental operating conditions for the superconductor. Superconducting wires provide significant advantages over conventional copper wires because they conduct electricity with little or no resistance and associated energy loss and they can transmit much larger current density than conventional wires.

### 2.3.1 Design of fusion magnets

A promising approach to produce energy is the use of controlled thermonuclear fusion machines, whose development is performed since many decades all over the world. The most studied configuration to achieve magnetic confinement of the very hot plasma, where the fusion process evolves, is called *tokamak* (toroidal chamber machine, by the original Russian acronym). A huge superconducting magnetic system is used in a tokamak fusion machine to generate the strong fields required in a wide region [9]: for this purpose, conventional resistive magnets are not attractive due to the large energy needed to feed such magnets, in addition to technological issues. The magnetic system is composed by a set of coils wound with superconducting cable: the design of such coils has to be properly processed in order to fulfill the wanted requirements. The project ITER (International Thermonuclear Experimental Reactor) has gathered worldwide significant research and development efforts about superconducting magnets and conductors. In the framework of the ITER project, two model coils have been built and are now under testing: one of these, the TFMC (toroidal field model coil), is shown in Figure 2.1.

### 2.3.2 Design of MRI superconducting magnets

Superconducting magnets for Magnetic Resonance Imaging (MRI) are designed to provide very strong magnetic fields with quite high levels of homogeneity [10]. Suitable optimisation techniques can be effectively used to choose the magnet geometrical parameters (*e.g.* dimensions and position of each coil), while satisfying mechanical and physical constraints (*e.g.* dimensions of the wires and packaging factors or superconductor critical currents) [11].

For the design of MRI magnets, the main performance figure is the homogeneity of the magnetic field in the Volume of Interest (VOI). In the analysis



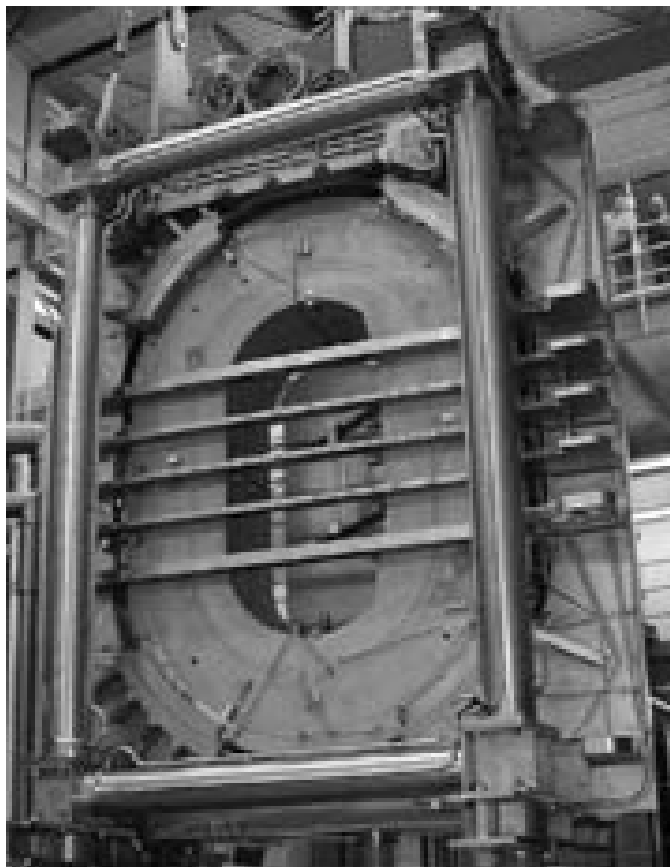


Figure 2.1: ITER project: toroidal field model coil (TFMC).

of MRI magnets, a spherical harmonics expansion of the flux density field can be used inside the sources free VOI:

$$B_z = \mu_0 \sum_{n=1}^{\infty} r^{n-1} \sum_{m=0}^{n-1} \left[ (n-m) \cos \vartheta P_n^m(\cos \vartheta) + \sin \vartheta P_n^{m+1}(\cos \vartheta) \right] \times \quad (2.1)$$

$$[A_{nm} \cos m\varphi + B_{nm} \sin m\varphi]$$

where  $(r, \theta, \varphi)$  are the coordinate of the field point, with the axis  $z$  aligned with  $\theta = 0$ , and  $P_n^m$  are the Legendre functions of the first kind. Only the field component along the axis  $z$  of the coil system is considered, because other components are negligible with respect to the main component, on condition that the needed field is highly uniform.

The coefficients  $A_{nm}$  and  $B_{nm}$  provide an effective measure of the field homogeneity: for a perfectly homogeneous field, all the coefficients are equal to zero except for the first one, which is equal to the field magnitude. Rather effective techniques have been proposed to evaluate  $A_{nm}$  and  $B_{nm}$  with good accuracy and limited computation time, allowing to perform analysis with a large number of runs even on a PC-class computer [12].

For axial-symmetric fields, there is no dependence by the azimuthal coordinate  $\varphi$  and only the terms with  $m = 0$  are not vanishing. The field expansion (2.1) reduces to:

$$B_z = \mu_0 \sum_{n=1}^{\infty} A_{n0} r^{n-1} \left[ n \cos \vartheta P_n^0(\cos \vartheta) + \sin \vartheta P_n^1(\cos \vartheta) \right] \quad (2.2)$$

The lack of homogeneity  $Unif(\mathbf{x})$  for the magnets configuration  $\mathbf{x}$  is defined as the ratio between the maximum field variation inside the VOI and the central field  $B_z(0)$ .  $Unif(\mathbf{x})$  is measured in ppm (parts per million) as

$$Unif(\mathbf{x}) = 10^6 \frac{|B_z(p_{\max}) - B_z(p_{\min})|}{B_z(0)} \quad (2.3)$$

where  $p_{\max}$  e  $p_{\min}$  are respectively the points in the VOI where the field get its maximum and minimum values. Due to the analyticity of the field, the  $p_{\max}$  e  $p_{\min}$  points are on the VOI boundary.

# Chapter 3

## Optimisation Problems and Objective Functions

In this chapter, the multi-objective optimisation problem is defined and some mathematical and statistical background are recalled, in particular the concept of Pareto optimality. Topics related to the definition of the Objective Function are introduced. Then, some test cases, used in the following, are presented.

### 3.1 The optimisation problems

USUALLY THE OPTIMISATION problems are defined by using a scalar Objective Function that is used to evaluate the solution quality, as recalled in the previous chapter. The *OF* imposes a total order on the set of potential solutions and the task is *simply* to search for an optimum.

For many real world applications, however, when it is required to find solutions that *simultaneously* optimise two or more *distinct* criteria of preference, other approaches are possible. These multi-objective problems present a number of challenges that do not arise in scalar optimisation. In most cases, for example, there do not exist solutions that are an optimum on all problem objectives, and so there is no ideal solution: rather, there are a number of solutions that represent different tradeoffs of the objectives. In this context, the aim of the search has to be properly defined together with a method to compare the solutions in order to drive the search.

### 3.2 Definition of the problem

Single objective optimisation problems (SOPs) involve the minimisation of a scalar function  $f(\mathbf{x})$  (the objective function), where  $\mathbf{x} = (x_1, \dots, x_n)$  is a point in the optimisation parameter space  $\mathbf{R}^n$ . The general problem class to be considered is known as nonlinearly constrained single-objective optimisation problem and can be expressed in mathematical terms as [13]:

$$\begin{aligned} \min! \quad & f(\mathbf{x}) & \mathbf{x} \in \mathbf{R}^n \\ \text{subjected to} \quad & c_j(\mathbf{x}) = 0, & j \in E \\ & c_j(\mathbf{x}) \geq 0, & j \in I \\ & x_i \in [x_i^{low}, x_i^{up}] & i = 1, \dots, n \end{aligned} \tag{3.1}$$

where  $c_j(\mathbf{x}), j = 1, \dots, p$  are the *constraint functions*,  $E$  is the index set of equality constraints and  $I$  is the index set of inequality constraints, where both sets  $E$  and  $I$  are finite. The  $x_i^{low}$  and  $x_i^{up}$  are the lower and upper range limits of the  $i$ -th variables  $x_i$ . The objective function  $f(\mathbf{x})$  and the constraint functions  $c_i$  are real valued scalar functions. Any point  $\mathbf{x}$  satisfying all constraints of the optimisation problem is called *feasible*. The set of all feasible points is called the *feasible region*.

Multi-objective optimisation problems (MOPs) involve the "minimisation" of a vectorial function  $\mathbf{F}(\mathbf{x}) = (f_1(\mathbf{x}), \dots, f_k(\mathbf{x})) \in \mathbf{R}^k$ , where  $f_i(\mathbf{x})$  are the partial objectives. Because the  $\mathbf{R}^k$  space is not ordered, the meaning of the minimisation of the vectorial function  $\mathbf{F}$  has to be properly defined by introducing some ordering technique (for instance by using the Pareto dominance concept presented in the following). The multi-objective optimisation problems is defined as:

$$\begin{aligned} \min! \quad & \mathbf{F}(\mathbf{x}) & \mathbf{F} \in \mathbf{R}^k & \mathbf{x} \in \mathbf{R}^n \\ \text{subjected to} \quad & c_j(\mathbf{x}) = 0, & j \in E \\ & c_j(\mathbf{x}) \geq 0, & j \in I \\ & x_i \in [x_i^{low}, x_i^{up}] & i = 1, \dots, n \end{aligned} \tag{3.2}$$

The conditions for the existence of solutions of the problems (3.1) and (3.2) are reported in [13].

For solving a MOP, a *human* Decision Maker (DM) is necessary to state the often difficult tradeoffs between conflicting objectives [14]. Depending

on how optimisation and the decision process are combined, multi-objective optimization methods can be broadly classified into three categories:

**Decision making before search** The objectives of the MOP are aggregated into a single objective which implicitly includes preference information given by the DM.

**Search before decision making** Optimisation is performed without any preference information given. The result of the search process is a set of (ideally Pareto-optimal, see next sections) candidate solutions from which the final choice is made by the DM.

**Decision making during search** The DM can articulate preferences during the interactive optimisation process. After each optimisation step, a number of alternative trade-offs is presented on the basis of which the DM specifies further preference information to guide the search.

The aggregation of multiple objectives into one optimisation criterion has the advantage that the classical single-objective optimisation strategies can be applied without further modifications. However, it requires knowledge of the search domain, which is usually not available. Performing the search before decision making overcomes this drawback, but excludes preference articulation by the DM, which might reduce the search space complexity. Another problem with this second and also with the third algorithm category might be the visualisation and the presentation of non-dominated sets for higher dimensional MOPs [15]. Finally, the integration of search and decision making is a promising way to combine the other two approaches, uniting the advantages of both.

### 3.3 Partial and total order

For the multi-objective optimisation problem, the concept of order of a multi-dimensional space has to be introduced by the following definitions [3]:

**Definition 3.1** *Order*

**Partial order** *Binary relation  $\mathcal{R}$  is a partial order on domain  $D$  if and only if it satisfies the following three properties:*

1. **reflexivity**: for all  $x \in D$ ,  $\mathcal{R}(x, x)$ ;

2. **antisymmetry**: for all  $x, y \in D$ , if  $\mathcal{R}(x, y)$  and  $\mathcal{R}(y, x)$  then  $x = y$ ;
3. **transitivity**: for all  $x, y, z \in D$ , if  $\mathcal{R}(x, y)$  and  $\mathcal{R}(y, z)$  then  $\mathcal{R}(x, z)$ .

**Total order** Binary relation  $\mathcal{R}'$  is a total order on domain  $D$  if:

1. It is a partial order;
2. For all  $x, y \in D$ ,  $\mathcal{R}'(x, y)$  or  $\mathcal{R}'(y, x)$ .

**Strict order** Binary relation  $\mathcal{R}''$  is a strict (partial) order on domain  $D$  if it satisfies the following two properties:

1. **irreflexivity**: For all  $x \in D$ ,  $\neg \mathcal{R}''(x, x)$ ;
2. **transitivity**: For all  $x, y, z \in D$ , if  $\mathcal{R}''(x, y)$  and  $\mathcal{R}''(y, z)$  then  $\mathcal{R}''(x, z)$ .

The notations  $\leq$  and  $\geq$  are commonly used for partial and  $<$  and  $>$  for strict orders.

### Definition 3.2 Chain

Subset  $D' \subseteq D$  is called chain with respect to partial order  $\leq$  if every two elements of  $D'$  are comparable, i.e. for all  $x, y \in D'$ ,  $x \leq y$  or  $y \leq x$ .

## Examples

- The usual order on a set of real numbers is a total order: it is always possible to say for any two real numbers  $x$  and  $y$  if  $x \leq y$  or  $y \leq x$ .
- If  $D = \{(x, y) \mid x, y \in \mathbb{R}\}$  and  $\{(x, y) \leq_2 (x_1, y_1) \stackrel{def}{\iff} (x \leq x_1) \wedge (y \leq y_1)\}$  then
  1. Order  $\leq_2$  is (non-total) partial order on  $D$  since, for example,  $(2, 3) \not\leq_2 (3, 2)$  and  $(3, 2) \not\leq_2 (2, 3)$ ;
  2. Sets  $\{(x, 0) \mid x \in \mathbb{R}\}$  and  $\{(0, x) \mid x \in \mathbb{R}\}$  are examples of chains according to  $\leq_2$ .

For the multi-objective optimisation problems, the multi-dimensional component-wise order relation  $\leq$  is not a *total order*: it is not fulfilled that for every two vectors  $\mathbf{x}, \mathbf{y} \in \mathbf{R}^n$ ,  $\mathbf{x} \leq \mathbf{y}$  or  $\mathbf{y} \leq \mathbf{x}$ , *i.e.* not every two elements are comparable. In multi-dimensional case, this ordering relation is a *partial order*. Instead of one total order, we have (possibly many) chains where every two elements within a chain are comparable. The greatest element of a chain is called a *maximal element* [3].

### 3.4 Mathematical background

Some definitions used in the following are here presented.

**Convexity** The set  $K \in \mathbf{R}^n$  is *convex* if, for any points  $\mathbf{x}_1, \mathbf{x}_2$  in the set, the line segment joining these points is also in the set, *i.e.*:

$$\forall \mathbf{x}_1, \mathbf{x}_2 \in K \quad : \quad \mathbf{x}_\theta = (1 - \theta)\mathbf{x}_1 + \theta\mathbf{x}_2 \in K \quad \forall \theta \in [0, 1]$$

#### 3.4.1 Pareto dominance

**Pareto Dominance** A vector  $\mathbf{u} = (u_1, \dots, u_n)$  is said to dominate  $\mathbf{v} = (v_1, \dots, v_n)$  and is denoted by  $\mathbf{u} \preceq \mathbf{v}$ , if and only if  $\mathbf{u}$  is partially less than  $\mathbf{v}$ , *i.e.*,

$$\forall i \in \{1, \dots, n\} \quad u_i \leq v_i \quad \wedge \quad \exists j \in \{1, \dots, n\} : u_j < v_j \quad (3.3)$$

**Pareto (Optimal) Set** For a given multi-objective problem  $\mathbf{F}(\mathbf{x})$ , defined as in (3.2) in a set  $\Omega \subset \mathbf{R}^n$ , the Pareto optimal Set  $\mathcal{P}$  is defined as:

$$\mathcal{P} := \{\mathbf{x} \in \Omega \mid \neg \exists \mathbf{x}' \in \Omega : F(\mathbf{x}') \preceq F(\mathbf{x})\} \quad (3.4)$$

$\mathcal{P}$  is the set of all elements in  $\Omega$  whose image is non-dominated.

**Pareto (Optimal) Front** For a given multi-objective problem  $\mathbf{F}(\mathbf{x})$ , defined as in (3.2), and Pareto optimal Set  $\mathcal{P}$ , the Pareto Front  $\mathcal{PF}$  is defined as:

$$\mathcal{PF} := \{\mathbf{u} = \mathbf{F}(\mathbf{x}) \mid \mathbf{x} \in \mathcal{P}\} \quad (3.5)$$

The Pareto Front is therefore the maximal set of *nondominated feasible solutions*.

### 3.4.2 Statistical definitions

These statistical definitions [16] will be used later.

**PMF** The probability distribution of a *discrete* random variable  $Y$  is represented by its Probability Mass Function (PMF), defined as:

$$p_Y(y) = P\{Y = y\} \quad (3.6)$$

where  $P\{Y = y\}$  is the probability of  $Y$  to have the value  $y$ .

**Probability distribution function** If  $X$  is a continuous random variable and  $x$  the generic value of  $X$ , the probability distribution function of the random variable  $X$  is defined as

$$F_X(x) = P\{X \leq x\} \quad \forall x \in R \quad (3.7)$$

where  $P\{X \leq x\}$  is the probability of  $X$  to have values not greater than  $x$ .  $F_X(x)$  is also called the cumulative probability function or Cumulative Distribution Function (CDF). By the definition, the probability in an interval  $]a, b]$  is:

$$P(]a, b]) = F_X(b) - F_X(a) \quad (3.8)$$

**PDF** The Probability Density Function (PDF)  $f_X(x)$  of a continuous random variable  $X$  is defined by:

$$P(x) = \int_{-\infty}^{\infty} f_X(x) dx \quad (3.9)$$

Since the probability of the event is 1, the PDF is normalised:

$$\int_{-\infty}^{\infty} f_X(x) dx = 1 \quad (3.10)$$

**Expecter value E** Also referred as *mean* or first order moment:

$$E[X] = \int_{-\infty}^{\infty} x f_X(x) dx \quad (3.11)$$



**Variance**  $\sigma_X^2$  Also referred as second order moment:

$$\sigma_X^2 = \int_{-\infty}^{\infty} (x - E[X])^2 f_X(x) dx \quad (3.12)$$

The square root  $\sigma_X$  of the variance is called *standard deviation*.

**Uniform PDF** The continuous uniform PDF is defined as:

$$\begin{aligned} f_X(x) &= \frac{1}{b-a} & \text{if } x \in [a, b[ \\ f_X(x) &= 0 & \text{otherwise} \end{aligned}$$

For the uniform PDF it results:

$$E[X] = \frac{a+b}{2} \quad \sigma_X^2 = \frac{(b-a)^2}{12}$$

**Gaussian (normal) PDF** For two real parameters  $\mu > 0$  and  $\sigma > 0$ , the continuous Gaussian PDF is defined as:

$$f_X(x) = \frac{1}{\sqrt{2\pi}\sigma} e^{-\frac{(x-\mu)^2}{2\sigma^2}} \quad (3.13)$$

For the Gaussian PDF it results:

$$E[X] = \mu \quad \sigma_X^2 = \sigma^2$$

The special case  $\mu = 0$  and  $\sigma^2 = 1$  is called *standard normal PDF*.

**Central Limit Theorem** The Central Limit Theorem is an important mathematical result which states that for a continuous random sample of observations from *any* distribution with a finite mean and a finite variance, the sample mean will tend to follow a normal distribution for large samples.

**Confidence Interval** It is a statistic value constructed from a set of data to provide an interval estimate for a random variable. The confidence level associated with the interval, usually 90%, 95% or 99%, is the percentage of times, in repeated sampling, that the intervals will contain the value of the random variable.

### 3.5 Definition of the Objective Function

The multi-objective optimal design can be performed by using vector or scalar optimisation techniques. The former are based on the separate evaluation and optimisation of the different partial objectives, while in the latter the partial objectives are combined in some global cost function. For scalar optimisation the problem is therefore reduced to the minimisation of a single Objective Function. Therefore the *OF* provides a compact quantitative value to the satisfaction of the several design goals, as a function of all design parameters. The "quality" of each design solution is described by the value of the *OF* in the actual configuration.

The single objectives can be commensurable, if they are expressed in the same units, or non-commensurable: usually, for engineering optimisation problems, the objectives are non-commensurable.

Scalar *OFs* are typically assumed as the weighted sum of the different objectives, which have to be properly normalised and adimensionalised:

$$OF(\mathbf{x}) = \sum_{i=1}^k w_i f_i(\mathbf{x}) \quad (3.14)$$

where  $k$  is the number of the partial objectives,  $f_i$  is the  $i$ -th partial objective normalised in  $[0,1]$ ,  $\mathbf{x}$  is the design parameters vector and  $w_i$  are suitable weights, with  $w_i \geq 0$  and

$$\sum_{i=1}^k w_i = 1 \quad (3.15)$$

Of course,  $OF(\mathbf{x}) = f(\mathbf{x})$  for SOP. The choice of the weights is made to keep the order of magnitude and the sign of the partial objectives. The optimal selection of the weights  $w_i$  has to be performed by the designer on the basis of the relative importance of the various objectives: the weights are an a-priori articulation of the designer preferences and typically they strongly influence the final results. Different strategies to express the designer preferences among the objectives and to address the choice of the weights are reported in [17].

In many industrial design problems, the *OF* is non-continuous or non-analytic. In addition, for a wide class of optimal design problems, due to non-linear relationship with the design parameters, the *OF* presents multiple local minima, each corresponding to one of possible quasi-optimal solutions. When

the attraction basin of the minimum is unknown, to prevent the trapping into local minima, the whole parameters space has to be therefore scanned.

### 3.6 Constraints handling: penalty functions

Constraint handling methods used in classical optimization algorithms can be classified into two groups: (i) generic methods that do not exploit the mathematical structure (whether linear or nonlinear) of the constraints (*i.e.*  $c_i$  functions in (3.1) or (3.2)) and (ii) specific methods that are only applicable to a special type of constraints.

Generic methods, such as the penalty function method, the Lagrange multiplier method, and the complex search method are popular, because each one of them can be easily applied to any problem without significant changes in the algorithm [13]. However specific methods, such as the cutting plane method, the reduced gradient method and the gradient projection method, are applicable either to problems having convex feasible regions only or to problems having a few variables, because of the increased computational burden with large number of variables [18].

From here, I will refer, for simplicity, just to SOP. A very common approach to handling constraints (linear or not linear) is to transform the constrained problem into an unconstrained one by adding *penalty functions* to the objective function  $f$ :

$$\Phi(\mathbf{x}) = f(\mathbf{x}) + \sum_{i=1}^{N_{con}} P_i(\mathbf{x}) \quad (3.16)$$

where  $\Phi(\mathbf{x})$  is the modified objective function,  $N_{con}$  is the number of violated constraints and  $P_i(\mathbf{x})$  is the penalty function for the  $i$ -th constraint. These penalty terms weight the constraints violations, penalising non-feasible solutions.

The penalty function method presents the following properties:

1. The  $\Phi$  value of a feasible solution is equal to its objective function value  $f$ .
2. The  $\Phi$  value of an infeasible solution is always worse than that of a feasible solution.
3. The  $\Phi$  value of a infeasible solution having smaller constraints violation than another infeasible solution is better than the latter one.

A deeper discussion about penalty functions will be developed later in the Section 4.4.1, with their application to stochastic optimisation.

## 3.7 Test problems

In this Thesis some benchmark problems have been used to test different optimisation strategies. For the selection of an effective benchmark problem, it is important that the problem should be as much as possible similar to the typical "real world" electromagnetic models. In particular the benchmark function to minimise should be non-linear, non continuous, multimodal with multiple minima and its definition domain should be non connected. In addition, the function minima should be close to the non-feasible solutions region.

### 3.7.1 Rastrigin function

For preliminary studies, the widely used Rastrigin analytic function has been considered. It is defined by:

$$f = nA + \sum_{i=1}^n [x_i^2 - A \cos(2\pi x_i)] \quad (3.17)$$

where the parameter  $A = 10$ ,  $n$  is the dimension of the search space,  $i \in [1, n]$  and  $x_i \in [-5.12, 5.12]$ . This multimodal function has a global minimum at  $x_i = 0$ , where it values zero, and several local minima: for example, the function values 1 in the points located at  $x_i = 1$  and  $x_{j \neq i} = 0 \quad \forall j$ . To introduce some of the characteristics of the typical electromagnetic problems, not feasible regions have been set for the  $x_i$  variables, with  $i$  odd, in the ranges  $[-1.8, -1.1]$  and  $[1.1, 1.8]$ : is such a way the search space becomes not connected and some of the minima are located close to the border of the space. In addition, a discontinuity has been introduced at  $x_i = \pm 2.1$ , with  $i$  even. In Figure 3.1 a section of the modified Rastrigin function with  $n = 2$  is plotted in the plane  $x_2 = 0$  for  $x_1 \in [0, 5.12]$ : it is visible the not-allowed interval  $x_1 \in [1.1, 1.8]$ . In Figure 3.2 it is plotted the section in the plane  $x_1 = 0$  for  $x_2 \in [0, 5.12]$ : it is visible the discontinuity in  $x_2 = 2.1$ .

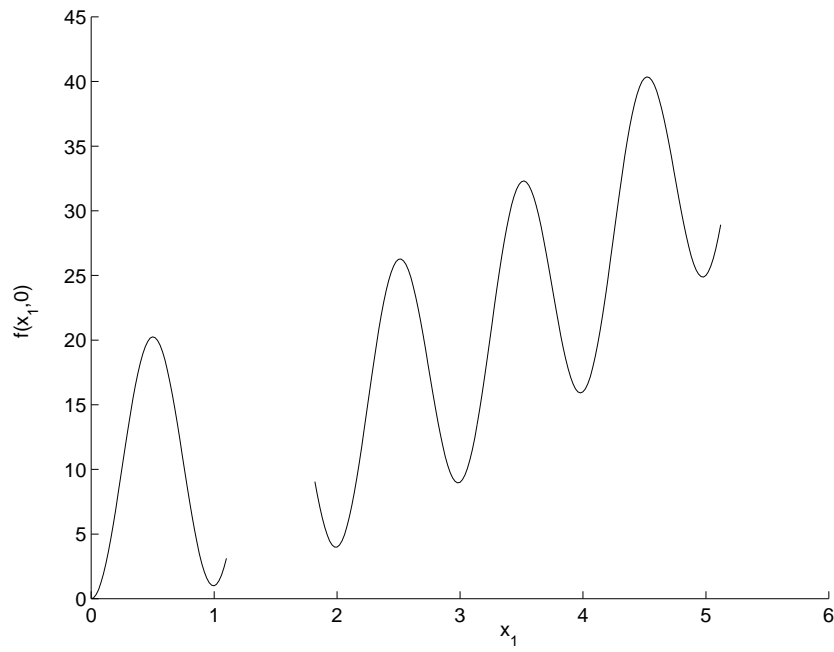


Figure 3.1: Section of the Rastrigin function on the plane  $x_2=0$  for  $n = 2$ .

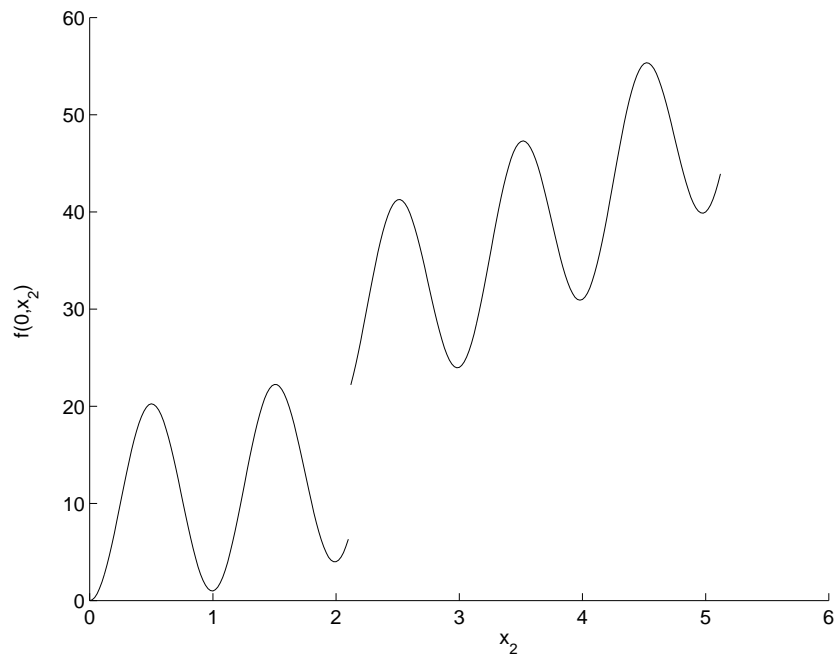


Figure 3.2: Section of the Rastrigin function on the plane  $x_1=0$  for  $n = 2$ .

### 3.7.2 TEAM 22 Problem

As an example of a "real world" benchmark problem, the optimisation design has been performed for a superconducting system called SMES (Superconducting Magnetic Energy Storage) [19]. SMES systems are devices used to store energy in magnetic fields generated by coils wound with superconducting wires. These devices can be applied for electrical load levelling and peak load supply in power network or for protection of critical user facilities against voltage dips. Due to the increase of power quality demand, SMES can be also used for filtering the harmonic content in power transmission lines.

SMES are mainly characterised by the maximum stored energy: depending on the particular application, the SMES systems are designed for a maximum energy in the range  $0.1 \div 200$  MJ. In a SMES device design, beside to satisfy the specific device requirements, attention has to be given to other cost factors, such as the superconductors volume and the overall dimensions.

For construction reasons, the most effective configuration for SMES windings is a short solenoid. Unfortunately, such structures generate stray magnetic fields in a wide surroundings area: these stray fields can be non-conforming with environmental specifications related to human safety and they can also interfere with the correct operation of other equipment. For this reason, SMES devices include a second coil as an active shield, whose position, shape and currents are included in the design parameters set.

A shape optimisation is then required to find a good choice of the free parameters, according to the design constraints. Note that the dependence of the device performance on the design parameters is quite complex, taking also into account that the superconductors critical current conditions should not to be violated. Due to the presence of multiple local optima, scattered in the parameters search space, a global search algorithm is strongly recommended to perform the SMES design.

Here the SMES design has been performed according to TEAM (Testing Electromagnetic Analysis Methods) Problem 22 (see TEAM Web Page at <http://ics.ascn3.uakron.edu/>), treating of an optimal SMES design with the following specifications:

- The stored energy in the device should be 180 MJ.
- The stray field should be as small as possible.
- The current density inside superconducting coils must not violate critical conditions, depending on the magnetic field intensity, required to

guarantee the superconducting state.

The critical condition, relating the current densities  $\|\mathbf{J}\|$  with the maximum values of the magnetic flux density  $\|\mathbf{B}\|$  within the coils, for an industrial superconductor is approximated by:

$$\|\mathbf{J}\| = (6.4\|\mathbf{B}\| + 54) \text{ A/mm}^2 \quad (3.18)$$

The following Objective Function is used:

$$OF = F_1 + F_2 = \frac{|E - E_{ref}|}{E_{ref}} + \frac{B_{stray}^2}{B_{norm}^2} \quad (3.19)$$

where:  $E$  is the magnetic energy of the device,  $E_{ref} = 180 \text{ MJ}$ ,  $B_{norm} = 2E^{-4} \text{ T}$  and

$$B_{stray}^2 = \sum_{i=1}^{22} \frac{|\mathbf{B}_{stray,i}|^2}{22} \quad (3.20)$$

$B_{stray}$  is evaluated at 22 equidistant points along line  $a$  and line  $b$  in Figure 3.3. From the numerical point of view, the coils are schematised by a set of filamentary circuits. Due to the linearity of the problem, analytical formulas can be adopted to evaluate the field energy and the magnetic fields by superposition. The magnetic energy  $E$  is calculated by:

$$E = \frac{1}{2} \mathbf{I}^t \mathbf{L} \mathbf{I} \quad (3.21)$$

where  $\mathbf{L}$  is the inductance matrix and  $\mathbf{I}$  is the filamentary current vector. The inductance matrix elements are evaluated using well known approximate formulas [20]. The stray field and the magnetic field inside the coils, needed to check the critical condition, are evaluate using the Urankar's formulas [21].

### Three parameters problem

Two subproblems are defined in the TEAM 22 benchmark. For the small problem, the three design parameters are the dimensions of the outer coil ( $R_2$ ,  $h_2/2$ ,  $d_2$  defined in Figure 3.3), while the inner coils dimensions and the current densities are fixed. The geometrical boundaries for the design parameters and the fixed parameters ( $R_1$ ,  $h_1/2$ ,  $d_1$ ,  $J_1$ ,  $J_2$ ) values are given in Table 3.1.

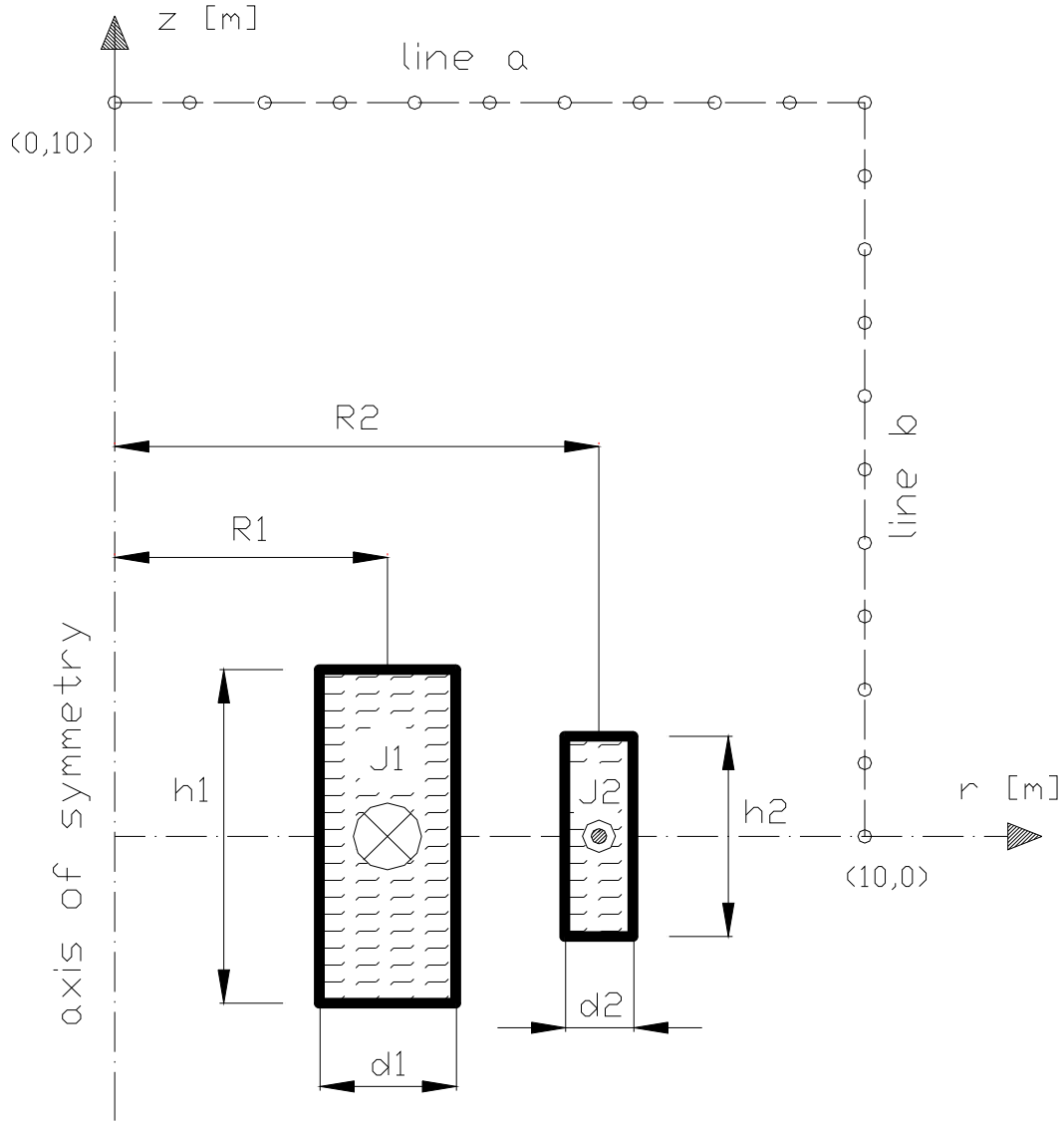


Figure 3.3: TEAM 22 problem: SMES geometry.

|       | $R_1$<br>(m) | $R_2$<br>(m) | $h_1/2$<br>(m) | $h_2/2$<br>(m) | $d_1$<br>(m) | $d_2$<br>(m) | $J_1$<br>(MA/m <sup>2</sup> ) | $J_2$<br>(MA/m <sup>2</sup> ) |
|-------|--------------|--------------|----------------|----------------|--------------|--------------|-------------------------------|-------------------------------|
| Min   | -            | 2.6          | -              | 0.204          | -            | 0.1          | -                             | -                             |
| Max   | -            | 3.4          | -              | 1.1            | -            | 0.4          | -                             | -                             |
| Fixed | 2.0          | -            | 0.8            | -              | 0.27         | -            | 22.5                          | -22.5                         |

Table 3.1: Geometrical constraints and fixed parameters of the SMES design parameters: three parameters problem.



|     | $R_1$<br>(m) | $R_2$<br>(m) | $h_1/2$<br>(m) | $h_2/2$<br>(m) | $d_1$<br>(m) | $d_2$<br>(m) | $J_1$<br>(MA/m <sup>2</sup> ) | $J_2$<br>(MA/m <sup>2</sup> ) |
|-----|--------------|--------------|----------------|----------------|--------------|--------------|-------------------------------|-------------------------------|
| Min | 1.0          | 1.8          | 0.1            | 0.1            | 0.1          | 0.1          | 10                            | -10                           |
| Max | 4.0          | 5.0          | 1.8            | 1.8            | 0.8          | 0.8          | 30                            | -30                           |

Table 3.2: Allowable ranges for the SMES design parameters: eight parameters problem.

### **Eight parameters problem**

For this quite more difficult problem, there are eight design parameters: the dimensions of the two coils and the two current densities ( $R_1$ ,  $R_2$ ,  $h_1/2$ ,  $h_2/2$ ,  $d_1$ ,  $d_2$ ,  $J_1$ ,  $J_2$  in Figure 3.3) with their allowable boundaries given in Table 3.2.

# Chapter 4

## Search Algorithms

*"If there is a set of strategies with the property that no player can benefit by changing her strategy while the other players keep their strategies unchanged, then that set of strategies and the corresponding payoffs constitute the Nash Equilibrium"* (by John F. Nash Jr. [22]).

In this chapter, different strategies to solve the multi-objective optimisation problem are presented, together with the Pareto optimality and sensitivity analysis concepts. The main attention is focused on the Genetic Algorithms. The developed and implemented algorithms have the principal aim to increase the robustness of the problem solutions.

### 4.1 Pareto optimality and $OF$ minimisation

TWO OF THE STRATEGIES for multi-objective problems resolution are to cast it as the minimisation of a scalar  $OF$  or as a Pareto Set search. As already reported, usually the multi-objective problem defined in (3.2) is solved by introducing a scalar  $OF$ , as in (3.14), defined as the weighted sum of the single objectives to minimise. Each set of weights codes a different choice made by an expert of the design problem (the Decision Maker) about the relative importance of the single objectives. By varying the weights, the objectives space can be spanned by modifying the  $OF$  landscape, where the term *OF landscape* refers to the hypersurface in  $\mathbf{R}^{n+1}$  space obtained by applying the  $OF$  to every point in the search space  $\mathbf{R}^n$  [23].

A different way to approach the multi-objective optimisation problem was introduced by the Italian economist Vilfredo Pareto in XIX<sup>th</sup> century [24]. Such a method is based on the concept of non-dominated solutions, as defined

in Section 3.4.1. A solution of a multi-objective optimisation problem is non-dominated if does not exist another solution which gains better values of each partial objective: in other words, given a non-dominated solution, it is not possible to improve a partial objective without getting worse another one. The Pareto Set is the locus of all non-dominated solutions and the Pareto Front is the image of the Pareto Set in the objectives space [25].

The Pareto Front gives a global view of the optimisation problem without assuming any particular decision about the relative importance of the partial objectives and including the solutions related to all possible combinations of relative weights among objectives.

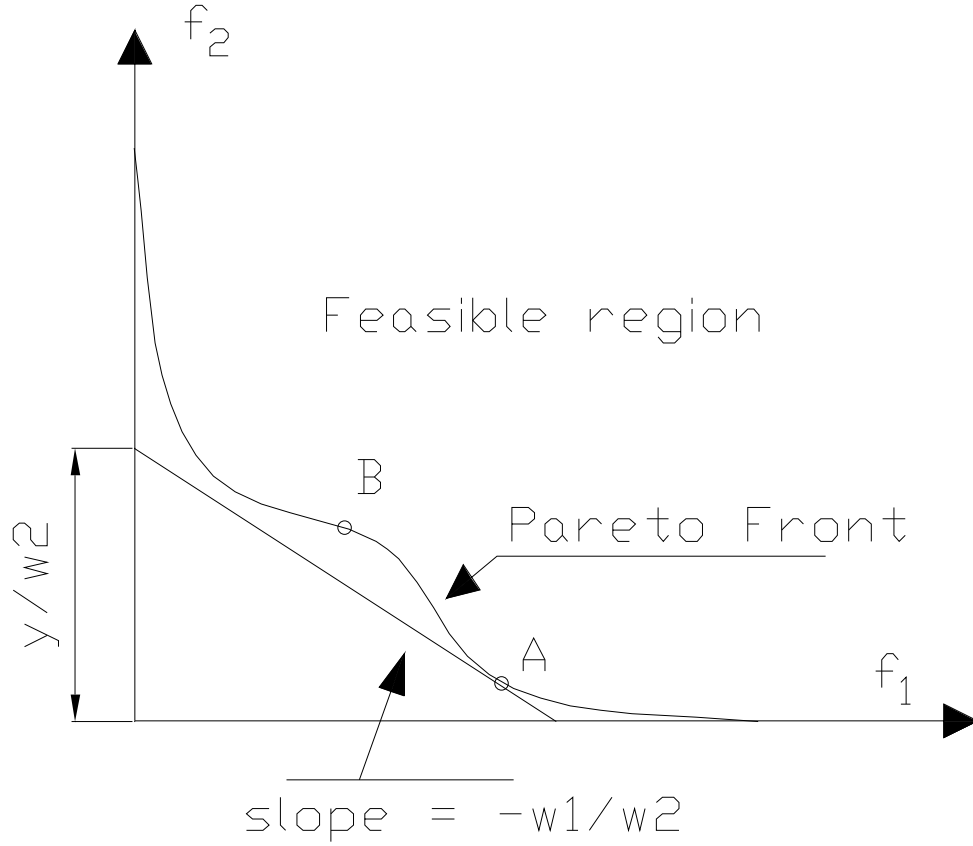
In the ideal case, each global minimum of the  $OF$ , with its particular weights set, is a point of the Pareto Front of the problem [26], [27]. Therefore, solving the weighted optimization problem (3.14) for a certain number of different weight combinations yields a set of Pareto optimal solutions: on condition that an exact optimization algorithm is used and all weights are positive, this method will only generate Pareto optimal solutions, as it can be easily shown [28]. Assume that a feasible decision vector  $\mathbf{a}$  minimises  $OF$  for a given weight combination and is not Pareto optimal. Then, there is a solution  $\mathbf{b}$  which dominates  $\mathbf{a}$ , *i.e.*, without loss of generality  $f_1(\mathbf{b}) < f_1(\mathbf{a})$  and  $f_i(\mathbf{b}) \leq f_i(\mathbf{a})$  for  $i = 2, \dots, k$ . Therefore,  $OF(\mathbf{b}) < OF(\mathbf{a})$ , which is a contradiction to the assumption that  $OF(\mathbf{a})$  is minimum.

The disadvantage of this technique is that it cannot generate all Pareto optimal solutions with non-convex Pareto Front surfaces [5]. This is illustrated in Figure 4.1 for a two-objectives example. For fixed weights  $w_1, w_2$ , the solution  $\mathbf{x}$  is sought to maximize  $y = w_1 f_1(\mathbf{x}) + w_2 f_2(\mathbf{x})$ . This equation can be reformulated as  $f_2(\mathbf{x}) = -\frac{w_1}{w_2} f_1(\mathbf{x}) + \frac{y}{w_2}$ , which defines a line with slope  $-\frac{w_1}{w_2}$  and intercept  $\frac{y}{w_2}$  in the objectives space  $(f_1, f_2)$ . Graphically, the optimisation process corresponds to move this line downwards until no feasible objective vector is below it and at least one feasible objective vector (here the vector ending in the point  $A$ ) is on it. However, the point  $B$ , in a non-convex region, will never minimise  $OF$  because no tangent line totally below the Pareto Front can pass through it.

In order to be able to locate points on non-convex parts of the Pareto Front, the weighted  $\mathcal{L}_p$ -norm problem could be solved instead [29]. The weighted  $\mathcal{L}_p$ -norm problem is actually a generalization of the weighted sum formulation (3.14) and it is defined as:

$$OF(\mathbf{x}) = \left\{ \sum_{i=1}^k [w_i f_i(\mathbf{x})]^p \right\}^{\frac{1}{p}} \quad (4.1)$$

where  $p$  is an integer satisfying  $1 \leq p \leq \infty$ . With an appropriate value of  $p$ ,

Figure 4.1: Pareto Front and  $OF$ .

all Pareto optimal points could be obtained but, however, such a value for  $p$  is unknown in advance. Moreover, a high value of  $p$  increases the difficulty of solving the optimization problem. In the extreme case where  $p = \infty$ , the problem to minimise the (4.1) is known as the weighted *minmax formulation*.

In practical applications, the (approximate) Pareto Front of the problem can be found by numerically solving many problems (3.14) by using different weights set and to retain the non-dominated approximate minima solutions.

#### 4.1.1 Pareto front: analytical test case

The previous procedure to find Pareto optimal solutions has been tested with an analytical multi-objective problem with one DOF (the "design parameter"  $x$ ) and two partial objectives defined by:

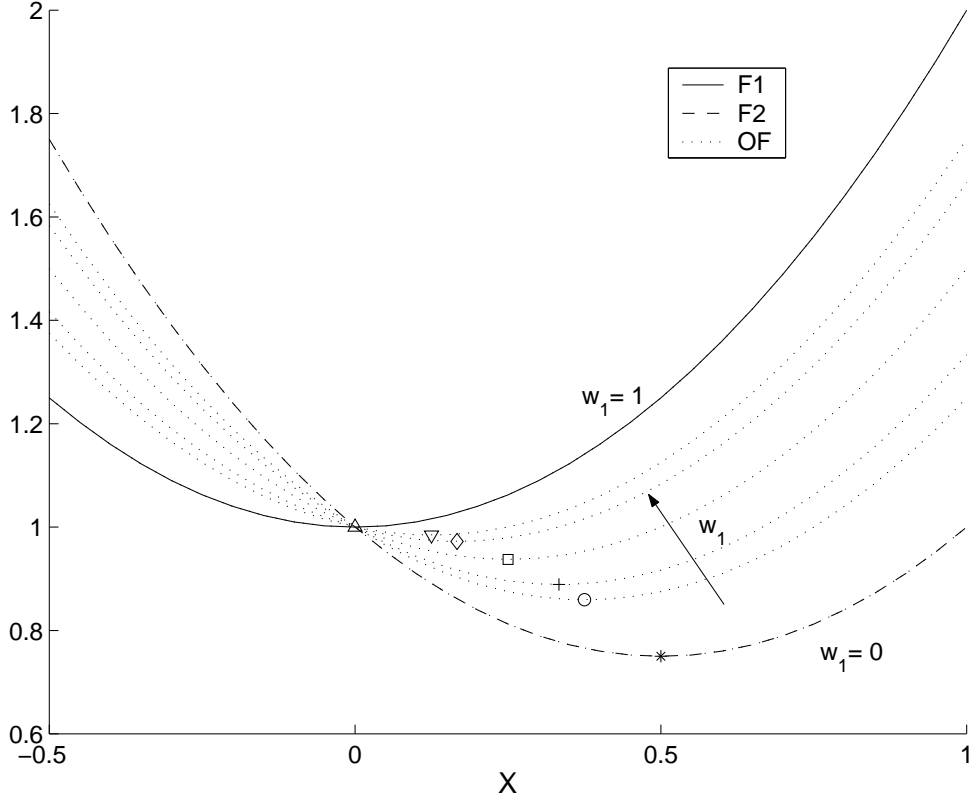


Figure 4.2: Pareto Front analytical test case: partial objectives plots and  $OF$ s for different weight sets (the minima of each  $OF$ s are plotted with marks).

$$\begin{aligned} F_1(x) &= 1 + x^2 \\ F_2(x) &= 1 - x + x^2 \end{aligned} \quad (4.2)$$

$F_1$  has a minimum  $F_1 = 1$  for  $x = 0$  and  $F_2$  has a minimum  $F_2 = 3/4$  for  $x = 1/2$ . The partial objectives are plotted in Figure 4.2 together with the scalar  $OF = w_1 F_1 + w_2 F_2$  for seven different sets of weights: for each  $OF$  the minimum is plotted with a mark. The seven weight sets are reported in Table 4.1 together with minima values of  $OF$  and the corresponding  $x$  values.

The Pareto Set of the multi-objective problem is the interval  $x = [0, 1/2]$ , where the first objective  $F_1$  increases with  $x$  and the second one  $F_2$  decreases: note that the Pareto Set is simply connected. The corresponding Pareto Front is plotted in Figure 4.3 with continuous line in the objectives plane:

| $w_1$ | $w_2$ | $OF_{min}$ | $x_{min}$ |
|-------|-------|------------|-----------|
| 0     | 1     | 0.750      | 1/2       |
| 1/4   | 3/4   | 0.859      | 3/8       |
| 1/3   | 2/3   | 0.889      | 1/3       |
| 1/2   | 1/2   | 0.937      | 1/4       |
| 2/3   | 1/3   | 0.972      | 1/6       |
| 3/4   | 1/4   | 0.984      | 1/8       |
| 1     | 0     | 1          | 0         |

Table 4.1: Pareto Front analytical test case: minima  $OF$ s for different weight sets.

similarly to the Pareto Set, the Pareto Front is simply connected.

As reported before, the Pareto Front can be computed by finding the minima of the  $OF$  for different weights. Each minimum of  $OF$  corresponds to a point in the Pareto Front when plotted in the objectives plane: in Figure 4.3 the points are plotted with different marks, as listed in legend. Note that, for each of such points, the corresponding weights give also the values of the local tangent to the Pareto Front, as:

$$\frac{\partial F_2}{\partial F_1} = -\frac{w_1}{w_2} \quad (4.3)$$

For the points inside the Pareto Set, small variations of the  $x$  variable keep the point inner to the Set: therefore the corresponding point in the objectives space moves along the Pareto Front. In other words, *tolerances* on the design variable give no effect, in the sense that we get another Pareto optimal solution. At the boundaries of the Pareto Set and in their neighbourhood, small variations of the  $x$  variable can fall out of the Set and the solutions can become not Pareto optimal.

## 4.2 Stochastic and deterministic methods

The algorithms for the resolution of an optimisation problem can be classified in two general classes [13]: deterministic methods and stochastic methods. A method is *deterministic* if, for a given initial point (*guess*), its trajectory in the search space is predetermined and depends by the algorithm strategy: the deterministic methods find always the same solution for each instance, if they start from the same initial guess. The *stochastic* methods perform instead some kind of random walk in the search space and their results are usually non "deterministic".

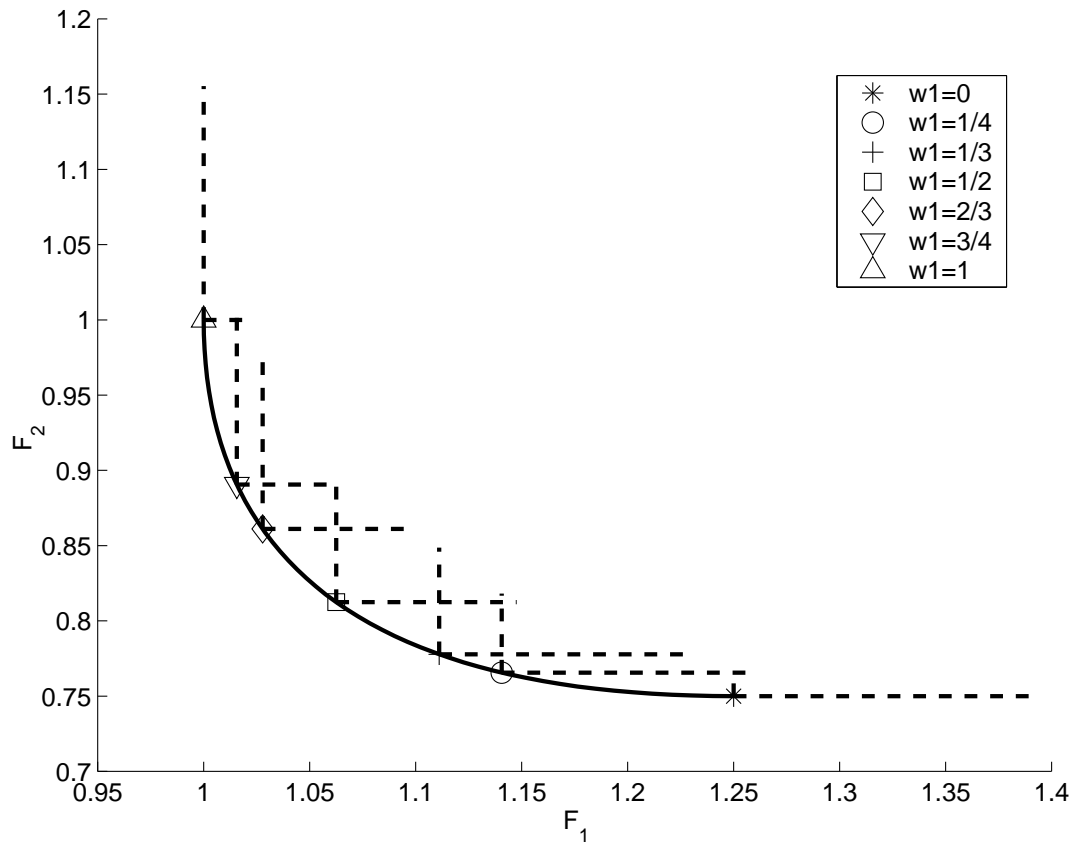


Figure 4.3: Pareto Front analytical test case: Pareto Front with MC worst cases bars in dashed lines for partial objectives.

Deterministic methods are both theoretically well analysed and numerically well tested tools to determine the optimal solution, if the starting point is chosen in an appropriate way. Stochastic methods results do not depend by a starting guess and, therefore, they can be seen as more "robust" methods for applications where no preliminary suggestions about the minimum position are provided. Sometimes a two steps strategy is adopted, with a preliminary global search by a stochastic approach followed by a deep local optimisation by a deterministic algorithm [30].

Beside evolutionary approaches widely presented in the following, Monte Carlo (MC) methods can be classified as a stochastic strategy: they employ a pure random search where any selected trial solution is fully independent of any previous choice and its outcome [31].

Optimisation methods can also be classified by the *order of the algorithm*, which is the maximum derivative order of the objective functions used by the algorithm. For simplicity, in the following I will just refer to problems defined by a scalar  $OF$ . The  $OF$  is in general not differentiable and, if its derivatives are needed, an interpolation of the  $OF$  has to be introduced by assuming some model of its local or global behaviour in the search space (for instance a quadratic model). By using zero-th methods, no derivative of  $OF$  are needed and therefore, no model of the objective function  $OF$  is established. On the other hand, the heuristic nature of these interpolating methods is reflected by a more or less large number of strategy parameters to be selected: the success of the different methods often crucially depends on the choice of these parameters.

The choice of the minimisation method follows the characteristics of the function  $OF$ , which is generally nonlinear and usually presents for industrial problems one or more of the following properties:

- Calculation of  $OF$  is very expensive or time-consuming. For example, each value of  $OF$  may be obtained by solving a costly numerical subproblem or performing a sequence of laboratory experiments.
- Exact first partial derivatives of  $OF$  cannot be calculated. Either the gradient does not exist, for example, when  $OF$  is discontinuous, or  $OF$  is defined from a complex or convoluted computational structure that obviates application of automatic differentiation techniques.
- Numerical approximation of the gradient of  $OF$  is impractically expensive or slow.
- The values of  $OF$  are 'noisy'. For example, the calculated value of  $OF$  may depend on discretisation, sampling on a grid, inaccurate data, or



an adaptively solved subcalculation (such as numerical quadrature or Finite Elements Analysis).

A possible approach to deal with the  $OF$  computational cost and with noisy data is to use curve-fitting or other data modelling techniques based on a set of evaluated  $OF$  data points to derive new simpler objective functions that represent the original ones explicitly and with acceptable accuracy. These new models are sometimes referred to as *surrogate models* or *metamodels*. Any subsequent call of the  $OF$  during the optimization phase is replaced by the surrogate models containing the explicit functions: using surrogates may reduce drastically the computational load in a large design model. When a final design is reached, the original algorithms can be used to obtain more precise estimates. Surrogate modelling methods include traditional polynomial curve-fitting techniques, as well as other employed strategies such as neural networks.

### 4.2.1 Deterministic methods

Some short references about deterministic methods are here presented: for a deeper survey see [13], [32]. Among the deterministic methods to optimise unconstrained problems, it is possible to recall the simplex algorithm and the Pattern Search method as direct search zero-order methods [33], or the Newton method as second derivative method and the Quasi-Newton method as first derivative method. When the function to be minimised has suitable smoothness properties, unconstrained problems can often be solved routinely using techniques based on Newton's method. The underlying approach is to develop a model function, usually quadratic, derived from local gradient and Hessian information about  $OF$ , and then to calculate a 'good' step based on the model. The fundamental theory of Newton-based methods has been understood for more than twenty years, although a few open issues remain. The most active areas of research about smooth unconstrained optimization today involve the large-scale case, particularly the associated linear algebraic issues. For constrained optimisation, among main techniques there are linear, quadratic or non-linear programming, where the term *programming* is historically used as synonymous for optimisation.

Deterministic algorithms are available via a number of well tested mathematical libraries, such as NAG, IMSL, Netlib (see <http://www.netlib.org>) or Matlab.

## 4.3 Evolutionary computation

Evolutionary Strategies (ES) and Genetic Algorithms (GAs) are members of a class of powerful stochastic, heuristic and adaptive procedures generally called *Evolutionary Computation* techniques, which are based on the imitation of the genetic processes of biological organisms. ES and GAs may be used to solve search and optimisation problems [11] and they are suitable for problems described by non-continuous, multimodal or multi-objective *OF*. These techniques are usually simple and robust and, like other zero-order methods, they do not require computation of the *OF* derivatives or particular knowledge about *OF* properties. ES and GAs were independently (and almost simultaneously) developed, respectively by Ingo Rechenberg [34] and John H. Holland [35].

### 4.3.1 Biological basis

The origin of Evolutionary Computation was an attempt to mimic some of the processes taking place in natural evolution.

How can be seen in Nature, biological species evolve over many generations, according to the principles of natural selection and "survival of the fittest", first clearly stated by Charles Darwin in *The Origin of Species*. By mimicking this process, ES and GAs are able to "evolve" solutions to real world problems, if they have been suitably encoded.

Although the details of biological evolution are still not completely understood, there exist some fixed points supported by a strong experimental evidence:

- **Evolution** is a process operating over chromosomes rather than over organisms. The chromosomes are organic *tools* encoding the structure of a living being, *i.e.* a creature is "*built*" decoding a set of chromosomes.
- **Natural selection** is the mechanism that relates chromosomes with the *efficiency* of the entity they represent, thus allowing those efficient organisms, which are well-adapted to the environment, to reproduce more often than those which are not.
- The evolutionary process takes place during the **reproduction** stage. There exists a large number of reproductive mechanisms in Nature. The most common ones are **mutation** (that causes the chromosomes

of offspring to be different from those of the parents) and **recombination** (that combines the chromosomes of the parents to produce the offsprings).

## 4.4 Genetic Algorithms

Among the evolutionary techniques, the Genetic Algorithms are the most extended group of methods representing the application of evolutionary tools. They rely on the use of selection, crossover and mutation operators. Replacement is usually performed by generation of new individuals.

A GA proceeds by creating successive generations of better and better individuals by applying very simple operations. The search is only guided by the *fitness* value associated to every individual in the population: this value is used to rank individuals depending on their relative suitability for the problem being solved.

The process starts with a randomly generated population of *individuals* (or *phenotypes*), each one made by strings of the design variables, representing a set of points spanning the search (or design) space. Each individual is suitably coded into a *chromosome* (or *genotype*) made by a string of *genes*: each gene encodes one of the design parameters, by means of a string of bits, a real number or other alphabets.

New individuals (or *offsprings*) are then generated by using some genetic operators, the classical ones being the *crossover* (or recombination) and the *mutation*. The crossover operator combines two chromosomes to generate an offspring, while the mutation operator randomly changes some of the genes of a chromosome. The probability of survival of the newly generated individuals depend of their *fitness*: the individuals with higher fitness values are kept in the population for further mating and reproduction and those with lower fitness are discarded.

### Historical perspective

Here the main steps in the Genetic Algorithms history are presented, since their birth in 1962 by the hand of John H. Holland. Before that date, some attempts were made in modelling genetic systems by computer models (see A. Fraser in 1957 [36]): however the fundamental objective of these studies was to understand some biological phenomena. Holland and his students in the University of Michigan were the first to recognize the usefulness of using genetic operators in artificial adaptation problems. In 1971, John Holland sets the basis for the theory behind the use of Genetic Algorithms with the

*Schema Theorem.* In 1975 two important works were published: "Adaptation in Natural and Artificial Systems" of Holland [35] and "An Analysis of the behavior of a class of Genetic Adaptive Systems" of Kenneth De Jong [37], a Holland's student: these works served as a base for the vast majority of subsequent studies. In 1989, David Goldberg published "Genetic Algorithms in Search, Optimization and Machine Learning", a reference book for Genetic Algorithms [38]. In the present, GAs are reaching their adult phase, being used in several applications in different fields, especially where "conventional" methods are not applicable.

### Traditional GAs

A GA is defined by the following components, functions and parameters [38]:

- the search space (*i.e.* the space of *phenotypes*);
- the representation space (*i.e.* the space of *genotypes*), including alphabet and string length of genotypes;
- the mapping from phenotypes to genotypes spaces;
- the fitness function;
- the size of the population;
- the strategy for the initialization of the population;
- the selection mechanism (*e.g.* roulette wheel, ranking, tournament);
- the percentage of the population genetically operated on and inserted back;
- the genetic operators (including crossover and mutation) with their parameters (*e.g.* the probability of application);
- the replacement policy (*e.g.* worst, random);
- the termination criterion (*e.g.* predefined number of steps, stagnation).

The three commonly used methods for individuals selection are [39]:

1. *Random wheel*: in this scheme the probability of selection for each chromosome is proportional to its fitness.

2. *Ranking method*: chromosomes are sorted based on their fitness values and probabilities of their selection are fixed for the whole evolution process.
3. *Tournament selection*: a selected number of chromosomes is chosen randomly and then the chromosome with the best fitness in this group is selected.

A *traditional GA* works on binary strings of fixed length and applies random wheel selection, one point crossover and bit-flip mutation [35]. The initial population is generated by following an uniform random distribution, that is, every position in every string contains one 0 or one 1 with the same probability. The evolution model is represented by successive generations of populations, *i.e.*, a new population completely replaces the old one. The algorithm stops when a predefined number of generations have been reached. Finally the evaluation of any given string is made by mapping the genotype to the phenotype by means of a binary-to-decimal operation for every group of bits of the genotype representing one problem parameter.

The notion of evaluation and fitness are sometimes used interchangeably. However, it is useful to distinguish between the evaluation function (*i.e.* the objective function of the problem to be minimised) and the fitness function used by a genetic algorithm. The evaluation function provides a measure of performance with respect to a particular set of parameters. The fitness function transforms that measure of performance into an allocation of reproductive opportunities. The evaluation of a string representing a set of parameters is independent of the evaluation of any other string. The fitness of that string, however, can be defined with respect to other members of the current population. In the canonical genetic algorithm, fitness is defined by:

$$fitness = \frac{1}{OF_i} \quad (4.4)$$

where  $OF_i$  is the value of the  $OF$  associated with string  $i$ . Another possible definition is:

$$fitness = \frac{OF_{mean}}{OF_i} \quad (4.5)$$

where  $OF_{mean}$  is the average evaluation of all the strings in the population.

The computational effort in a GA usually resides in the evaluation of the fitness function of the initial and new strings. Operators like selection, mutation, crossover or replacement are of linear complexity and work at constant rates for a given problem

#### 4.4.1 Constraints handling in GAs

GAs are essentially unconstrained search techniques but most real life design problems involve constraints. Therefore there have been a number of approaches to handle constraints in GAs: a survey of methodologies is presented in [40]. Care must be taken in the choice of the method: the search can be extremely difficult in non-convex feasible regions especially if the optima are near the infeasible region.

The simplest approach has been to assign an arbitrarily low fitness to infeasible individuals [41]. An interesting attempt to incorporate the knowledge of constraint satisfaction during the selection phase was proposed in [42]: to match *the beauty with the brain*, constraints matching was employed during partner selection for crossover.

However the most used strategies are penalty functions (already defined in Section 3.6), where solutions with constraint violations are penalized. The naive method requires user to supply penalty parameters, which are usually difficult to set. Moreover, the performance of this approach largely depends on the penalty parameters used. Beside a number of dynamically updated penalty parameter approaches [43], a penalty parameter-less GA is suggested in [44].

Different forms of the penalty functions have been proposed. In [45] the following one is presented (supposing to have just greater-than-or-equal-to type constraints  $c_i$ ):

$$P_i(\mathbf{x}) = \begin{cases} 0 & \text{if } c_i(\mathbf{x}) \geq 0 \\ a_i [1 + c_i(\mathbf{x})] & \text{else} \end{cases} \quad (4.6)$$

This function enforce the penalty to allow some infeasible points near the constraint boundary to have fitness values which are competitive with nearby feasible points. These infeasible points may contain genetic information (as building blocks or *schema*) that is necessary to find the optimum, so it is important to allow these points a chance to survive [38]. However, it is also necessary that the final design be feasible.

Therefore a fundamental tradeoff to be considered, when using a penalty function, lies in the proper choice of the draw-down coefficient  $a_i$ , which is often arbitrary: a small coefficient will impose a smaller penalty than a large coefficient for the same magnitude of constraint violation. In the GA, a large penalty (resulting in a poor fitness) can quickly eliminate infeasible solutions from the search. Conversely, using a small draw-down coefficient may allow the survival of infeasible designs to the extent that the population converges at an infeasible point as the optimal fitness solution. Clearly, a compromise must be struck between these two extremes. The goal of an

adaptive penalty function is to change the value of the draw-down coefficient during the search allowing exploration of infeasible regions to find optimal building blocks, while preserving the feasibility of the final solution.

Two basic forms of draw-down coefficient strategies can be identified: generation number-based and population fitness-based.

- The *generation number-based strategies* increase the value of the draw-down coefficient with successive generations.
- The *fitness-based strategies* are meant to increase the penalty coefficient when the population fitness is diverse, causing the population to move toward an optimal feasible design; and to decrease the coefficient when the population begins to become homogeneous, allowing some infeasible designs with important design information to survive. These forms can use the variance of the population's fitness values.

In [44] another approach is presented, based on a penalty function which does not require any penalty parameter: a pairwise comparison is exploited to make sure that:

1. when two feasible solutions are compared, the one with better objective function value is chosen;
2. when one feasible and one infeasible solutions are compared, the feasible solution is chosen;
3. when two infeasible solutions are compared, the one with smaller constraint violation is chosen.

The resulting objective function (3.16), modified by this penalty function, is then defined as:

$$\Phi(\mathbf{x}) = \begin{cases} f(\mathbf{x}) & \text{if } c_i(\mathbf{x}) \geq 0 \\ f_{\max} + \sum_i \langle c_i(\mathbf{x}) \rangle^2 & \text{else} \end{cases} \quad \forall i \quad (4.7)$$

where the operator  $\langle \ \rangle$  returns the operand, if the operand is negative and returns a value zero, otherwise. The parameter  $f_{\max}$  is the maximum function value of all feasible solutions in the population: therefore objective function of an unfeasible solutions not only depends on the amount of constraints violations but also on the population of solutions at hand.

An alternative approach to handling constraints in GAs is to *repair* or to cancel infeasible solutions. After an individual has been generated during the population initialization, crossover or mutation phases, if it is an unfeasible

one, it is wiped out and substituted by new individual, which can be created by scratch or by using some pre-evaluated "gene pool" [46].

Constraints can be also handled as objectives as presented in [47] for multi-objective Pareto GAs.

#### 4.4.2 Initial population selection

To increase the efficiency of GAs in terms of quality of the final solution found and of the computing burden, the set up of a "good" initial population is an important topic to deal with. The generated initial individuals should, in general, satisfy the problem constraints and efficiently span the search space. The generation can be performed randomly or by using some heuristic problem-specific approaches [48].

##### Adopted strategy

The recalled concept of avoiding unfeasible solutions has been here adopted, mainly for problems with a large number of constraints. Usually the constraints satisfaction test of an individual is much more less computationally time-consuming than the  $OF$  evaluation: therefore it is important to check the constraints before performing the  $OF$  computing.

An iterative procedure has been exploited to randomly generate (with an uniform PDF) all individuals inside the admissible range for each parameter: if an individual does not satisfy the constraints, it is substituted by a new individual until a good feasible one is found, without evaluating the  $OF$  and saving therefore a great computing load. In this phase, the available knowledge about the problem at hand is also exploited: the problem parameters can be correlated (for instance, there could be some implicit geometric relations among parameters), therefore their generation has to suitably performed. After the initial population has been created, the fitness of each individual is evaluated.

#### 4.4.3 Evolutionary stall

As already recalled, GAs are more robust than deterministic search strategies. However, if multiple minima are present, also the GAs can fall and be trapped in a local minimum. In this case, the evolution of the population can arrive to a situation of *stall* or premature convergence, where neither crossover nor individuals mutation can improve the mean population fitness or the best individual. To avoid the stall, the genetic diversity of the population has to be saved during the evolution: a possible way is to use a proper population



size or to adopt a *hill-climbing* strategy. In addition, the termination criterion has to be able to discriminate between the stall and the finding of the wanted problem optimum.

#### 4.4.4 Meta-optimisation of GAs

It is clear that Genetic Algorithms performances and their ability to solve our problems depend by a number of parameters which has to be properly set. This task belongs to the meta-optimisation of the algorithm. Parameters like the population dimension, the selection strategy, the crossover and mutation probabilities, the stopping criterium are key points for the GAs behaviour.

#### No Free Lunch Theorem

It is not useful to look for "general problem" evolutionary parameters. The recent so-called "No Free Lunch" (NFL) theorem by Wolpert and Macready [49] proves the following result:

*There is no universal genetic parameters setting for GA and there is no universally best method for optimisation i.e. there is no method that will in all cases outperform other methods.*

The simple corollary of the NFL theorem is that, averaged on the class of all functions, no algorithm performs better than random search. On the other hand, the result of NFL theorem is "too general" and mostly theoretically important: we do not need an algorithm which will outperform all other algorithms on all functions. Desired is a better performance on a certain class of functions. In order to achieve this, careful choice of operators and parameters is needed. In particular, the optimal values of the genetic operators probability of application is specific for the particular problem at hand.

### 4.5 Proposed and implemented strategies

In this section, the strategies implemented in the Thesis to increase the efficiency of the GA and the quality of the found solution are presented.

#### 4.5.1 Operators adaptation and hybrid GA

During the GA evolution, it is generally useful to change the genetic operators probabilities [50]: in the early evolution steps, the genetic diversity of the

individuals is high and the crossover operator should have a high probability of application to efficiently mix this inheritance and therefore to widely span the search space. In this phase the mutation operator should be not often applied to not destroy useful genes. On the other hand, during the last part of the evolution, the genetic diversity is low because all individuals have been attracted by a (hopefully global) minimum: the mutation operator achieves therefore a more important role while the crossover is no more able to get new genetic information. Following the previous comments, the application probabilities of the crossover and mutation operators are varied in opposite way: the crossover probability decreases during the evolution, while the mutation probability increases. The change of probabilities can be previously fixed or self-adapted during run-time. The two implemented strategies are:

**Self-adapted operators probabilities** The evolution of the population is monitored and the operators probabilities are adapted during the evolution process to improve the rate of convergence and to escape from both the local minima and from too early convergence: for an example, if a stall condition is detected, the probability of mutation increases. As an index of the evolution, the generational finite increment, defined later (see definition 5.4), can be used.

**Deterministic mutation** A local minimum hill-climbing deterministic step is introduced: it is a directional mutation operator, that forces mutation in the opposite direction of the maximum gradient. This operator can be used when it is possible to get the gradient, by using the analytical derivative of the  $OF$ , when available, or by a numerically computed derivative in other cases.

### 4.5.2 Optimal design and uncertainties

The actual construction of a device solution selected by some optimisation strategy is generally different from the design one due to material or geometrical tolerances: the final values of the device parameters are different from the nominal ones and therefore the real device performances are in general worse than expected [51]. In addition, during the working conditions, the generated magnetic forces can deform the device geometry with the consequence that the working point is different from the design one [52]: for example, during the first charging cycles of a magnet, the coils naturally perform some small positioning adjustments (this is called the magnet *training*). These effects, as the mechanical and assembling tolerances, are usually modelled through random variables with Gaussian PDF: in all cases, a device performances degradation has to be expected.

It can be shown that some design solutions are more sensible with respect to the performances to little changes in the device parameters than other ones. Therefore it is useful for the designer to use some tool capable to evaluate the sensitivity of a design solution to construction errors [53], [54], [55].

After the optimisation procedure has provided one or more candidates for the design problem at hand, a post-processing phase can be applied to rank the different solutions against their sensitivities.

A design solution is defined *robust* when it is not very sensible to the variation of the construction parameters in a neighbourhood of their nominal values. The neighbouring region can be identified with the *tolerances range*, which is the interval of possible variation of each design parameter during the construction phase.

From this statement, it follows that can be preferred a solution characterised by a worse *OF* value than other configurations, if it is more robust.

### 4.5.3 Increasing the robustness of the design solution

The principal aim of this section is to shown as the effects of the uncertainty due to the manufacturing tolerances can be efficiently considered in an automatic fashion if it is included in the objectives a suitable term related to parametric sensitivity of performances.

The *OF* definition is modified in such a way to take into account some information about the behaviour of the *OF* in a neighbourhood of the candidate solution, defined by the expected uncertainty on the geometrical parameters.

When dealing with uncertain parameters values, the evaluation of the *OF* can be substituted by a modified  $\overline{OF}$  defined as the expected value of *OF* in the neighbourhood  $\Omega(\mathbf{x})$  of the nominal device configuration  $\mathbf{x}$  (the tolerances range):

$$\overline{OF}(\mathbf{x}) = \int_{\Omega(\mathbf{x})} p(\mathbf{x}') OF(\mathbf{x}') d\mathbf{x}' \quad (4.8)$$

where  $p(\mathbf{x}')$  is the probability density of the occurrence of the configuration  $\mathbf{x}'$ . Here a Gaussian PDF is adopted.

The integration of (4.8) for a multi-variable general PDF requires suitable integration techniques to be adopted, because the computational cost of multidimensional integration increases exponentially with the search space dimensionality (this phenomenon is referred as "the curse of dimensionality" [56]). A simple possible, but computationally heavy, approach for multiple design variables is to consider statistical independence among tolerances,

assuming the joint probability  $p(\mathbf{x})$  is the product of the single marginal probabilities  $p_i(x_i)$  of each parameter:

$$p(\mathbf{x}) = \prod_i p_i(x_i) \quad (4.9)$$

Due to technological and constructive issues, there could be some dependence among design parameters or tolerances caused by machine tools and construction methodologies: in these cases, the number of independent parameters decreases as the joint PDF should no longer be considered the product of marginal PDF, leading to a reduction of the computational cost for evaluation of (4.8). As an example, for MRI magnets the minimum radius of the coils wound in the drum caves are subjected to the same tolerance. The exploitation of such concepts provide a better exploration of the search space in the neighborhood of each design trial solution: the integration points for (4.8) can be reduced by locating them only in a subregion of  $\Omega(\mathbf{x})$  while keeping the same accuracy.

In the following, a one-variable SOP will be considered. A confidence interval of 99% is adopted (*i.e.* the percentage of times in repeated sampling that the interval contains the true value of the unknown parameter  $x$ ). By using the *error function*  $erf$  defined as:

$$erf(x) = \frac{2}{\sqrt{\pi}} \int_0^x e^{-t^2} dt \quad (4.10)$$

the probability (3.8) for an interval  $]-\Delta x, \Delta x]$  with a standard normal PDF can be expressed as [16]

$$P(-\Delta x, \Delta x) = erf\left(\frac{x}{\sqrt{2}}\right) \quad (4.11)$$

By the previous definitions, the root  $x'$  of the equation:

$$erf\left(\frac{x}{\sqrt{2}}\right) = 0.99 \quad (4.12)$$

is the upper limit of an interval corresponding to a 99% confidence for the standard distribution. By using the variable substitution  $\frac{x}{\sigma} = t$ , this interval corresponds to the wanted interval limit  $\Delta x$  for a Gaussian distribution with mean  $\mu = 0$  and standard deviation  $\sigma$  computed as

$$\sigma = \frac{\Delta x}{x'} \quad (4.13)$$

The probability density  $p(x)$  is truncated at the tolerance range  $]-\Delta x, \Delta x]$  and then normalised with the area inside the confidence interval.

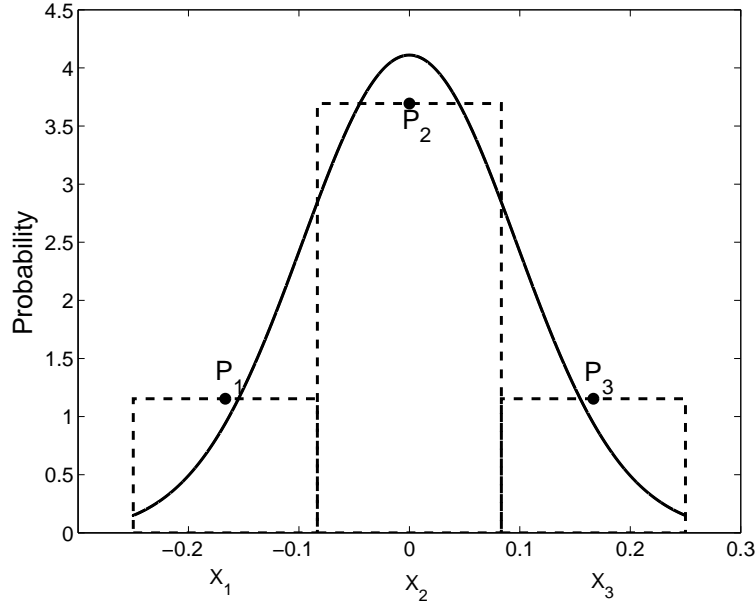


Figure 4.4: Continuous (continuous line) and discrete (dashed line) probabilistic density functions.

To be applied in the framework of an automatic optimisation procedure, (4.8) has to be properly discretised. Different approaches can be used for the approximate evaluation of (4.8). Here, for the one-variable case, the integral is evaluated by the rectangular rule with three equally spaced points  $x_1 = -\frac{2}{3} \Delta x$ ,  $x_2 = 0$ ,  $x_3 = \frac{2}{3} \Delta x$  (Figure 4.4). The discretised probabilistic densities (usually referred as Probability Mass Functions or PMF) is evaluated in such a way to conserve the total area. By using the CDF defined in (3.7), the points  $P_i$  are defined as:

$$\begin{aligned}
 P_1 &= \frac{F(-\frac{\Delta x}{3}) - F(-\Delta x)}{\frac{2}{3} \Delta x \text{ Area}} \\
 P_2 &= \frac{F(\frac{\Delta x}{3}) - F(-\frac{\Delta x}{3})}{\frac{2}{3} \Delta x \text{ Area}} \\
 P_1 &= P_3
 \end{aligned} \tag{4.14}$$

where *Area* is the area below the PDF in the tolerances range, equal to the wanted confidence:

$$\text{Area} = F(\Delta x) - F(-\Delta x) = 0.99 \tag{4.15}$$

Finally the  $\overline{OF}$  can be expressed as a weighted sum in the three integration points  $x_i$ :

$$\overline{OF}(x) = P_1 OF(x_1) + P_2 OF(x_2) + P_3 OF(x_3) \quad (4.16)$$

where the weights  $P_i$  have been normalised with respect to their sum.

### Developed software

By using the Matlab language, a code has here been developed to implement the previous concepts. The software is built on the *MATLAB Genetic Algorithm Toolbox* [57] by the Automatic Control and Systems Engineering Department of the University of Sheffield (UK). The toolbox is available at the Department web site [58] under the GNU licence. The GA Toolbox ver. 1.2 supports (*not parallel*) multi-populations with migrations and binary, integer and floating-point chromosome representations. A code fragment to compute the weights  $P_i$  is reported in Appendix A.1.

### A demonstration example

To illustrate the previous considerations, a very simple example is here presented. Let's consider a problem characterised by two objectives (  $\cos(x^3)$  and  $-x$  ) depending by just one parameter  $x$ . By assuming the weights equal respectively to 1/2 and to 1/5, we express the following analytic  $OF$  (Figure 4.5):

$$OF(x) = \frac{\cos(x^3)}{2} - \frac{x}{5} \quad (4.17)$$

The function (4.17) is characterized by two minima in the range  $[0, \sqrt[3]{4\pi}]$ , with the lower one (**B** in Figure 4.5) located in a narrower and steeper "valley" than the other minimum (**A**). It is assumed that the parameter  $x$  is affected by an uncertainty characterised in the range  $\Delta x = [x - 0.25, x + 0.25]$  by a Gaussian PDF with a confidence range=0.99 and a variance  $\sigma = 0.0971$ . By discretising the (4.8) with the previous technique, the  $OF$  has been modified as in (4.16) and it is plotted with dashed line in Figure 4.5. The three weights in (4.16) are:

$$P_1 = P_3 = 0.1922 \quad P_2 = 0.6156 \quad (4.18)$$

It can be observed that, in the modified  $\overline{OF}$ , the positions of the two minima move very slightly but the *more robust* point **A** becomes the new global minimum.

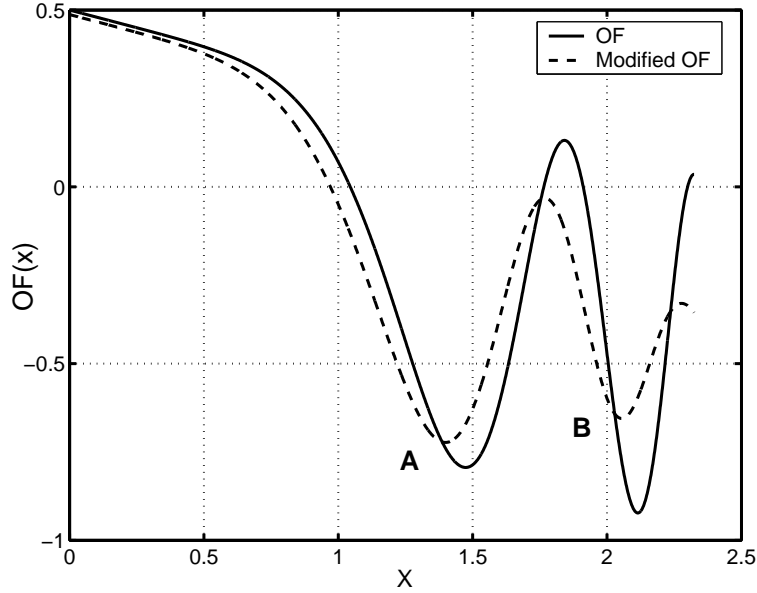


Figure 4.5: Robust Objective Function for the demonstration example.

#### 4.5.4 Sensitivity analysis

To evaluate the impact of mechanical tolerances on the actual device performance, two possible directions can be followed: *Sensitivity Analysis* (SA), and *Worst Case Analysis* (WCA). While SA is quite diffused in electrical engineering, WCA, which is a quite common tool in other field of engineering, deserves some further investigation.

SA is based on the evaluation of the  $OF$  partial derivatives with respect to the manufacturing input parameters. The partial derivatives, evaluated for an optimal configuration, can be estimated either using the raw "finite difference" method or by well-known methods such as the adjoint variable or the  $OF$  interpolation with multi-quadrics or splines approaches [59].

On the other hand, WCA is mainly aimed to effectively probe the constructive uncertainties distributions in order to localize the potentially most critical realization (worst case) of the device around the nominal design, in order to assess the performance of the actual device and to tune a possible correcting tool. Due to the large number of the design parameters in the usual engineering design problems, the principal methodology of probing the parameters space is a Monte Carlo analysis. The MC analysis is performed with the random generation of a quite large number of design configurations characterised by simultaneous variations of the parameters within the tol-

erance ranges centered on the reference design, possibly resulting from an optimisation procedure. This is typically a post-processing step. Note that, while the common methodologies to perform SA are based on the knowledge of  $OF$  derivatives, the MC analysis has the advantage on other methods of not requiring the computing of any derivatives.

MC makes available a large number of cases, that can be used, apart from performing WCA, also to evaluate the statistical properties of some further "performance index" characterizing the device: MC analysis provides therefore a number of information useful to evaluate the robustness of a design solution, such as correlation indices between the design objectives and the input parameters.

### Evaluation of the $OF$ gradient

The SA is usually performed through the evaluation of partial derivatives of the design performance. Sometimes, in the phase of the design process after the optimisation, some fixed parameters, not included in the previous optimisation phase, may be included or some constraints on the DOF can be released: in these cases, the  $OF$  derivatives are not all vanishing, although evaluated in the proximity of an optimum. In addition, the solution from a stochastic optimiser not always is a local minimum even if it is close to it: so first partial derivatives can be different from zero.

Unfortunately, typical approaches to compute the  $OF$  derivatives can be performed only if the dependence of the  $OF$  on the design parameters is regular enough, and of course do not apply straight to parameters not considered in the optimisation phase. In addition, the device sensitivity with respect to fixed parameters must be evaluated from scratch, as no information is available on this relationship at the end of optimisation process.

In the choice of a strategy to evaluate the partial derivatives, it is also important to remind the characteristics of the  $OF$ s usually involved in electromagnetic optimisation. These  $OF$ s can be not differentiable or discontinuous with steep behaviour in the neighbouring of a local optimum: the usual methods can therefore fail.

A different approach is here presented to performs SA with respect to both fixed parameters and DOF by using MC analysis. After a MC analysis, for instance used to perform a WCA, a random sampling of the  $OF$  centered on a reference device configuration is available. An analogue situation can happen after an evolutive optimisation, when the final population is usually clustered around the best individual. In both situations, the MC analysis and the evolutive optimisation, a quite big number of samples of the  $OF$  is available "for free" [60].



By expanding at the first order in Taylor series the  $OF$  starting from the reference configuration  $\mathbf{P}_0$  and by using the  $m$  already computed values of the  $OF$  in the MC points  $\mathbf{P}_i = [P_{i,1}, \dots, P_{i,n}]$  in a neighbourhood of  $\mathbf{P}_0 = [P_{0,1}, \dots, P_{0,n}]$ , it is possible to assemble the following overdetermined linear system for the unknown  $OF$  gradient:

$$\mathbf{A}\mathbf{x} = \mathbf{b} \quad (4.19)$$

where:

$$\begin{aligned} x_j &= \frac{\partial OF}{\partial P_{0,j}} && \text{are the components of the } OF \text{ gradient } \mathbf{x} \text{ in } P_0, \\ A_{i,j} &= P_{i,j} - P_{0,j} && \text{are the coefficient matrix } \mathbf{A} \text{ terms,} \\ b_i &= OF(\mathbf{P}_i) - OF(\mathbf{P}_0) && \text{are the known values,} \\ &&& \text{and } i = 1, \dots, m \end{aligned}$$

The "best fit"  $\mathbf{x}$  solution of the overdetermined linear system (4.19), representing the first order partial derivatives of  $OF$  in the reference point  $P_0$ , is obtained by computing the pseudoinverse of the rectangular  $m \times n$  matrix  $\mathbf{A}$  by singular value decomposition (SVD).

### Sensitivity analysis of the Rastrigin function

In order to test the previous sensitivity extraction method, the Rastrigin function, presented in Section 3.7.1 has been considered with three variables ( $n = 3$ ). The point  $P_0 = [1.1, -0.1, 0.1]$ , close to the local minimum  $[1, 0, 0]$ , has been considered to evaluate the function gradient.

The Monte Carlo analysis has been started around the point  $P_0$  with 500 sample points randomly generated with a Gaussian distribution with  $\mu = 0$  and standard deviation  $\sigma$  computed as in (4.13) inside a tolerance range of  $[P_0 - 0.01, P_0 + 0.01]$  with a confidence range=0.99.

The coefficients of the Taylor expansion have then been reconstructed using the MC data, as in previous section. In Table 4.2 is reported a comparison between the SVD computed derivatives and the analytical ones: the MC computed results show a good agreement within 0.4 % with the exact data.

### 4.5.5 Monte Carlo analysis and Pareto Front

When the Pareto Front of the optimisation problem is available, it is possible to carry out a MC analysis to test the robustness of the Pareto optimal solutions. Here a MC analysis is performed for the analytical test case presented in Section 4.1.1, by starting from each point of the Pareto Set, which

| Variable | SVD $\frac{\partial F}{\partial x_j}$ | Analytical $\frac{\partial F}{\partial x_j}$ | Difference % |
|----------|---------------------------------------|--|--------------|
| $x_1$    | 39.1316                               | 39.1263                                      | 0.0137       |
| $x_2$    | -37.1316                              | -37.2485                                     | 0.3138       |
| $x_3$    | 37.1316                               | 37.0192                                      | 0.3038       |

Table 4.2: Comparison between SVD computed (with 500 samples) and analytical derivatives for the Rastrigin function.

is randomly perturbed inside the tolerance range. The mean values and the variance of the partial objectives in the perturbed configurations are then used to assess the sensitivity of that particular configuration. In addition, the WCA gives the (approximate) worst cases of the partial objectives for each Pareto solution: after such a piece of information is known, it is possible to judge how far from the nominal performance will be, in the worst case, that particular optimal solution and to tailor consequently possible correction systems (*e.g.* shimming coils for high uniformity magnets).

This analysis can help to compare different Pareto solutions from the actual performance point of view, not only on the basis of the "nominal design". Note that the values of the partial objectives for the all perturbed configurations lie on the same side of the Pareto Front: following the definition of Pareto Set, there are no configuration with lower values of all objectives than a Pareto point. The worst cases can be plotted in the objectives plane to get uncertainty intervals for points alongside the Pareto Front and, for each objective, the width of the intervals is a direct measure of the sensitivity of a Pareto solution to the construction tolerances.

MC analysis has been performed for a tolerance of 5% on the design variable with 2000 runs for each point of Pareto Front. The worst cases for the two partial objectives are reported as error bars for each Pareto points in Figure 4.3. These figures help understanding the diverse sensitivities of the partial objectives at different Pareto Front points: they are somehow similar to the sensitivity ellipsoids presented in [60]. As an example, it is possible to observe that the sensitivity of  $F_1$  is much higher in points with small values of  $w_1$ . If needed, a more detailed perspective about the effect of uncertainties can be obtained by analysing the statistical behaviour of the different objectives around a particular solution (or, in other words, around a particular point of the Pareto Set).

Finally, it can be useful to have an understanding of the behaviour of the statistical parameters resulting from MC analysis when moving along the Pareto Front, in order to help selecting the most promising region. As an example, the PDF for the point of Pareto Front obtained with a weight

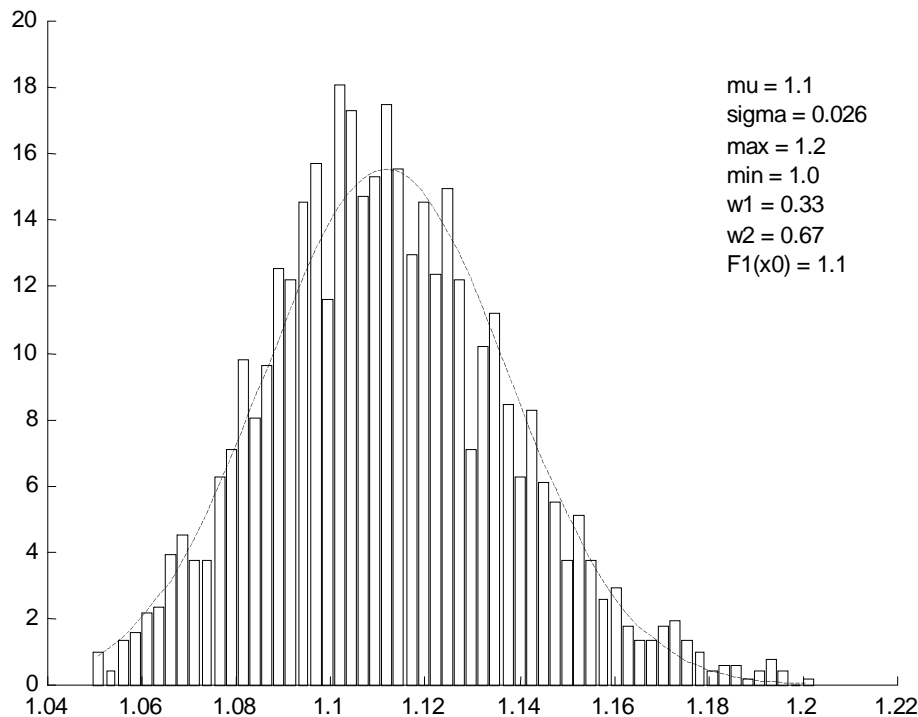


Figure 4.6: Pareto Front analytical test case: PDF of objective  $F_1$  for  $w_1 = 1/3$  and the Gaussian distribution with the same mean and standard deviation (in dashed line).

$w_1 = 1/3$  is reported in Figure 4.6 for the objective  $F_1$  and in Figure 4.7 for the objective  $F_2$ . The mean  $\mu$  and standard deviation  $\sigma$  of the objectives PDF are also computed and in Figure 4.6 and in Figure 4.7 the Gaussian distribution with such values of  $\mu$  and  $\sigma$  are also plotted.

In Figure 4.8 the standard deviations of  $F_1$  and  $F_2$  is plotted versus the corresponding values of the weight  $w_1$ : the monotonic decrease of the  $\sigma$  with increasing  $w_1$  weight suggests to select high values  $w_1$  if the objective  $F_1$  is the most critical one and vice-versa, to get small values of  $\sigma$  and therefore low solution sensitivity.

## 4.6 Appendix: the Nash equilibrium

In a multi-objective optimisation the goal is to find a good "equilibrium" point among different wanted objectives.

The situation is similar to a game theory concept, introduced by the

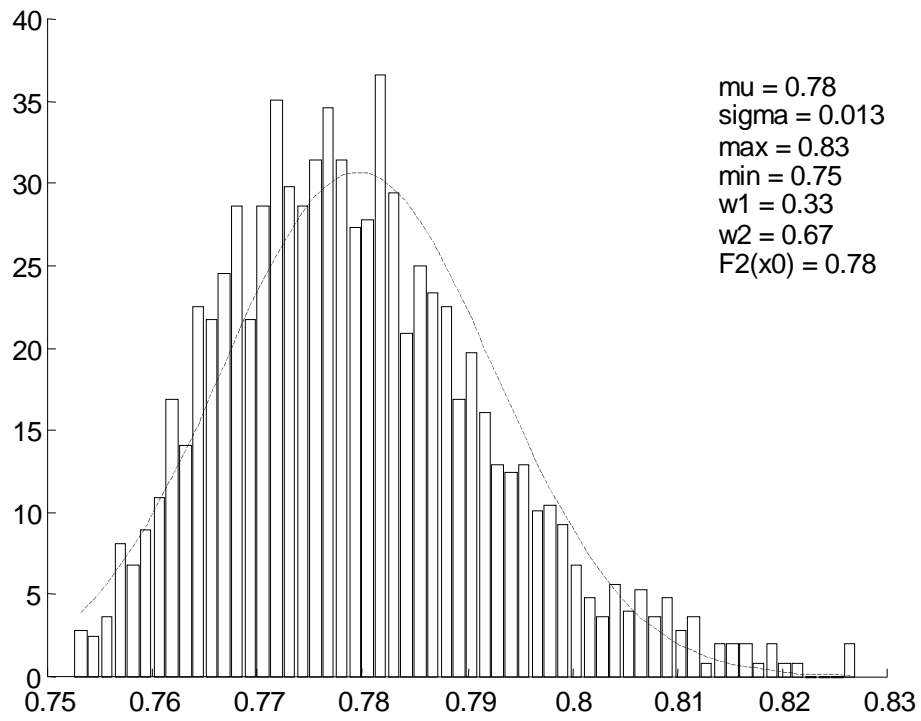


Figure 4.7: Pareto Front analytical test case: PDF of objective  $F_2$  for  $w_1 = 2/3$  and the Gaussian distribution with the same mean and standard deviation (in dashed line).

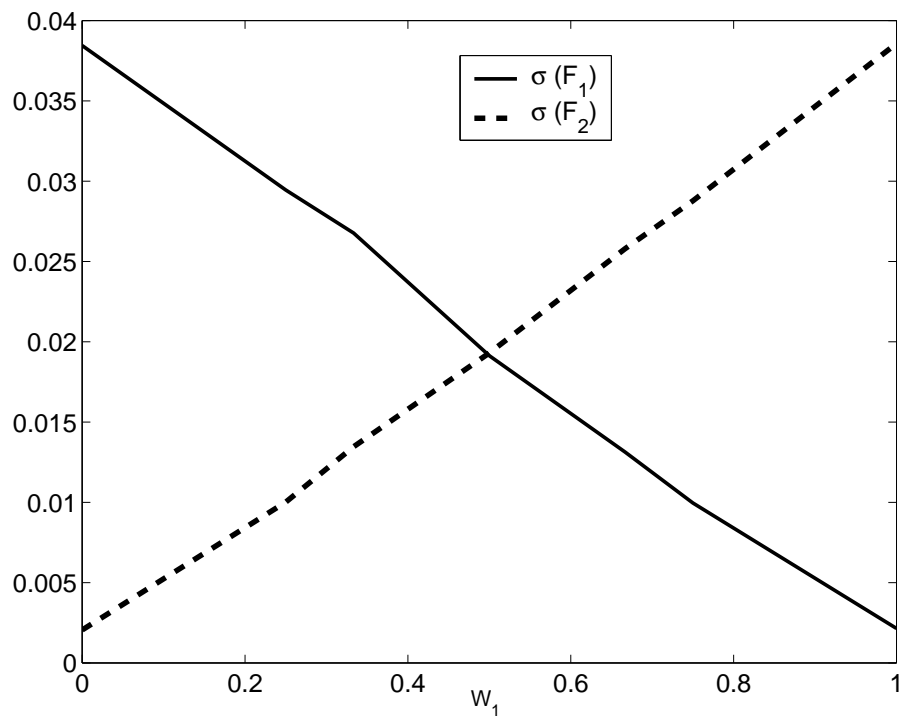


Figure 4.8: Pareto Front analytical test case: plot of standard deviation  $\sigma$  of objectives  $F_1$  (continuous line) and  $F_2$  (dashed line) versus weight  $w_1$ .

mathematician John Forbes Nash Jr. and therefore called "Nash equilibrium" [22]. A set of game strategies is a Nash equilibrium just in case no player could improve his payoff, given the strategies of all other players in the game, by changing his strategy. In a Nash equilibrium, all of the player's expectations are fulfilled and their chosen strategies are optimal.

On the cooperative game theory is based an approach of solving the multi-objective optimization problem with the search for Nash equilibrium points [23]. In a cooperative game, the players agree to cooperate with each other and each player corresponds to an objective.

Also the so-called evolutionary games are based on the Nash equilibrium concept. This type of games has been developed in biology in order to understand how the principles of natural selection operate in strategic interaction within and among species.

# Chapter 5

## Parallel Genetic Algorithms

*Life results from the non-random survival of randomly varying replicators.*  
(A sentence the evolutionist Richard Dawkins wrote to be put on a T-shirt.)

In this chapter, the main issues of parallel computing and its application to electromagnetics and optimal design are recalled. Then the parallel Genetic Algorithms are described and the implemented Island Parallel Model is introduced together with the evolution metric and population operators.

### 5.1 Computational Electromagnetics and Parallel Computing

COMPUTATIONAL ELECTROMAGNETICS (CEM) requires high computing power both in terms of hardware than in terms of algorithms and solving paradigms. Today many fields of computational physics, such as fluid dynamics, currently adopt parallel computing to simulate near-real-world cases (*e.g.* the shape optimisation of complete aircrafts) while in CEM the use of parallel computing is not so widely diffused [61] but in some military application (*e.g.* stealth technologies in the high frequencies sector and magnetic signature detection of submarines in low frequencies).

There are many reasons for this delay in CEM use of parallel computing. One reason is certainly due to the fact that field problems are generally neither confined to a structure nor set in very regular domains. The geometries involve substantial details and the domains of study have often to be considered to infinity: the needed spatial resolution spans many order of magnitudes increasing the numerical difficulties in recognising parallel tasks. Some examples of recent parallel CEM papers are in [62] and [63].

In addition, I think this situation is also partially due to the availability in electromagnetics of efficient simplified models, which can be used to solve many typical problems. Other important issues are the usual quite high costs of parallel computing, in terms of required computing resources and human investment.

### 5.1.1 Present trends in parallel computing

The past situation has been recently changed. Today parallel computing is no more restricted to huge expensive mainframes but low-cost parallel cluster high-performances machines can be directly assembled by an university department with a cost at the level of its normal research budget. Therefore new perspectives are at hand and new problem solving strategies and approaches can be explored.

At the moment, such cluster machines still require the knowledge of message passing programming model, which is not very easy to use: in fact, sometimes the message passing is called the "machine language" of parallel computing. In the near future, with the availability of faster network links among computing nodes, it will be possible to adopt easier programming models, such as the virtual shared memory environment [64].

In last years the CEM community began to use these new parallel computing machines to increase performances of existing algorithms requiring long computing time, such as the ones used in optimal design and field computation [65], [66], [67], [68].

## 5.2 Parallel Genetic Algorithms

The Genetic Algorithms are generally able to find good solutions in reasonable amounts of time, but as they are applied to larger and harder problems, like the electromagnetic optimal design, the time required to find adequate solutions can become very long. Therefore there have been multiple efforts to make GAs faster and one of the most promising choices is to use parallel implementations [69]. GAs structure is inherently parallel: the simultaneous search for different points in parameters space could be thus naturally distributed among many processes. Different strategies to parallelise GAs have been proposed [70], [71], [72], [73], [74]:

**Global models** These models introduce the parallel computing of new individuals among different processors to speed-up evolution without modifying the main structure and properties of the evolutionary procedure.



This method is relatively easy to implement and a significant speed-up can be expected, if the communications cost does not dominate the computation cost [75]. The evaluation of individuals is parallelized by assigning a fraction of the population to each of the processors available. Communication occurs only as each processor receives its subset of individuals to evaluate and when the processors return the fitness values. On a distributed memory computer, the population can be stored in one processor: this "master" processor would be responsible for sending the individuals to the other processors (the "slaves") for evaluation, collecting the results, and applying the genetic operators to produce the next generation.

**Coarse grained models** In these models, also named Island Genetic Algorithms (IGAs), the population of the GA is divided into multiple subpopulations or *islands* that evolve isolated from each other most of the time, but exchange individuals occasionally [76], [77]. The exchange of individuals is called *migration*. Coarse grained parallel GAs bring fundamental changes in the operation of the GA and have a different behavior than simple GAs: they introduce new evolution paradigms by using new relations among groups of individuals. Typically, each island explores a different area of the research domain increasing the probability to find a global minimum, but allowing also the possibility of tracking different "quasi-optimal" solutions (local minima): storing multiple quasi-optimal solutions can be useful in optimisation problems, where the possibility of multiple solutions has not to be ruled out, provided that the solutions all satisfy the design objectives. Sometimes coarse grained parallel GAs are known as *distributed* GAs because they are usually implemented on distributed-memory computers: these models are well suited for cluster computing with a little number of nodes connected by a local network.

**Fine grained models** This approach in parallelizing GAs uses fine-grained parallelism [78]. Fine grained parallel GAs partition the population into a large number of very small subpopulations. Indeed, the ideal case is to have just one individual for every processing element available. This model is suited for massively parallel computers.

**Hybrid and multilevel models** These models concurrently adopt different strategies, for instance with hierarchical multiple levels to perform some sort of meta-optimisation. Combining parallelisation techniques results in algorithms that share the benefits of their components and

promise better performance than any of the components alone. An example of a multi levels GA is presented in Bianchini and Brown [79], where an island model GA is combined with a master-slaves global model inside each island: migration occurs between islands and the evaluation of the individuals is handled in parallel. This approach can be useful when working with complex applications with objective functions that need a considerable amount of computation time.

### 5.3 Population moments

In a multiple populations GA environment, it is important to have a measure to describe in a compact form the features of each population: I have therefore introduced [80], in analogy with mechanics, the concept of population moments with respect to the problem fitness. Population moments act as a metric in the search space and are defined in the following:

- The *zero-order moment* could be called the population *mass* and it is computed as the sum of individuals fitness (where, for instance, the fitness can be the reciprocal of  $OF$  value) :

$$F_0 = \sum_{n=1}^{N_{indiv}} F_n \quad (5.1)$$

where  $F_n = F(\mathbf{x}_n)$  is the fitness for the  $n$ -th individual, described by the chromosomes vector  $\mathbf{x}_n$  of the design parameters, with dimension equal to number of the design parameters (DOF)  $N_{dof}$  and  $N_{indiv}$  is the number of individuals in the population. The zero-order moment is a measure of the total population fitness.

- The *first order moment* defines the position  $\mathbf{R}$  of the *center of mass* in the search space as:

$$F_0 \mathbf{R} = \sum_{n=1}^{N_{indiv}} F_n \chi_n \quad (5.2)$$

where  $\chi_n$  is the vector of the normalized chromosomes  $\chi_{n,i}$ , defined as the corresponding chromosomes  $x_{n,i}$  normalized to the diameter of their admissible range, which is usually provided as a design constraint. The first-order moment indicates the position of the "center" of the population.

- The *second-order moment* defines the *moment of inertia* with respect to each design parameter  $i$ , computed around the  $i$ -th component  $R_i$  of the center of mass:

$$F_0 \rho_i^2 = \sum_{n=1}^{N_{indiv}} F_n (\chi_{n,i} - R_i)^2 \quad (5.3)$$

where  $\rho_i$  is the  $i$ -th *inertia radius* component. The second-order moment measures the dispersion of the population with respect to its center.

These moments describe the global behaviour of a population during the evolution steps. For instance, they can be used to check the evolutionary stall of the population, when there are no more "important" changes in the population for a number of successive generations. For this purpose, a generational finite increment can be defined at each generation  $k$  as:

$$D_k = M_k - M_{k-1} \quad (5.4)$$

where  $M_k$  is the generic moment at the  $k$ -th iteration. The generational finite increment can be profitably used to describe the evolution process and the occurrence of the condition of stall.

However the main property of the moments is their possibility to compare different populations (or the subpopulations in a coarse grained model) by using them as a metric of the search space. As an example, if two compact populations (*i.e.* with low values of the second order moment) have distant centres (*i.e.* with different values of the first order moment), it is possible to say they are exploring different areas of the search space and they are also focusing towards different local minima. It is also possible to rank the populations, for instance against the robustness of solution found: during the last evolution steps, a population with a high global fitness (*i.e.* with a high value of the zero order moment) and quite spread around its center (*i.e.* with a high value of the second order moment) has found a more robust solution, with a big number of good fitness individuals around the best one, than a population with the same global fitness but a lower value of the second order moment.

## 5.4 Population operators

My attention focused mainly to IGAs parallel models: therefore next sections present some of the main topics about multi-populations GAs.

### 5.4.1 Migration policy

Parallel GAs are more complex than the serial ones and more parameters control their behaviour [81]. In particular, the migration of individuals from an island to another one is controlled by several parameters like:

1. the islands **topology**, that defines the connections between the sub-populations;
2. the **migration rate**, that controls how many individuals migrate;
3. the **migration interval**, that affects how often migrations occur.

An important index of the performance of parallel GAs is the topology of the interconnection among islands [82]: the topology determines how fast a good solution disseminates to other islands. If the topology has a dense connectivity, good solutions will spread fast and may quickly take over a new population. On the other hand, if the topology is sparsely connected, solutions will spread slower and the islands will be more isolated from each other, permitting the appearance of different solutions.

The communication topology is also important because it is a major factor in the cost of migrations. For instance, a densely connected topology may promote a better mixing of individuals but it also entails higher communication costs.

The general trend on coarse grained parallel GAs is to use *static topologies* that are specified at the beginning of the run and remain unchanged. Many implementations of parallel GAs with static topologies use the topology of the communications network of the computer available to the researchers. For example, implementations on hypercubes are common [83].

The other major choice on communication topologies is to use a *dynamic topology*. In this type of topology, an island is not restricted to communicate only with some fixed set of populations but instead it sends its migrants to those that meet some criteria. The motivation behind dynamic topologies is to identify those populations where the migrants are likely to produce some effect. Typically, the criteria used to choose an island as a destination include a measure of the diversity of the population [84] or a measure of the genotypic distance between the two populations (or some representative individual of a population, like the best one) [85]. A review of different migration policies and of their links to natural evolution is presented in [86].

Different *migration policies* can be adopted. The migrations can be *co-operative*, if the populations agree to exchange individuals, or *dominant*, if a more developed and high fitness population sends some of its best individuals to other islands, following some criteria. A master-slaves approach

to execute and control migrations has also been proposed to send the best individuals to all islands [87].

### 5.4.2 Resources allocation and aggression policy

To increase the efficient use of the computing resources for the resolution of optimisation problems defined by computationally intensive fitness functions, a new population operator has been here introduced [80]: the **aggression**. In the spirit of other GAs concepts, the new operator try to mimic a natural evolution aspect.

In natural ecosystems, different species can be viewed as evolutionary islands in competition to gain the limited available resources (*e.g.* food or vital space): the conquest of natural resources by one of the species could be performed for instance by hunting (*the strongest survive*) or resources can be allocated by some kind of "supervising" principle (*the best survive*).

In a similar way in the IGA, by adopting the concept of resources allocation, when two islands become too "near", a supervising aggression strategy can decide that the stronger or the more adapt one can conquer the other one by gaining its resources. On the other side, when there is a very weak island and when successive migrations are not able to give new impulse to it, the island can be destroyed and its resources can be given to the strongest island.

The evaluation of the strength of an island can be defined by using the already defined island moments. As a matter of fact, the higher are the available resources of an island, the higher are the probability and the velocity to find a good solution: the new acquired computing resources are used to speed-up the updating of the individuals fitness.

## 5.5 Implementation of Island GA

One of the main results of this Thesis is the implementation of the concepts of migrations on a dynamic topology among islands and of computing resources allocation for an IGA model. Some details about this implementation are given in the following.

The adopted parallel programming paradigm is the *message passing*, where the parallel running processes communicate, synchronise and exchange data through explicit messages, which have to be set by the programmer. In particular the Single Program, Multiple Data (SPMD) model is used: all processes run the same program, even if the execution of the code may be

different among the processes. The message-passing calls follow the Message Passing Interface (MPI) standard [88].

For the development of the computer code with the Fortran language, the parallel GAs library PGAPack [89], developed at the Argonne Laboratory (USA), has been used and extended with new operators and paradigms (see next section and also Section 7.3.1).

The GA has been adapted to the particular characteristics of the solved problems. A floating-point chromosomes representation has been adopted. For the generation of the initial population, the lower and upper problem limits for each design parameter set the initial ranges for the corresponding gene: each gene is uniformly randomly generated inside its range.

The classical GA operators, as previously defined in Section 4.4, have been suitably redefined in order to deal with floating point individuals:

- The selection phase allocates reproductive individuals on the basis of their fitness by using a tournament selection scheme: couples of strings are randomly chosen and for each couple the one with higher fitness is selected.
- The two-points crossover operator takes genes from each parent and combines them to create child strings.
- The mutation operator is in the form  $v \leftarrow v \pm p * v$ , where  $v$  is the existing gene value and  $p$  is selected from a Gaussian normal distribution with mean  $\mu = 0$  and standard deviation  $\sigma = 0.5$ . The change of a gene,  $p * v$ , is added or subtracted to the old value with a probability of 0.5. Individuals to mutate are randomly selected. Mutation operator may generate gene values outside the initialization range: if this happens, the gene value is reset to the lower (upper) value of the initialization range.

The population replacement is the steady state type, where the best individuals are copied to the new population, with a preset replacement value, while the other individuals are created by crossover and mutation.

An important element of all stochastic algorithms, is the (*pseudo*-)random number generator [90]: here the generator uses a starting seed value taken from the system clock and therefore the random sequences are always different for successive runs.

### 5.5.1 Load balancing issues: Master-Slave approach

Since the PGAPack only supports the single population global parallel model, to implement the multi-population model a master-slave algorithm has been

here developed: master process controls migrations and on each slave a single population GA runs. The flow chart of the proposed IGA is shown in Figure 5.1.

In parallel computing, an important aspect to deal with is load balancing. During parallel processing, care must be taken to maintain all participating processes busy performing useful computations and to minimise communication among the processes. In general, the SPMD model is not well suitable for parallel computing on a cluster of workstations: this model assumes an equal work load on each processor but, during the evolution, the actual slaves computing time could be unbalanced and non predictable, due, for example, to the presence of non-homogeneous computing nodes. To achieve good performance, it is necessary to use a *dynamic load balancing* algorithm.

This strategy has been assured by the adopted Master-Slave model: the work loads among the Slave processes are different and distributed by the Master process with a *task-farming* technique: a new task is sent to a Slave only when it has completed its previous task.

To avoid dead-locks of communication among processes, it has been necessary to develop an asynchronous and non-blocking islands migration strategy based on the master-slaves model [91], where master process controls migrations among islands using a dynamic network connection that randomly matches populations before migrations.

In addition, multiple processors can be assigned to each Slave island to increase individuals fitness evaluation speed. In this way, a **hybrid parallel** GA model is implemented, with a coarse grained GA running at the upper level among islands and performing aggression and migrations while a global parallel GA runs inside each multiple-processes island (Figure 5.2). The Slaves start different and separate global model GAs while master process enters in a loop waiting for messages from slaves (see Figure 5.1).

### 5.5.2 Implementation details

The system used to run the IGA is a Beowulf-class distributed-memory machine, which is described in the Chapter 7. An important issue of parallel codes (which usually require a long development work) is the portability of the codes across different platforms and architectures: here, to increase the portability, public domain libraries, such as MPICH and PGAPack, have been chosen. The code has been developed by using the always-available Fortran programming language.

Different MPI communicators are used: the global MPI\_Comm\_World, for the communications between the master and the slaves, and new communicators, one for each slave group of processes, where the GAs run. A

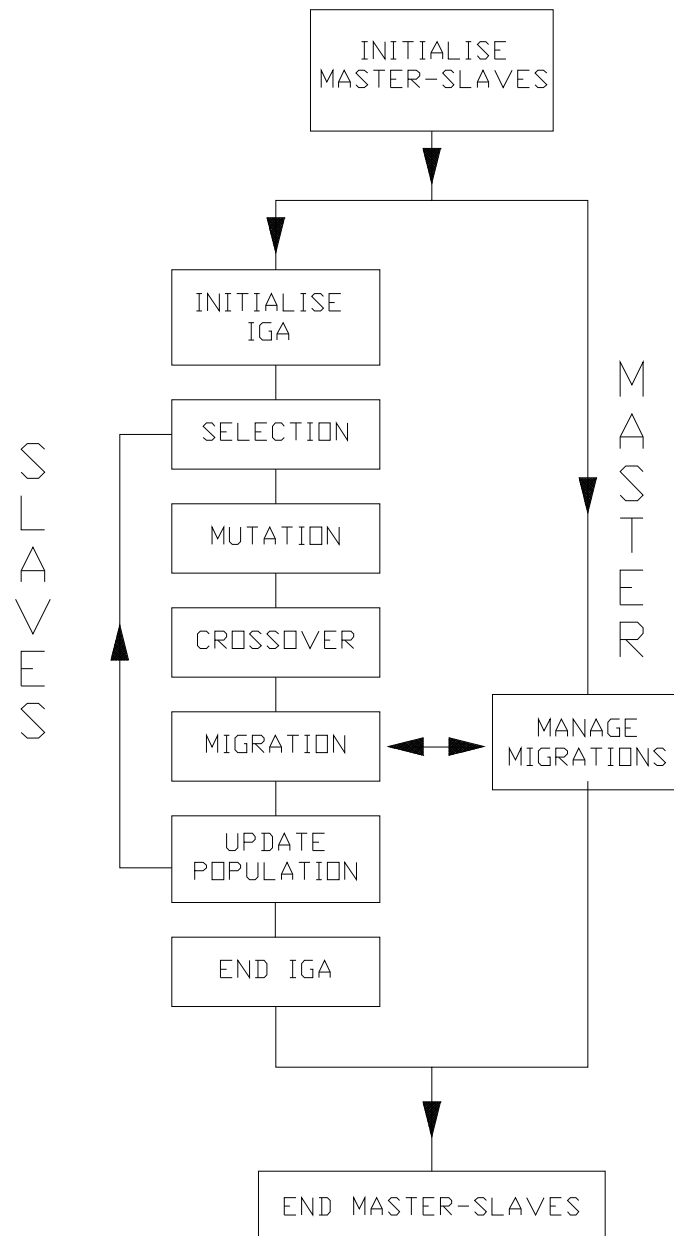


Figure 5.1: Proposed IGA flow chart.



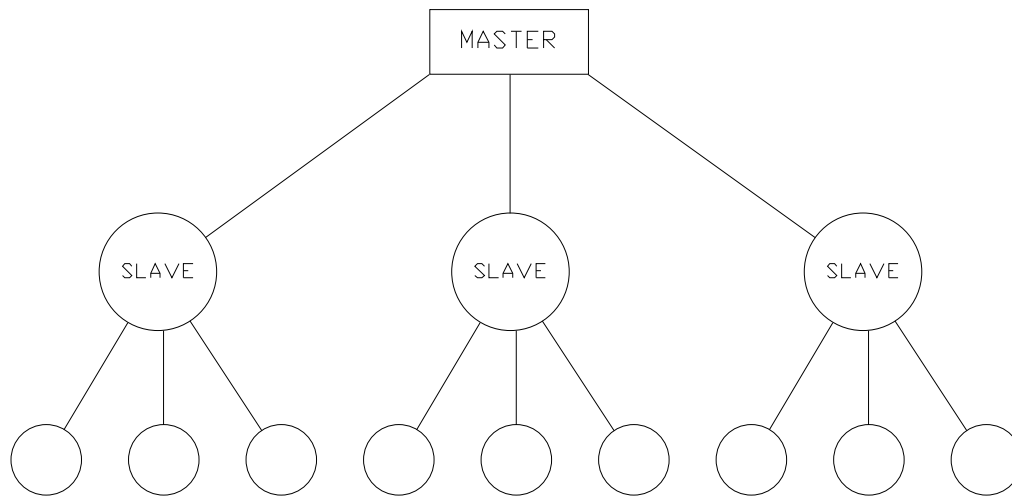


Figure 5.2: Hybrid multilevel IGA model structure.

Fortran-MPI code fragment to create the new communicators is reported in Appendix A.2.

The migrations start after an initial "genetic development" (*e.g.* set to 200 generations) to let each population to properly exploit its genetic material: by calling a migration genetic operator every  $N_g$  generations, each island sends  $N_c$  copies of its best individuals to master and then it receives  $N_c$  new individuals from master replacing some of its worst ones. In Figure 5.3 and in Figure 5.4 the detailed flow charts of the Master and of the Slave processes are respectively reported, with the migrations management in evidence. To perform migrations, the master process stores in a pool the individuals received from the slaves, then it randomly sends to each querying slave new individuals from another island (Aggression phase A, Figure 5.5).

After the first half of the preset total number of generations, the aggression phase begins (Aggression phase B, Figure 5.6): the weaker islands are destroyed and their processors are assigned to the other ones. For example, in Figure 5.6, the islands 0, 1 and 2 inherit the P4, P5 and P6 processors from the destroyed island 3, 4 and 5. Due to the present limitation of the used MPICH 1.2 release, it is not possible to have full asynchronous processes but the aggression phase requires a general processes synchronization: the creation of new topologies with new groups and new communicators has to be performed on all processes.

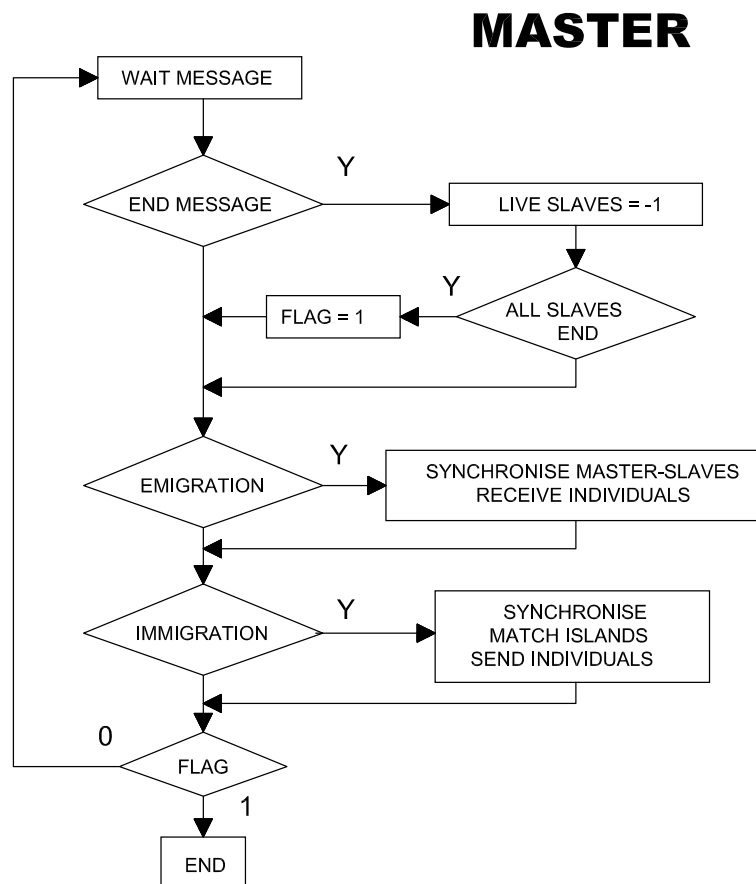


Figure 5.3: IGA: master process flow chart.

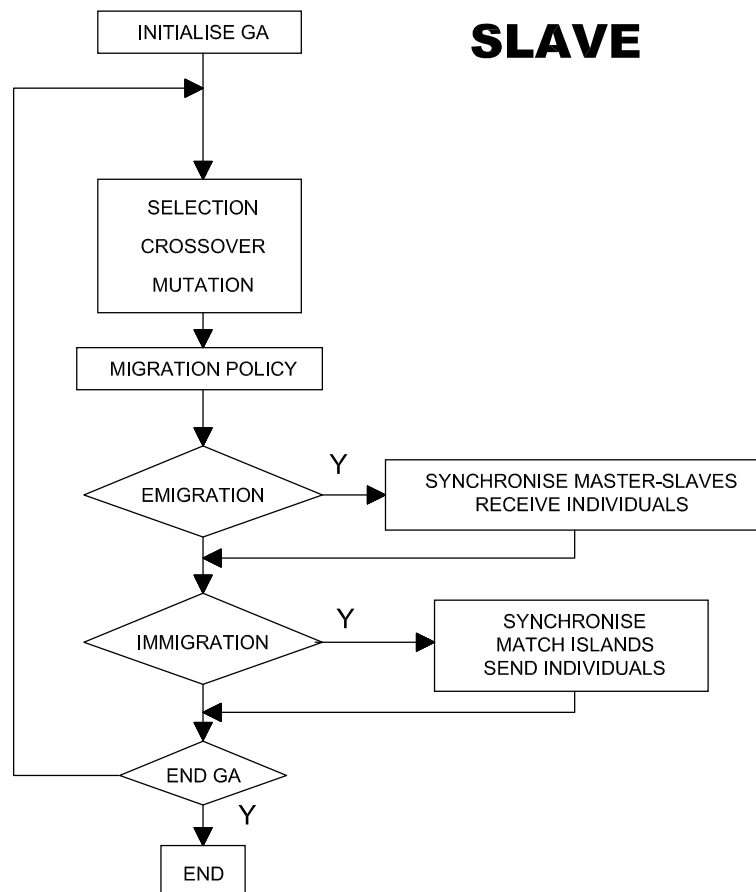


Figure 5.4: IGA: slave processes flow chart.

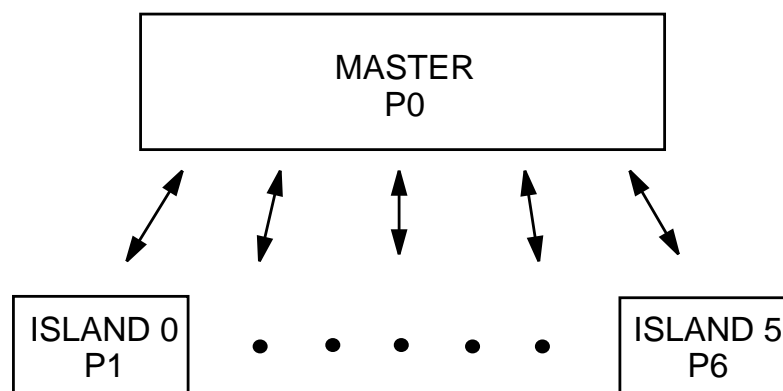


Figure 5.5: IGA aggression: Phase A.

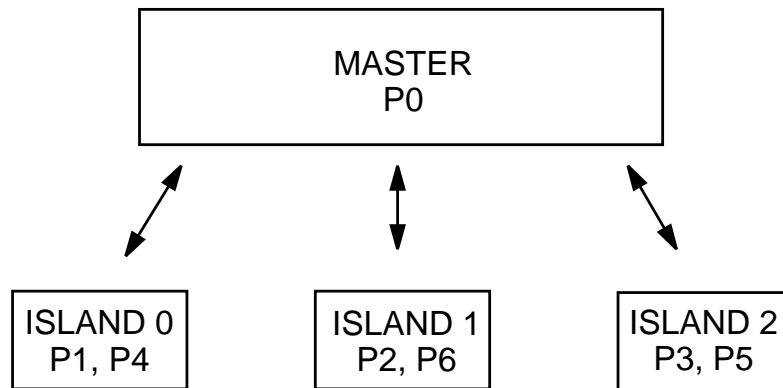


Figure 5.6: IGA aggression: Phase B.

By numerical experiments, it has been shown that there is a best value for the migration rate ( $N_g$ ) and for the number of migrating individuals ( $N_c$ ) [92]: too frequent or too populated migrations can destroy the genetic diversity of the populations and this can bring to the evolutionary stall.

## 5.6 Exploring the Biodiversity

A quite new strategy is here explored, once again borrowing from nature the concept of biodiversity: different species evolve in quite similar environments and they cooperate to achieve their not-the-same goals.

The multi population evolutionary environment has been used to find the Pareto Front, with each population specifically finalised to minimise the problem defined by a different weights set and, consequently, by a different  $OF$ : therefore the search landscape is slightly different for each population. If each population is characterised by its evolution goals, it is possible to refer such a situation as biological variety or biodiversity: the populations aim to the same objectives, which have different relative importance. The solving algorithm is based on the multi-population IGA model [93]: the structure is sketched in Figure 5.7, where each island has a different weights set and exchanges evolutionary information with the other islands.

A similar approach has been used for the resolution of inverse problems, as reported in the next Chapter 6.

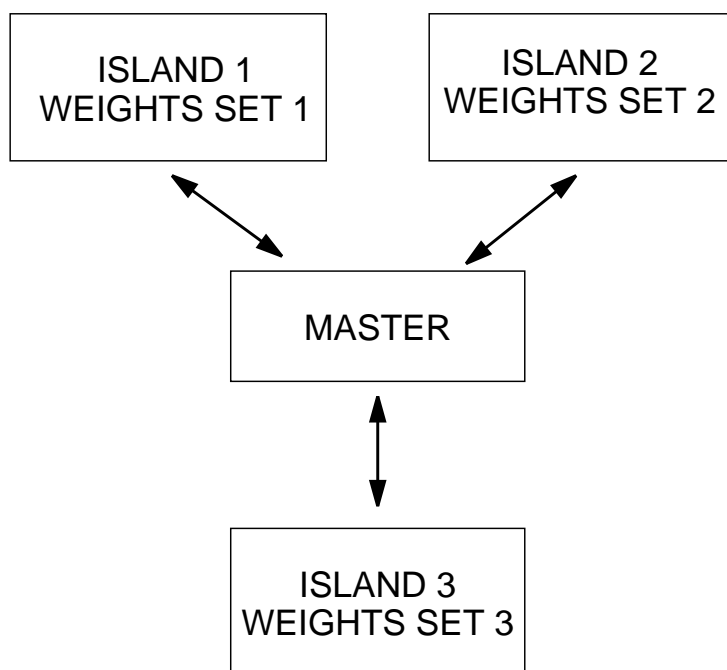


Figure 5.7: IGA: biodiversity model structure.

## Chapter 6

# Inverse problems: minimisation of error functionals in ECT

*Natural selection is the blind watchmaker, blind because it does not see ahead, does not plan consequences, has no purpose in view. Yet the living results of natural selection overwhelmingly impress us with the appearance of design as if by a master watchmaker, impress us with the illusion of design and planning.*  
by Richard Dawkins [94].

THE MODELS and methods used in optimal design can be adopted for the resolution of the inverse problems arising in *Non Destructive Testing* (NDT), where the task is to identify flaws in critical structural parts by using external measures of physical parameters [95]. Inverse problems are usually formulated as the minimisation of some error functionals, whose role is similar to the *OFs* used in optimisation problems. The difference between these two classes of problems is that the minimisation of the error functional should give the "real" unknown flaw geometry while in an multi-objective optimisation in general there is no globally defined minimum to find. In this chapter, the problem for electromagnetic NDT is formulated and the proposed solution strategy is introduced with the application to a classical benchmark.

### 6.1 Eddy Current Testing

Many technological productions, for instance in the aerospace or nuclear reactor industry, present increasing quality and safety demands that require in turn the detection of very small cracks or hidden flaws in critical parts.

One of the usual non-destructive evaluation techniques for the detection of defects in conductive specimens is the *Eddy Current Testing* (ECT) [96]. While early ECT-based systems adopted single frequency exciting signals, the most recent techniques make use of more complex waveforms, characterised by a richer spectral content.

One of these methodologies is the use of multiple frequencies, which increase the reliability of ECT by improving the capability to discriminate between the flaw signal and the noise due to the presence of external structures [97], and providing a better resolution in terms of defect depth [98]. In addition, a multiple frequency scanning can provide additional information about the flaw we are looking for [99]: for example, in multi-layer structures containing rivets, the use of different optimal frequencies helps to detect hidden cracks and to mask the noise from the rivet [100]. The use of a multiple frequency exciting signal has also been proposed as an input to a neural classifier for the flaw geometrical parameters [101], [102].

Of course, the adoption of more complex waveforms introduces additional difficulties and increases the complexity of the mathematical model to be inverted. As an example, ECT data from different frequencies can be affected by non equal measurement uncertainties and noises due to dissimilar behaviour of the probe with the frequencies or due to the use of different probes specialised for each frequency. In addition, suitable *data fusion* strategies must be applied to take the greatest advantage from the available data sets.

A novel strategy for the resolution of the inverse problems arising in the treatment of data from multi-frequency ECT is presented here [103]: the strategy is based on a multi-objective type parallel approach. The eddy currents pattern is determined by using a finite element code while the inverse problem solver is based on a stochastic algorithm.

### 6.1.1 Problem formulation

In order to determine the presence of possible structural defects and their characteristics, the usual approach is to solve an inverse problem, in which a set of measurements taken on the actual sample is the input, while the defect parameters represent the output. To accomplish such a task, a number of "trial solutions", for which the "trial crack" parameters are iteratively fixed by the inverse problem solving algorithm, must be analysed and compared to the actual solution in terms of the "measurement" generated. The presence of a flaw corresponds to a change of the conductivity inside the material: therefore the detection of the crack can be casted as the reconstruction of the material conductivity map.

The resolution of the inverse problem passes then through the resolution

of a number of "direct problems", which must be solved with the maximum efficiency, as this task represents the most demanding part of the process in terms of computational burden [104]. On the other hand, the effectiveness and the accuracy of the detection process depend also on the inversion strategy. Therefore, here the main attention is focused on the performance of the inverse problem solving algorithm, while a very simple, yet not trivial, direct problem has been considered, namely the JSAEM (Japan Society of Applied Electromagnetics and Mechanics) benchmark problem #2 [105], and solved using quite standard procedures.

### 6.1.2 Direct problem resolution

The solver for the direct problem is a finite edge-element integral code, based on the electric vector potential formulation in the framework of the magneto-quasi static modelling [106]. The formulation leads, via Galerkin finite elements discretisation, to the solution of the following equation:

$$\mathbf{L} \frac{d\mathbf{I}}{dt} + \mathbf{R}\mathbf{I} = \mathbf{U} \quad (6.1)$$

where:

$$\begin{aligned} L_{ij} &= \frac{\mu_0}{4\pi} \int_{\Omega_c} \int_{\Omega_c} \frac{\nabla \times \mathbf{T}_i(\mathbf{x}) \cdot \nabla \times \mathbf{T}_j(\mathbf{x}')}{|\mathbf{x} - \mathbf{x}'|} d\Omega d\Omega' \\ R_{ij} &= \int_{\Omega_c} \nabla \times \mathbf{T}_i(\mathbf{x}) \cdot \eta \nabla \times \mathbf{T}_j(\mathbf{x}') d\Omega \\ U_i &= - \int_{\Omega_c} \nabla \times \mathbf{T}_i(\mathbf{x}) \cdot \frac{\partial \mathbf{A}_s}{\partial t} d\Omega \end{aligned} \quad (6.2)$$

$\mathbf{T}_i$  is the  $i$ -th edge shape function,  $\mathbf{A}_s$  is the source field vector potential,  $\Omega_c$  is the conducting region,

$$\mathbf{J}(\mathbf{x}, t) = \sum_{k=1}^N I_k(t) \nabla \times \mathbf{T}_k(\mathbf{x}) \quad (6.3)$$

is the unknown current density distribution,  $\eta$  is the material conductivity, and the gauge condition  $\mathbf{T} \cdot \mathbf{w} = 0$  is assumed on the edges of a mesh tree to assure the uniqueness of the vector potential. The integral formulation adopted in this model allows to discretise only the region where an eddy current density is induced.

It should be noted that, when the same mesh can be used for the different trial solutions and just the conductivity  $\eta$  of the various elements is updated to locate the crack, the inductance matrix  $\mathbf{L}$  has to be computed only once; therefore  $\mathbf{L}$  can be inverted in advance, thus sparing quite a big amount of computational effort [107].



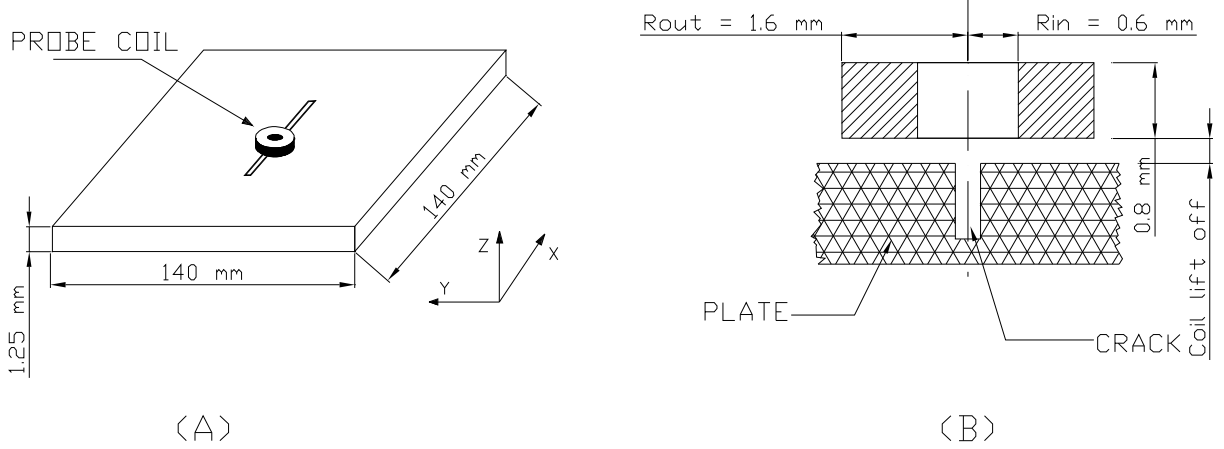


Figure 6.1: Schematics for JSAEM benchmark problem #2.

In order to improve the efficiency of the direct solution process, the reciprocity principle or smarter treatment of DOF can be adopted [108], [109].

In the JSAEM Problem #2 the test specimen is a square plate, with dimensions 140 x 140 x 1.25 mm (Figure 6.1, letter (A)), made of nickel-based non-magnetic superalloy INCONEL 600 MA showing a relative permeability  $\mu_r = 1$  and a conductivity  $\eta = 106$  S/m. The plate presents in the centre a rectangular crack characterised by the following dimensions: length = 10 mm; width = 0.2 mm; depth varying from 100% to 40% of plate thickness. Both inner and outer defects are considered.

The eddy current probe is a cylindrical coil, with inner and outer radius equal respectively to  $R_{in} = 0.6$  mm and  $R_{out} = 1.6$  mm and 0.8 mm height; the lift-off from plate is assumed equal to 0.5 mm (Figure 6.1, letter (B)). The coil is excited with AC current with RMS value equal to 1/140 A, at different working frequencies. In the Table 6.1.2, the skin depths for the three frequencies 150 kHz, 300 kHz and 600 kHz are reported for the case of INCONEL 600 MA alloy.

A finite elements mesh has been here properly chosen to guarantee a suitable precision and spatial resolution while limiting the number of elements

| Frequency       | 150 kHz | 300 kHz | 600 kHz |
|-----------------|---------|---------|---------|
| Skin depth (mm) | 1.30    | 0.92    | 0.651   |

Table 6.1: Skin depths for different frequencies in the INCONEL 600 MA alloy.

(i.e. the number of unknowns), using a higher discretisation level in the region close to the probe (*search region*) and a coarser one in the remaining part of the plate. In the present study, only cracks aligned to an axis (here the  $x$ -axis) and with a high aspect ratio have been considered, representing a class of quite common defects in the practical applications.

In the search region, in order to improve the overall effectiveness, a non-uniform mesh step along the crack direction ( $x$  axis) and normal to it has been used: in this way it is achieved almost the same spatial resolution along the two  $x - y$  directions (see Figure 6.2). Each of the finer elements (crack elements) have the same width and half the length of the JSAEM crack (i.e.  $0.2 \times 5$  mm). In Figure 6.3 is shown a zoomed view of the search region mesh indicated by a dashed circle in Figure 6.2.

With such assumptions, a generic crack is described by five integer parameters: the row  $ny$  position along  $y$ -axis, the initial ( $nx_{in}$ ) and the final ( $nx_{fin}$ ) element along  $x$ -axis, the initial ( $nz_{in}$ ) and the final ( $nz_{fin}$ ) element along the vertical  $z$ -axis on the mesh (see Figure 6.3).

Finally, note that, to prevent new evaluations of already calculated trial configurations, a data base of the computed trial cracks is built and updated during the inverse problem resolution process. In this way, before evaluating the measurements for a trial crack, the resolution strategy looks whether it is already available in the look-up table: if not, the new crack is processed and added to the data base, otherwise the data base is simply read.

### 6.1.3 Inverse problem model

As highlighted above, the actual crack is usually searched with an iterative process by generating a sequence of "trial cracks", possibly converging towards the actual crack to be detected, or, more reasonably, towards its best representation among all the possible cracks generated by the representation basis chosen. The effectiveness of an inverse problem resolution strategy must then be judged on the basis of its efficiency in the search process and, in addition, on the basis of its ability in finding such a "projection" of the crack in the search space, without being puzzled by "phantom" solutions.

The most usual approach is to formulate the problem in terms of a suitable Objective Function  $OF$ , expressing the difference of the actual measurements and the "trial" ones (generated by the direct problem solver) in terms of the parameters defining the crack (e.g. position, length or width).

Taking into account the nature of the  $OF$  (poor smoothness with multiple local minima), the latter can be efficiently solved by an evolutionary strategy, such as the Genetic Algorithms [110], thanks to their capability to span the complete parameters region. Of course, a suitable coding of the

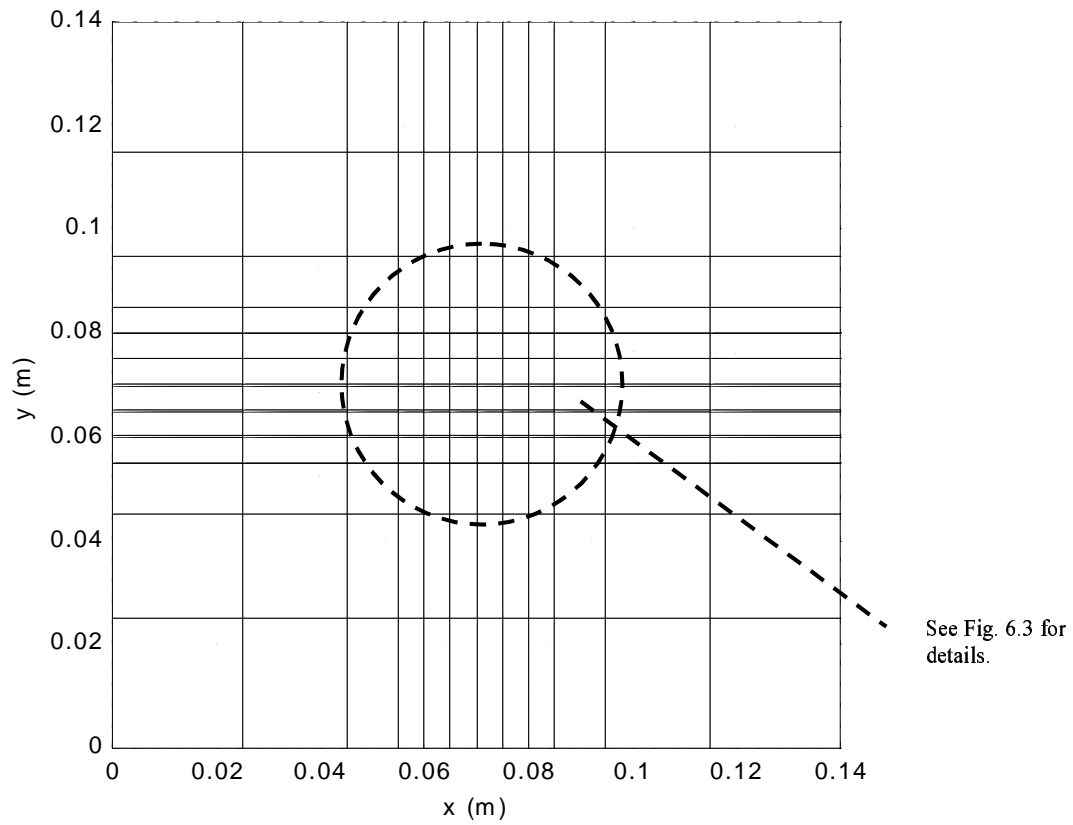


Figure 6.2: ECT analysis: top view of the plate mesh. The dashed circle indicate the region zoomed in Figure 6.3

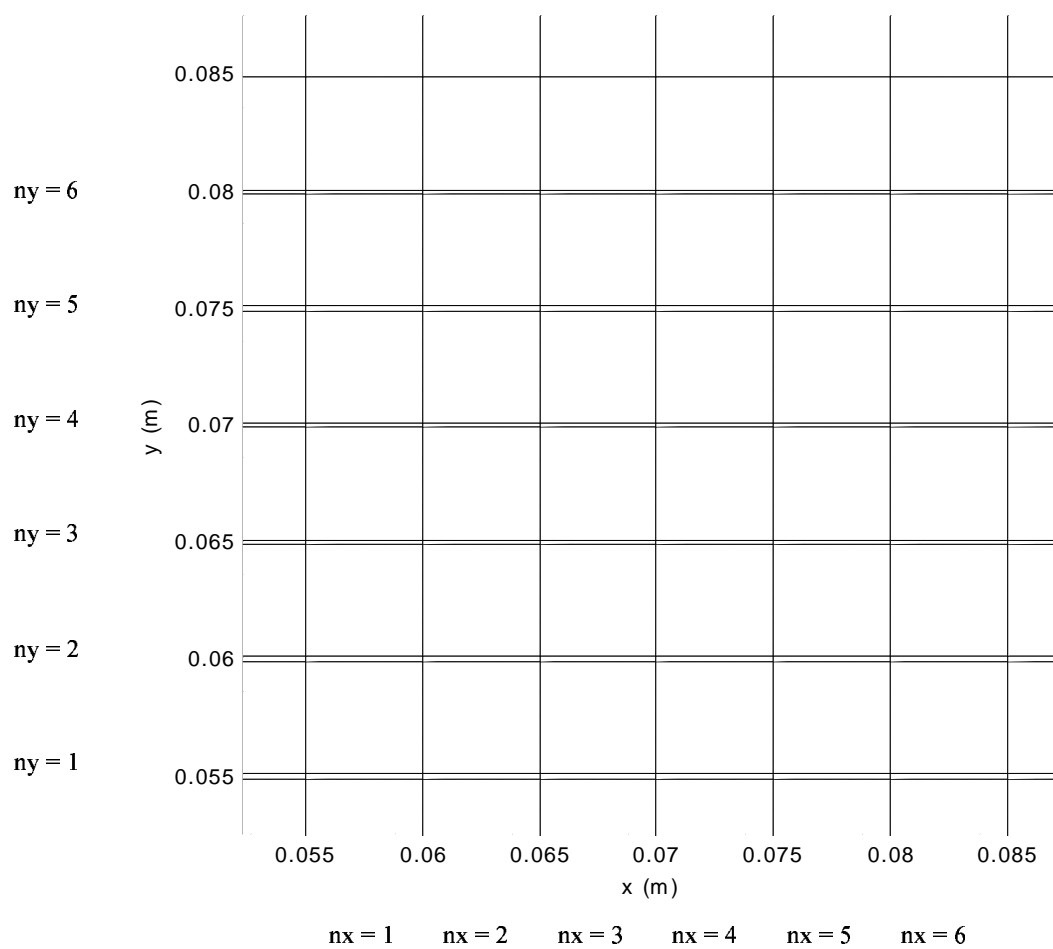


Figure 6.3: ECT analysis: zoom plot of the fine mesh region.

crack parameters and a suitable  $OF$  have to be chosen in order to relate the measurement discrepancies with the defect parameters.

Note that when using a multi-frequency ECT, the  $OF$  should be able to treat data from different frequencies. A possible, very simple, solution is to use a scalar  $OF$  defined as the sum of the errors by the signals for different frequencies [111], even if a scalar  $OF$  in multi-objective optimisation problem is affected by well known problems arising from the non-convexity of the search region.

In the following, on the other hand, the multi population environment presented in Chapter 5 is adopted, where each population is specifically finalised to reconstruct the defect by using only one of the frequencies. To this purpose, an Objective Function  $OF_i$  for the  $i$ -th population is defined by:

$$OF_i = \frac{\|\mathbf{S}_i - \mathbf{S}_{si}\|}{S_{si,norm}} \quad (6.4)$$

where  $\mathbf{S}_{si}$  and  $\mathbf{S}_i$  are the vectors of the measured and computed signal values at the  $i$ -th frequency for the actual flaw geometry,  $S_{si,norm}$  is a normalisation parameter (*i.e.* the maximum value of the signal).

The inverse problem solving algorithm is based on the previously introduced multi-population Island Genetic Algorithms (IGA). The presented strategy is somehow similar to the solution of a multi-objective optimisation even if, in this problem, a global optimum does exist (the true flaw geometry) and therefore the partial  $OF_i$  have the same global minimum (but different local minima). Of course, if the different signals are affected by noise, the global minimum can no more exist and the solution of the multi-objective problem gives therefore a Pareto Front, which has to be suitably post-processed in order to localise the actual solution.

The direct problem has been faced with the described finite element approach. A fixed mesh has been adopted in order to simplify the problem resolution, because the main concern of this chapter is on the inverse problem. Therefore the individuals (*i.e.* each "trial crack") can be described by an integer chromosome in the form  $(ny, nx_{in}, nx_{fin}, nz_{in}, nz_{fin})$ . For each evaluation of the  $OF$ , the chromosome is translated in a conductivity map of the mesh elements to generate the trial crack geometry: to prevent numerical instabilities, the crack elements are set to a much lower conductivity than the material elements. The trial solution is then processed (either by solving a FEM problem, or only by looking in the  $OF$  values table) and its fitness is evaluated.

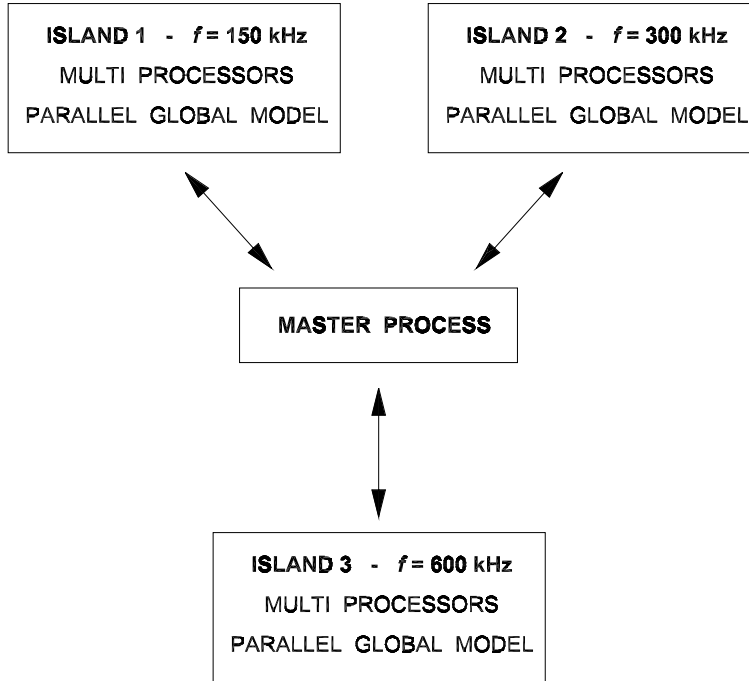


Figure 6.4: ECT: master-slaves IGA structure.

#### 6.1.4 Parallel computing environment

To achieve the needed performances, the concurrent stochastic search of the IGA model takes advantage of the computing power of a parallel distributed computing environment.

The multi level structure of the IGA utilises the different frequency-specialised  $OF$ s landscapes inside the different islands (Figure 6.4). The migration policy exploits the ranking of the populations following the skin depths to properly allow the propagation of the flaw information towards other populations.

#### 6.1.5 Results

To assess the validity of the proposed method, a mesh made up of 648 brick elements with 108 elements in the fine crack mesh region has been used to solve the direct problem. The calculations have been performed on a 10 processors cluster machine; three frequencies have been used for the exciting coil (150 kHz, 300 kHz and 600 kHz) leading to three populations, one for each frequency with three different  $OF$ s, as described above. The computing

|   | Crack A | Crack B |
|---|---------|---------|
| Case A : $f = 150$ kHz                  | 0%      | 0%      |
| Case A : $f = 300$ kHz                  | 10%     | 70%     |
| Case A : $f = 600$ kHz                  | 70%     | 50%     |
| Case B : scalar $OF$                    | 10%     | 10%     |
| Case C : migration gap = 3 generations  | 100%    | 60%     |
| Case C : migration gap = 6 generations  | 100%    | 90%     |
| Case C : migration gap = 12 generations | 100%    | 70%     |

Table 6.2: Results of the ECT numerical experiments: percentage of the success on localising the crack.

resources of the cluster machine have been equally distributed among the populations, each composed of 20 individuals and allowed to evolve for 60 generations in all numerical experiments.

Two different cracks have been considered, among those defined in the JSAEM #2 benchmark: namely a first crack (crack A, of kind 66% inner defect ID) described by the string [3,3,4,1,2] and a second one (crack B, of kind 66% outer defect OD) described by [3,3,4,2,3]. Random noise has been added to the computation results in order to simulate measurement noise.

In order to compare the effectiveness of different migration policies among populations, the measurements of each of the crack have been processed using the following strategies for the inverse problem resolutions:

- *Case A*: Three different, not interacting, populations;
- *Case B*: A single population with a classical scalar  $OF$  constituted by the sum of the various terms (6.4) for the three frequencies;
- *Case C*: Three different populations, each communicating with the others, with different migrations gaps (*i.e.* the number of generations between successive migrations).

For each numerical experiment, to average the results, ten runs of the GA have been considered, starting from the same initial population. In Table 6.1.5 the percentages of the success on localising the crack are reported for each of the strategies and, limiting to the case C, for different migrations gaps ranging from 3 (equal to 1/20 of the total number of generations) to 12 (equal to 1/5 of the total number of generations). For all runs, the total number of direct problem resolutions is the same.

From the results presented, it appears that, for the non-migrating GA, the lower frequency was unable to find both the cracks, due to a local minima

trapping with the used little population, while the other frequencies perform better respectively with one of the two cracks. The scalar  $OF$  performs quite badly for both cracks. The proposed strategy with migrations scores very good for the inner defect (crack A) with full marks; for the outer defect (crack B) the results show that there is an optimal value of the migration gap, approximately equal to 1/10 of the total number of generations, as already reported [80].

### 6.1.6 Section summary

An inverse problem solution strategy has been proposed for the multiple-frequencies ECT data treatment. The model is based on a multiple populations Island Genetic Algorithm, with each population specialised to locale cracks using data at one single frequency. The method has been tested with JSAEM problem #2 with three frequencies and it shows significant better performances than the other usual techniques.

The developed model for multiple frequency ECT can be also efficiently exploited for a *data fusion* strategy, with the concurrent use of data from different technologies and sources data by submitting a typology of data to each population, for instance with ultrasonic scanning coupled with ECT data.



# Chapter 7

## Computing environment

*In a famous lecture, Alan Turing said: "Tell me what you think a computer cannot do and I will make one which can do exactly that". I answered him by letter: "What do you mean by tell me? Perhaps I need to give you a description, because in that case it would be an easy challenge. Clearly what must be avoided is the description itself. There is one thing a computer certainly lacks and that is initiative. And I do not know how one can describe initiative"*

(by Karl R. Popper) [112].

In this chapter the current trends of parallel cluster computing are illustrated. Then the developed parallel computing environment and the cluster prototype are described.

### 7.1 Beowulf Clusters

BEOWULF SYSTEMS are networks of fast personal computers configured with large quantities of RAM and hard disk space and usually running the Linux operating system [113]. These machines are also known as "piles of PCs" or "cluster of workstations". Thanks to their scalability and easy upgrade possibility, such systems are becoming more and more attractive as cheap and efficient platforms for distributed parallel applications and High Performance Computing (HPC) and also for high availability and high reliability systems [114].

The cluster scalability can be exploited to an extreme level to build very huge systems: at the moment, in the position number 5 of the world most-powerful installed computers list there is a cluster machines with 2304 processors (Intel Xeon) with a computing speed of 5.69 TFlops (millions of millions

of floating point operations per second), built in part with the Italian technology of Quadrics (see <http://www.top500.org>).

Beowulf clusters provide universities, which often have limited resources, cost effective computing power and provide as well a platform to teach parallel programming courses. Also in the today always changing and evolving situation of the computer market, it is possible to say that clusters can achieve equivalent computing performances of classic "industrial" machines which have an order of magnitude higher price.

One of the first projects of this class was started at the NASA Goddard Space Flight Center in 1994: at Goddard a machine was built and its name was "Wiglaf", after one of the characters from the Beowulf epic British saga [115]. Commodity clusters subsequently became known as Beowulf-class clusters. More information is available from the dedicated web site <http://www.beowulf.org>.

Today there is an increasing interest in the use of "commodity off-the-shelf" (COTS) components as building blocks for HPC. The success of cluster machines is mainly due to the performance improvements in microprocessors and, perhaps more important, to the recent cost/performance gains in network technology: Fast Ethernet and, in some months, Gigabit Ethernet technology are becoming even more cheap.

A key component to forward compatibility is the system software used on Beowulf. With the maturity and robustness of Linux, GNU software and the standardization of message passing via PVM and MPI, programmers now have a guarantee that the programs they write will run on future Beowulf clusters, regardless of who makes the processors or the networks [116].

The cost-saving factor of Beowulf clusters is beginning to draw the attention of the mainstream computing world. Today many major corporations are beginning to use them and large computer companies, such as IBM, SGI and Compaq, offer clusters to their customers community.

The future of the Beowulf project will be determined collectively by the individual organizations contributing to the Beowulf project and by the future of mass-market COTS. As microprocessor technology continues to evolve and higher speed networks become cost effective and as more application developers move to parallel platforms, the Beowulf project will continue to evolve [64].

## 7.2 Beosun

To efficiently run the developed IGA code, a Beowulf machine has been designed and built in the laboratory of the Department of Information Engi-

neering of the Second University of Naples: its name is **Beosun**. The **Beosun** machine is assembled with 8 PC-class rack-mounted nodes and connected in island with a dedicated Fast Ethernet network. In Figure 7.1 a picture of the final **Beosun** machine is shown. The components of the **Beosun** machine are the following:

- **Master Node**

- Motherboard with chipset Intel 850, PC800 Rambus DRAMs support, ATA 100 and Fast Ethernet onboard controllers.
- Intel Pentium IV 1.9 GHz CPU, cache L2 256kB, 400 MHz FSB.
- 512 MB PC800 ECC Rambus DRAMs.
- 2 x 40 GB ATA 100 hard disks, 7200 RPM.
- Floppy disk.
- 2 Fast Ethernet NICs.
- 32 MB AGP graphics card.
- CD-ROM writer.

- **Compute Slave Nodes**

- Motherboard with chipset Intel 850, PC800 Rambus DRAMs support, ATA 100 and Fast Ethernet onboard controllers.
- Intel Pentium IV 1.9 GHz CPU, cache L2 256kB, 400 MHz FSB.
- 512 MB PC800 ECC Rambus DRAMs.
- 40 GB ATA 100 hard disks, 7200 RPM.
- Floppy disk.
- Fast Ethernet NIC.
- 8 MB graphics card.

- Fast Ethernet switch, 24 ports, 10/100BASE-TX, Layer 4.
- Master switch for monitor, keyboard and mouse, 32 ports.

All the compute nodes are configured in the same way, with a minimal Linux installation. All nodes are connected to a single monitor, keyboard and mouse via the master switch: this provides the ability to directly login to the compute nodes if something goes wrong whilst avoiding unnecessary



Figure 7.1: The Beosun Beowulf machine

cost and space. All the components, but the monitor, are mounted on a 19" rack cabinet.

The master node and the compute nodes are attached via 2 NICs to the Ethernet switch: one card is for message passing communications with the rest of the nodes and the second card for IP, DNS and other network data traffic. The master node is connected via its third NIC to the external site network.

The Beosun machine has been also connected to the previous generation cluster machine built two years ago, with 6 nodes powered by AMD K7 processors (550 MHz) with 550 MB SDRAM per node: the resulting cluster counts therefore 14 computing nodes.

## 7.3 Software

The used operative systems are Linux (Red Hat 7.2, Kernel 2.4.7) and Microsoft Windows XP, with the machines configured for dual boot. For parallel applications development, Linux with the Fortran language is mainly adopted: both Fortran 77/90 and High Performance Fortran (HPF) are available. The parallel environment is message passing using the standard MPI library, in the MPICH implementation.

### 7.3.1 Libraries

The software environment is completed by mathematical libraries such as the standard BLAS (linear algebra), LAPACK (scalar linear equations systems) and ScaLAPACK (parallel linear equations systems).

#### PGAPack

The parallel GAs library PGAPack [89] has been used to implement the IGA model. PGAPack is a general-purpose, data-structure-neutral, parallel genetic algorithm library. It supports the parallel implementations of the single population global model. Key features in PGAPack include:

- Routines callable from Fortran or C.
- Runs on uniprocessors, parallel computers and workstation networks.
- Binary-, integer-, real-, and character-valued native data types.
- Full extensibility to support custom operators and new data types.

- Parameterised population replacement.
- Multiple crossover, mutation, and selection operators.
- Easy integration of hill-climbing heuristics.

PGAPack is available by anonymous FTP from *ftp.mcs.anl.gov* in `pub/pgapack` as `pgapack.tar.Z`.

### 7.3.2 Graphical user interfaces

The IGA code is linked to a Graphical User Interface (GUI), developed by using the Matlab language, in a mixed environment Fortran-Matlab. The GUI is used for I/O and during the computation to show the results. For instance, to efficiently show the behavior of the different islands during the evolutions, different windows are displayed on the screen showing, for each of the best islands, the motion of the local first-order moment in the parameters space or the evolution of the zero-order and second-order moment. In each window the values of the best  $OF$  and of the generation are displayed together with the number of processes running for the island.

The GUI is also used to set some of the input GA parameters, such as the size of the populations and the GA stopping criteria (*e.g.* the maximum number of generations) by using pop-down menus. At the end of the optimization process, it is possible to show in each windows the obtained final solution with the  $OF$  value.

### 7.3.3 Parallel Matlab

Matlab is widely adopted as a computing development tool in many scientific and technological working groups. The underlying numerical routines, its interactive environment, matrix-oriented language and graphical tools are some of the reasons for its widespread use.

In the last years a number of parallel libraries (known as *toolboxes*) for Matlab have been made available by several researchers and institutions: these toolboxes are mainly developed by adopting the message passing concept for the use on cluster of computers. A survey of the available parallel toolboxes is presented in [117].

Here a different approach has been implemented. Rather than looking for interactive parallel capabilities, the previously presented mixed Fortran-Matlab environment has been exploited to run parallel mixed MPI-Fortran code sections from a Matlab program.

# Chapter 8

## Results

In this chapter the main results obtained from the previous analysis by using the developed and implemented techniques are introduced with the application to test cases and real world problems, such as the design of superconducting magnets. In particular, the software prototype *Marides* is described.

### 8.1 Island GA for the TEAM 22 Problem

THE PREVIOUSLY INTRODUCED Island GA has been tested on the TEAM 22 problem with eight parameters described in Section 3.7.2. Each SMES configuration, corresponding to an individual, has been represented by 8 chromosomes coded with double precision floating points variables, corresponding to the 8 design parameters  $(R_1, R_2, h_1/2, h_2/2, d_1, d_2, J_1, J_2)$ , as defined in Figure 3.3.

#### 8.1.1 Migrations without aggression

First studies were performed for a multi population IGA with migration but without aggression strategy among islands [118]. A preliminary analysis has been carried out to tune IGA migration parameters: in particular, the number of individuals involved in exchange process  $N_c$  and the frequency  $N_g$  of the migration have been varied, computing for each case the mean value of the minima found on 3 runs with 1000 generations. Table 8.1 shows a summary of the best values of the objective function  $OF$  obtained for each island population with 1000 individuals: lowest values of the  $OF$  (*i.e.* better solutions) are achieved with  $N_c = 20$  and  $N_g = 50$ , letting therefore 2% of the population to migrate with rather frequent migrations.

These values of  $N_c$  and  $N_g$  have been then selected and the IGA has been

|            | $N_g = 50$ | $N_g = 100$ | $N_g = 200$ |
|------------|------------|-------------|-------------|
| $N_c = 10$ | 0.1000     | 0.1310      | 0.2961      |
| $N_c = 20$ | 0.01933    | 0.06638     | 0.1892      |
| $N_c = 40$ | 0.05888    | 0.07865     | 0.4887      |

Table 8.1: Best  $OF$  values for different migration IGA parameters, with populations of 1000 individuals.

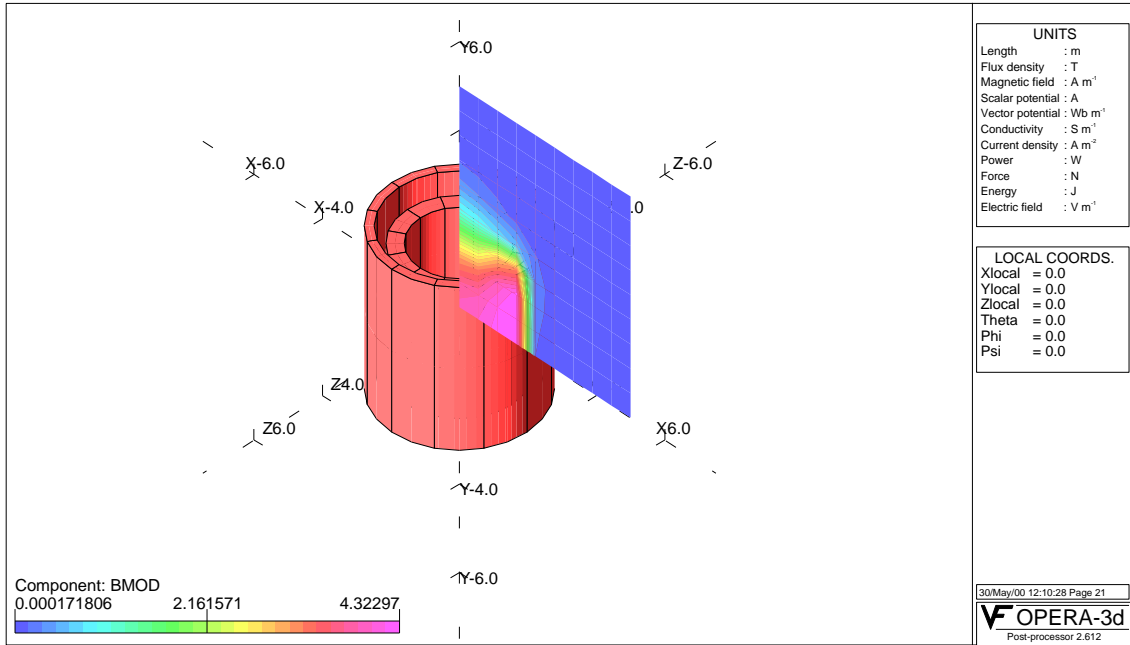


Figure 8.1: Best SMES configuration for migration IGA with magnetic field map on a radial plane sector.



| Case          | $OF$           | Energy<br>(MJ) | $B_{\text{stray}}^2$<br>( $T^2$ ) | $R_1$<br>(m)          | $R_2$<br>(m)          | $h_1/2$<br>(m) |
|---------------|----------------|----------------|-----------------------------------|-----------------------|-----------------------|----------------|
| <b>Best A</b> | 7.480e-3       | 180.0060       | 2.979e-10                         | 1.1042                | 1.8483                | 1.7557         |
| <b>Best B</b> | 1.553e-2       | 180.8708       | 4.272e-10                         | 1.3354                | 1.8661                | 1.4495         |
| <b>TEAM</b>   | 5.520e-3       | 179.9924       | 2.191e-10                         | 1.5703                | 2.0999                | 0.7846         |
|               |                |                |                                   |                       |                       |                |
| Case          | $h_2/2$<br>(m) | $d_1$<br>(m)   | $d_2$<br>(m)                      | $J_1$<br>( $MA/m^2$ ) | $J_2$<br>( $MA/m^2$ ) |                |
| <b>Best A</b> | 2.1851         | 0.4006         | 0.1394                            | 17.0572               | -14.2191              |                |
| <b>Best B</b> | 1.8380         | 0.3764         | 0.2184                            | 19.9071               | -13.9534              |                |
| <b>TEAM</b>   | 1.4184         | 0.5943         | 0.2562                            | 17.3367               | -12.5738              |                |

Table 8.2: Best TEAM 22 results with migration IGA.

let to optimize the  $OF$  for a higher number of generations. As expected, a number of "optimal" configurations have been found, each satisfying the design goals, but characterized by different layouts. In Table 8.2 two of the best results are reported: these results are obtained with 5 islands, each one evolving with a population composed of 1000 individuals during 2000 generations, and they are compared with the currently best TEAM 22 solution. A sketch of the first best configuration (case with letter **A**) is shown in Figure 8.1 together with the magnetic field modulus map on a radial plane. Slight differences with the current best solution have been observed in the energy and field values, probably due to different computational approaches to the field and inductance evaluations.

The solutions found here have layouts different from the TEAM one: in the following section, a strategy able to rank "best" solutions will be presented.

### 8.1.2 Aggression strategy

The TEAM 22 problem has been solved again by adopting the aggression concept for the IGA. The population moments, introduced in Section 5.3, have shown during the tests their ability to describe the behavior of the islands: the aggression and migration strategies, based on the moments concept, can efficiently improve the optimization process [80].

The parameters adopted for the IGA with aggression to tackle the TEAM 22 optimization problem are listed in Table 8.3. The number of initial islands is six with one process for each island; after the aggression phase, the final number is three, where each island owns two processes. By the previous analysis performed to tune IGA migration parameters, the number of individuals

|                                   |      |
|-----------------------------------|------|
| <b>Initial populations</b>        | 6    |
| <b>Final populations</b>          | 3    |
| <b>Generations</b>                | 4000 |
| <b>Individuals per population</b> | 2000 |

Table 8.3: IGA parameters for aggression.

involved in exchange process has been set to 2% of the overall population and the frequency of the migrations has been set to 50 generations.

After the IGA evolution, in each of the three final islands an "optimal" configuration has been found: each configuration satisfies the assigned design goals with a particular and different layout. In Table 8.4 the best results are reported for the three islands, compared with currently best TEAM 22 solution. The best SMES geometry found (corresponding to Island 1) is shown in Figure 8.2 together with the current best TEAM geometry.

As usual in a multi-objective optimization, different quasi-optimal solutions exist and they can be ranked by using some criterion in addition to the *OF* values, such as some auxiliary design requirements not coded in the *OF*. In the case of SMES, some of the main characteristics of the device are the total volume of the coils, that measures the amount of required superconducting wire and therefore the cost of the apparatus, and the compactness of the system (defined as the external coil radius by the maximum of the coils heights), that measures its external size. Among the three solutions of Table 8.4, the first one (Island 0) has the lowest coils volume and is the most compact one although its fitness is the worst, whereas TEAM solution has a bigger volume but is more compact than the present best one, as reported in Table 8.5. The final word among these solutions is a designer choice.

The comparison between IGA results on the TEAM 22 problem without aggression (Table 8.2) and with aggression (Table 8.4) shows that, while the adoption of the aggression strategy increases by sure the overall computing performances, however it can decrease the exploration capabilities in the search space due to the lowering number of islands, getting therefore sometimes worse results.

## 8.2 Design of high $T_c$ superconducting magnets

High Temperature Superconductors (HTS) are ceramic-type materials that exhibit zero-resistance properties at temperatures between 20 to 130 K, therefore requiring less expensive cooling systems than those needed for low tem-

| Case     | $OF$           | Energy<br>(MJ) | $B_{\text{stray}}^2$<br>( $T^2$ ) | $R_1$<br>(m)          | $R_2$<br>(m)          | $h_1/2$<br>(m) |
|----------|----------------|----------------|-----------------------------------|-----------------------|-----------------------|----------------|
| Island 0 | 3.398e-2       | 178.5766       | 10.428e-10                        | 1.9283                | 2.4253                | 0.7043         |
| Island 1 | 1.424e-2       | 180.0007       | 5.6940e-10                        | 1.9288                | 2.4275                | 0.7190         |
| Island 2 | 1.569e-2       | 180.0058       | 6.2655e-10                        | 1.9306                | 2.4268                | 0.7220         |
| TEAM     | 5.520e-3       | 179.9924       | 2.191e-10                         | 1.5703                | 2.0999                | 0.7846         |
|          |                |                |                                   |                       |                       |                |
| Case     | $h_2/2$<br>(m) | $d_1$<br>(m)   | $d_2$<br>(m)                      | $J_1$<br>( $MA/m^2$ ) | $J_2$<br>( $MA/m^2$ ) |                |
| Island 0 | 1.4199         | 0.4358         | 0.1908                            | 22.5600               | -16.2376              |                |
| Island 1 | 1.4663         | 0.4280         | 0.1879                            | 22.6135               | -16.0162              |                |
| Island 2 | 1.4717         | 0.4279         | 0.1882                            | 22.6001               | -16.0208              |                |
| TEAM     | 1.4184         | 0.5943         | 0.2562                            | 17.3367               | -12.5738              |                |

Table 8.4: Best results for IGA with aggression, compared to the TEAM 22 results.

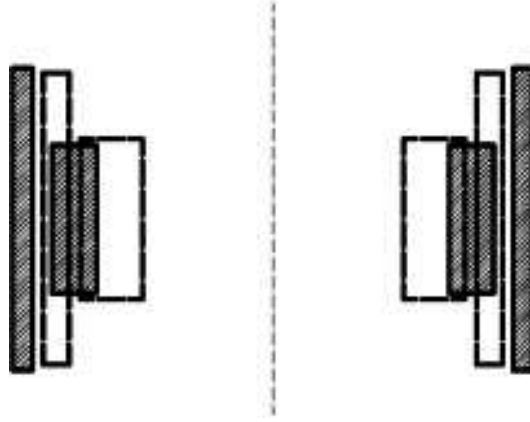


Figure 8.2: Axial section of the best computed SMES geometry by aggression IGA (filled boxes) and present TEAM solution (empty boxes).

| Case     | $OF$     | Volume<br>$m^3$ | Compactness<br>( $R * L$ ) |
|----------|----------|-----------------|----------------------------|
| Island 0 | 3.398e-2 | 15.69           | 7.158                      |
| Island 1 | 1.424e-2 | 15.85           | 7.394                      |
| Island 2 | 1.569e-2 | 15.93           | 7.420                      |
| TEAM     | 5.520e-3 | 18.78           | 6.320                      |

Table 8.5: Aggression IGA solutions ranking.

perature superconductors ( $< 10$  K, see Section 2.3). Recent progress in *Ag* or *Ag*-alloy-sheathed *Bi* based HTS fabrication allows to produce suitably long superconductor tapes.

For a number of power applications, in the near future, such new materials could represent an appealing actual alternative to the classical technology, based on *NbTi* and *Nb<sub>3</sub>Sn*, operating at low temperature of liquid helium. However, the characteristics of HTS conductors are still to be assessed, and many efforts are being carried out in order to improve their performance, such as the critical current densities, and to optimise the fabrication process [119].

From the design point of view, one of the most critical characteristics of HTS is their anisotropic relationship between the critical current density and the magnetic flux density [120], with a different behaviour between parallel  $B_{//}$  and perpendicular  $B_{\perp}$  field components with respect to the tape surface. Just for an exemplification, in Figure 8.3 the critical currents versus both the flux density components, namely  $J_{c1} = f_1(B_{//})$  and  $J_{c2} = f_2(B_{\perp})$ , are shown for a commercial HTS tape at a fixed temperature of 27.9 K.

Due to these technological issues and to the sensitivity to the bending stress, HTS tapes are usually wound in "double-pancake" configuration coils, which are then suitably arranged in order to build high field magnets: this configuration allows to reduce the tape performance degradation due to winding procedure.

The optimal design of a HTS magnet has been here performed. The adopted Objective Function  $OF$  is a combination of the different goals to be fulfilled. A first term  $f_v(\mathbf{x})$  takes into account the overall volume of superconductor, which represents the main cost factor:

$$f_v(\mathbf{x}) = \frac{1}{V_{MAX}} \sum_{i=1}^{N_{coils}} V_i \quad (8.1)$$

where  $N_{coils}$  is the number of the magnet coils,  $V_i$  is the volume of  $i$ -th coil,  $\mathbf{x}$  is the vector of the DOF defining a particular configuration and  $V_{MAX}$  is a normalizing term related to the volume of the region admissible for the coils allocation.

The second term  $f_s(\mathbf{x})$  of the Objective Function takes into account the relative amplitude of the magnet feeding current with respect to the minimum critical current within the coils: the lower this term is, the better the coils are working because, in principle, it is possible to decrease the amount of superconductor by downsizing the configuration and consequently by augmenting the feeding current. The expression adopted is:

$$f_s(\mathbf{x}) = \frac{I}{I_c} \quad (8.2)$$

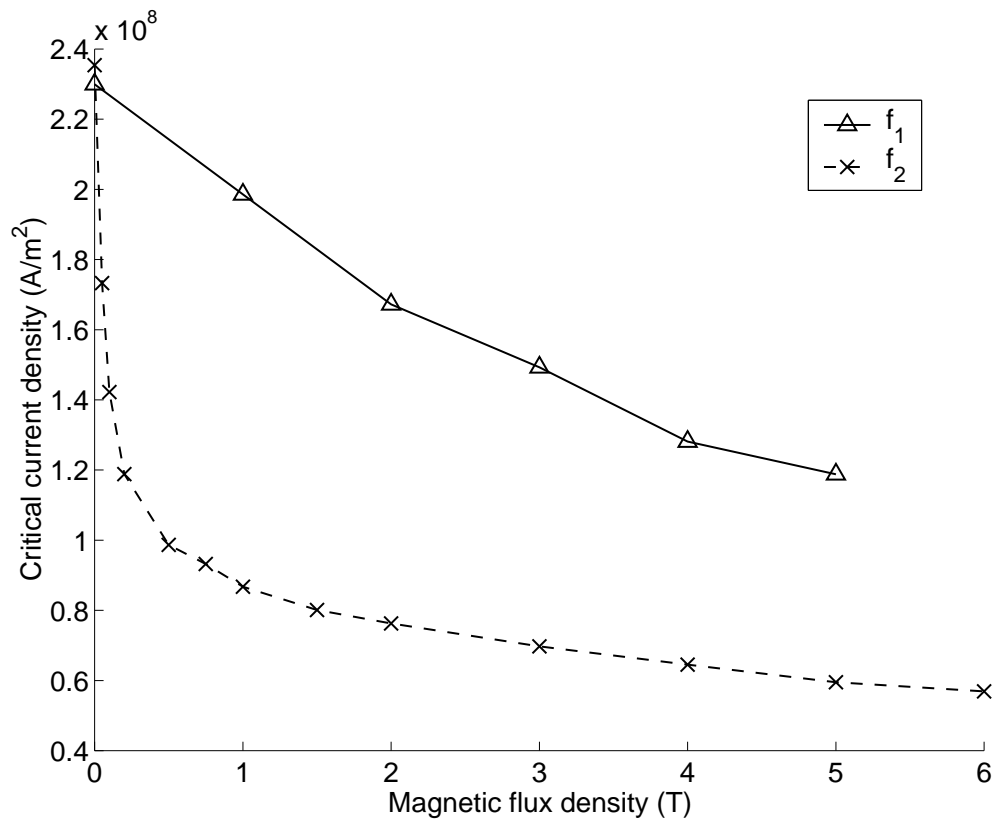


Figure 8.3: HTS magnet: critical current densities versus  $f_1(B_{//})$  and  $f_2(B_{\perp})$  for a commercial HTS tape.

where  $I$  is the current needed to generate the assigned central field  $B_{des}$  using the tentative geometry  $\mathbf{x}$ , and  $I_c$  depends of the field map inside the coils and is evaluated using the anisotropic superconductor characteristics. The  $OF$  can be then written as:

$$OF(\mathbf{x}) = w_V \cdot f_V(\mathbf{x}) + w_s \cdot f_s(\mathbf{x}) \quad (8.3)$$

where  $w_V$  and  $w_s$  are the weights of the objectives in the optimization function. As usual, the weights can be chosen in different fashions, depending on the relative importance of the various design issues.

In addition, a number of constraints should be satisfied. The first ones are the geometrical limits as, for example, the coils allocation inside suitable areas. Further constraints set the maximum tape length that can be used to wind each double-pancake and also the overall tape length.

The second ones can be termed "physical constraints": a typical physical constraint is represented by the critical current limits. Although the term  $f_s(\mathbf{x})$  acts in the direction of keeping the current below the critical value, it is necessary to explicitly impose this constraint to prevent from accepting solutions with a very small volume but working above critical conditions. A simple and efficient way to take into account the dependence of the critical current from both the field modulus and direction is to verify the two conditions:

$$J \leq f_1(B_{//}) = J_{c1} \quad (8.4)$$

$$J \leq f_2(B_{\perp}) = J_{c2} \quad (8.5)$$

where  $f_1$  and  $f_2$  are the functions already introduced,  $J_{c1}$  and  $J_{c2}$  are the critical parallel and perpendicular current densities and  $J$  is the current density inside the superconductor, given by the ratio between the current  $I$  and the tape cross section.

Conditions (8.4) and (8.5) are very demanding in terms of the computational effort required by the optimisation algorithm, as both the conditions are to be verified at each optimisation step in the points inside the windings where  $B_{//}$  and  $B_{\perp}$  respectively reach their maximum values. This step requires a maximum value search for each  $\mathbf{B}$  component and therefore an effective strategy for the maximum points localisation would result highly beneficial for the optimisation process. An example of such "fast localization strategy" will be discussed in the next section.

To assess the ability of the proposed design strategy, here a double-pancake magnet has been considered [121], composed by a bulk field coil (coil A in Figure 8.4) and two couples of symmetrical compensation coils

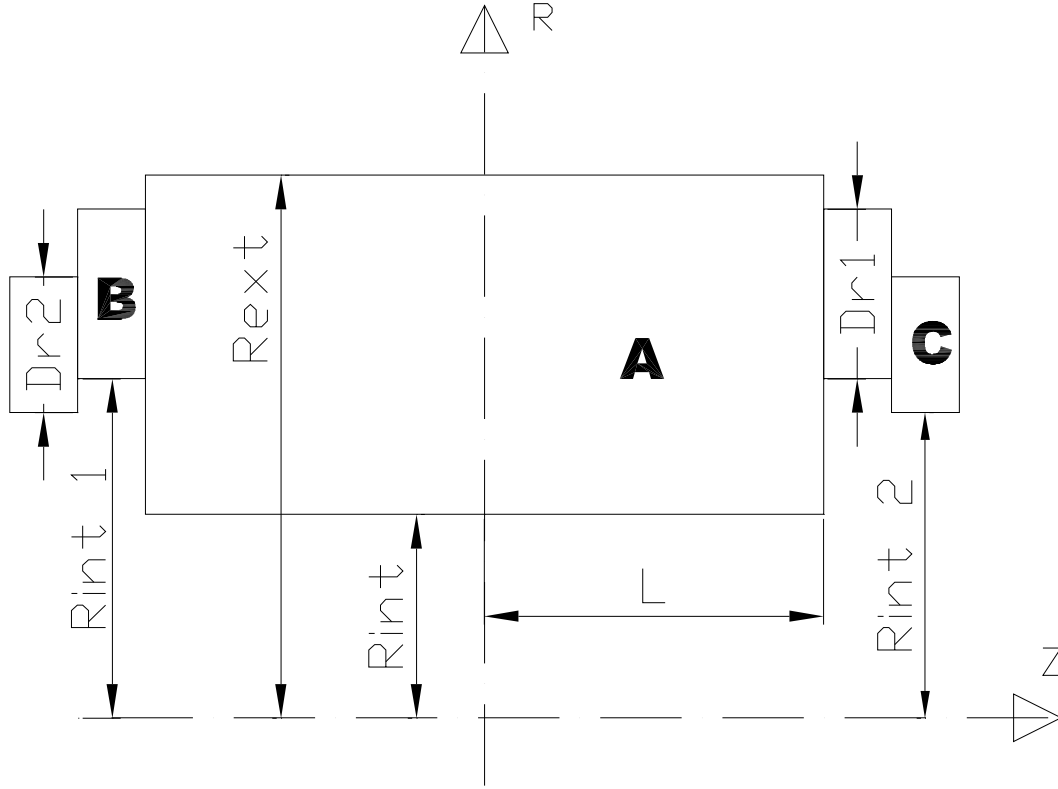


Figure 8.4: HTS magnet poloidal cross section describing the geometrical parameters.

(coils B and C in Figure 8.4). Each compensation coil is realised with just one double-pancake, while the number of double-pancakes in the bulk magnet is a design parameter. Only geometrical parameters have been considered for optimisation because the coils are series connected and then the feeding current, common to all of them, can be deduced from the knowledge of the desired field and of the tentative geometry. The optimal configuration is searched by varying the design parameters of the compensation coils, while the double-pancake coils forming the bulk magnet are forced to be equal, with the inner radius  $R_{int}$  fixed. Of course, symmetry is taken into account to reduce the number of design parameters to be optimised. This results in an objective function depending on 6 parameters: the thickness and the length of the bulk magnet, plus the inner radius and the radial thickness of the two compensation coils.

### 8.2.1 Optimisation strategy

The optimisation task has been performed in two phases. During the first one, a set of quasi-optimal configurations has been found by using an adaptive-hybrid GA. The results of the first phase have been used as starting points for a deterministic "deep" optimisation based on a deterministic gradient search.

The adaptive-hybrid GA, already described in Section 4.5.1, incorporates, inside a genetic structure, a deterministic search operator and an adaptive operators choosing rule. Here the possibility of a deterministic step is introduced with a directional mutation operator, that forces mutation in the direction opposite to the gradient: the gradient is computed by using numerically computed derivatives [11]. In addition, the operators occurrence probabilities are adapted during the evolution process to improve the rate of convergence and to escape from both the local minima and too early convergence: during the evolution, the probability of the recombination operator decreases, while the probabilities of the mutation and directional mutation operators increase.

In the "quasi-stochastic" phase the goal is thus to find some good starting points for the following deterministic step. In this second phase, the number of optimisation parameters decreases to 5. As a matter of fact, the bulk magnet length varies in a discrete way, as it depends on the number of double-pancakes. In the first step, it has been neglected the discrete character of this parameter, allowing a "continuous" optimisation. In the second phase, the discrete approximation of the optimum found is kept fixed, as the main interest is on the correction coils.

The coils radial thickness is a discrete parameter too, given by the number of tape turns, but it is treated as a continuous variable thanks to the small value of aspect ratio of tape.

Another difference from the previous step is the way adopted to locate the maximum field points, which is based on a sensitivity analysis approach applied to the relationship among the magnet shape and the field map in the outer region of the magnet. Even for optimised configurations, the most critical working point lays at the end of the magnet (Figure 8.5) due to the high radial field component still achieved in the outer coils. Therefore the region to be searched for the minimum critical current can be restricted to the external double-pancakes of the bulk magnet and to the two compensation coils.

In order to minimise the computational burden while keeping a suitable precision in the maximum field localisation, only the field variation due to difference between the present configuration and a reference one has been



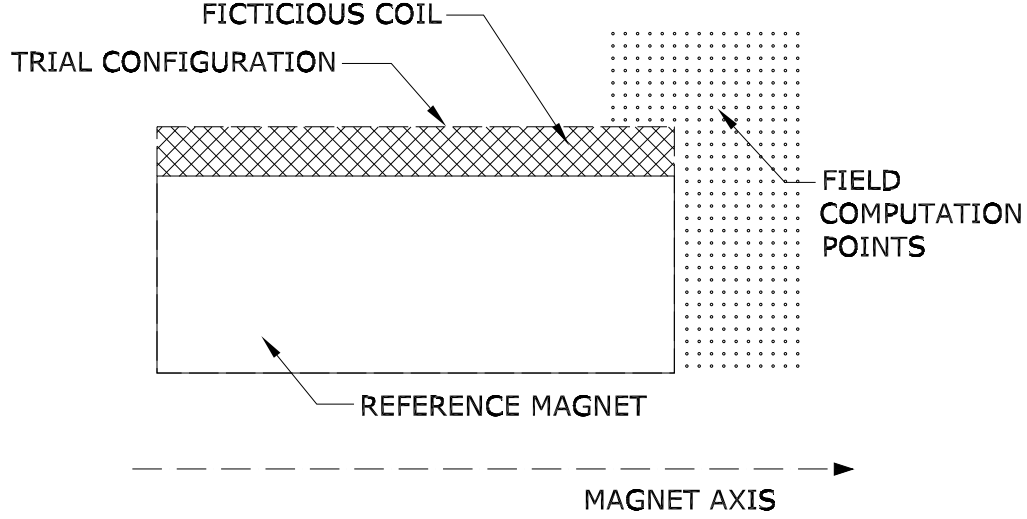


Figure 8.5: HTS magnet: sketch of the computational approach for the fast field map evaluation scheme (just one fictitious coil is reported).

computed at each step. As the procedure starts, a high accurate field interpolation based on spline functions is found for a set of predefined evaluation points in a region which includes the most external three coils. Then, in the due course of the optimisation, a coarser spline interpolation of the field due to a set of five fictitious coils (one for each DOF) representing the difference between the starting configuration and the current one is computed inside each of the three outer coils of the present configuration. Thanks to the linearity of the problem, the field map inside the outer coils is then assumed to be the superposition of the fine map and the coarser ones, and its maximum is localised. The difference field at each step is compared with the fine one: if it is higher than a fixed threshold, the fine map interpolation is updated by using the present configuration, which becomes the new reference geometry. In Figure 8.5 a schematic drawing is reported to illustrate the fast field computation scheme: note that, for the sake of simplicity, in this picture just one of the fictitious coil needed to compute the difference field is reported.

### 8.2.2 Results

The optimisation scheme described has been adopted for the design of a HTS double-pancake magnet with a central field of  $B_{des} = 4 \text{ T}$ . The inner bulk

|   | Min | Max |
|---|-----|-----|
| <b>L</b> (mm)                           | 30  | 100 |
| <b>R<sub>ext</sub></b> (mm)             | 35  | 90  |
| <b>R<sub>int1,2</sub></b> (mm)          | 25  | 90  |
| <b><math>\Delta R_{1,2}</math></b> (mm) | 5   | 65  |

Table 8.6: HTS magnet geometrical limits.

| Coil                         | Tape length<br>[m] | Length L<br>[mm] | R <sub>ext</sub><br>[mm] | R <sub>int</sub><br>[mm] | Turns |
|------------------------------|--------------------|------------------|--------------------------|--------------------------|-------|
| <b>Bulk</b>                  | 145                | 111              | 76.75                    | 25.0                     | 225   |
| <b>1<sub>st</sub> couple</b> | 66.5               | 7.4              | 76.74                    | 58.8                     | 78    |
| <b>2<sub>nd</sub> couple</b> | 98.5               | 7.4              | 72.75                    | 41.47                    | 136   |

Table 8.7: HTS magnet best configuration.

magnet radius has been set to  $R_{int} = 0.025$  m while the numerical ranges for the optimisation parameters are reported in Table 8.6. A population of 100 individuals has been bred for 50 generations, by adopting the operators probabilities according to the adaptive strategy described earlier. Then a deterministic step has been applied to the results achieved in the first stochastic phase.

The optimal solution found is reported in Table 8.7 and plotted in Figure 8.6: the width of each double-pancake is assumed equal to 7.4 mm. The working current to achieve the desired field is  $I = 67.2A$ , while the whole amount of superconductor tape for the magnet is about 2500 m.

The same central field can be achieved also with a standard solenoid configuration with optimised aspect ratio and the same inner radius. However, this latter configuration requires about 2800 m of superconductor, therefore more than 10% tape length can be saved with our optimised configuration.

In Figure 8.7 the field distribution at one end of the magnet is shown, in the case of presence and absence of the two outer double-pancake "correcting" coils. Both field distribution are normalised with respect to the central field. The figure shows clearly the effect of the outer coils, which modify the field distribution in the terminal region of the magnet, decreasing the radial field component and allowing to achieve higher critical current values.

### 8.3 Sensitivity analysis on tolerances

*"If you get enough data, whatever thing can be demonstrated by statistical methods" (from The Murphy's Law [122])*

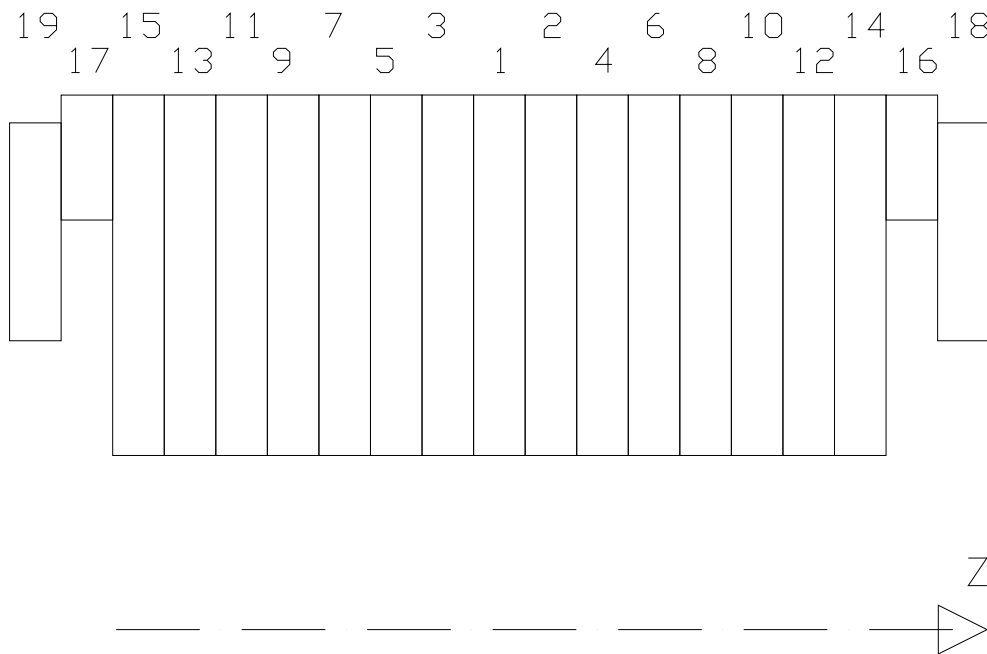


Figure 8.6: Proposed HTS magnet configuration.

As already recalled in Section 4.5.2, the available performances of an electromagnetic device can be strongly affected by manufacturing and assembling tolerances which make the actual machine somehow different from the project one. In particular, for the optimal design of superconducting magnets for MRI, little changes to the device geometry can deeply degrade the field uniformity.

It has been shown that some device configurations are more sensible than other ones with respect to the performances by little changes in the building parameters. Therefore it is useful for the designer to use some tool capable to evaluate the sensitivity of a design solution to construction errors. An effective designer-aiding tool is here presented [51].

The device specifications are usually satisfied by a number of different magnet layouts. If the optimisation procedure is able to provide a set of solutions characterised by the same "field quality" (*i.e.* the level of homogeneity inside the VOI), the designer can have the opportunity to select the final configuration.

An important element in ranking the solutions could be the robustness against the manufacturing tolerances. Here a possible ranking is proposed through a Monte Carlo method, based on the dependence of the field quality with respect to the mechanical tolerances. The most attractive solution can

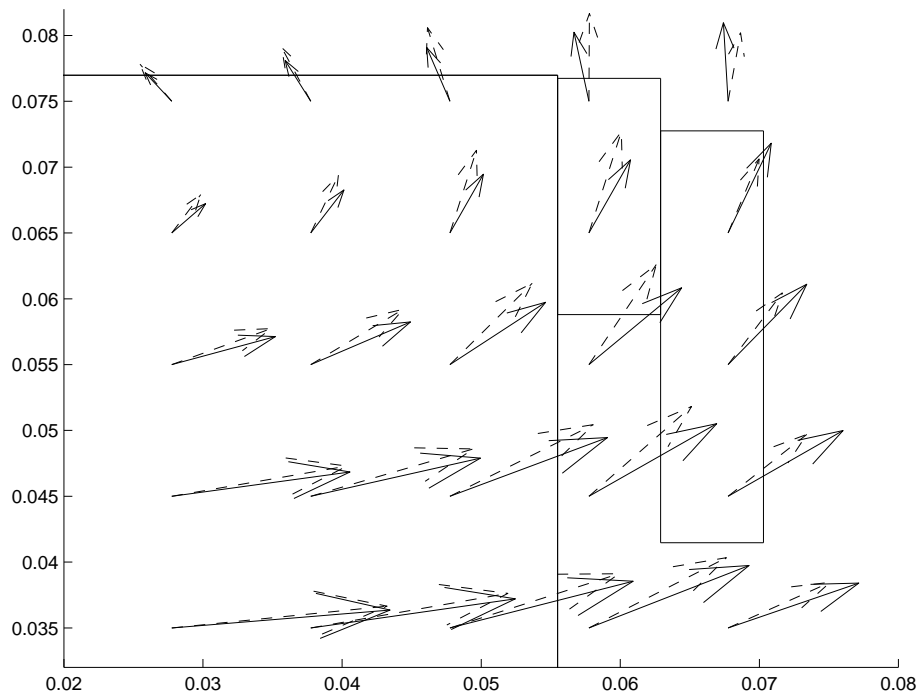


Figure 8.7: Optimised HTS magnet: field distribution in the terminal part of the windings, in the cases of presence (solid) and absence (dashed) of the compensation coils.

be chosen as the one characterised by the lowest values of the mean and the variance of the field dishomogeneity. In principle, other statistical moments can also be considered to have a wider description of the dependence of the magnet performance with respect to the design parameters.

In the following sections, the basis of the Sensitivity Analysis (SA) through statistical methods are briefly introduced; the concepts are then particularised to the design of MRI magnets, highlighting advantages and drawbacks; and finally a test case is presented and discussed to show the effectiveness of the approach.

### 8.3.1 Sensibility analysis in MRI magnet design

As a general rule, due to construction tolerances in coil manufacturing and magnet assembly, the actual performance of a MRI magnet usually does not meet the specifications, requiring an additional coil system to compensate such errors. Of course, a configuration less sensitive to constructional errors will be more attractive, because it would require lower correction. In addition, the knowledge of the homogeneity sensitivity with respect to the construction parameters also gives useful information for the magnet building phase, because it reveals the mechanical parameters requiring the most of attention in manufacturing.

It should be noted that the SA can also be performed with respect to others parameters than the design ones. As a matter of fact, in the design phase, in order to reduce the computational burden, the number of DOF has to be kept as low as possible. Afterwards, in the SA phase, further parameters can be considered. As an example, symmetry hypothesis can be abandoned to better describe the actual constructional issues.

In addition, it should be noticed that the derivative of the  $OF$  in the optimisation parameters vanish at the optimal solution because of the stationary condition. However, usually the  $OF$  is a complex function combining a number of elementary quality functions, including the homogeneity, the conductor volume and so on. In this case, the derivatives of each elementary function do not necessarily vanish, also because of numerical errors or optimisation issues, and their knowledge should be very useful.

The most common approaches to the error SA in the engineering practice can be classified in two main categories: Linearisation Methods (LM) and Statistical Methods (SM). In the latter category a prominent role is played by the Monte Carlo method (MC) [31] .

In the LM, the optimised configuration is perturbed by small variations of the design parameters. The performance of the "perturbed" device is then evaluated and, assuming a linear behaviour of the performance with

respect to the parameters, the sensitivity is evaluated with a simple finite difference approach. Such a method, although requiring a minimum amount of computation burden, allows only "local" SA. In addition, only the effect of one parameter at a time can be considered.

In the SM, on the other hand, a large number of different configurations are considered, by randomly varying the design parameters around a reference configuration according to their statistical properties, in a range given by the uncertainty on the various parameters. At the expense of a much higher computational burden, SM provide a better assessment of the device performance within the uncertainties space defined by the mechanical tolerances. In addition, the correlation between the design parameters and the device performance can be also easily estimated, giving information on the most sensible parameters.

Obviously, the reliability of a statistical approach depends on the level of accuracy reached in the probability density function (PDF) approximation; therefore, the number of configuration in the statistical population should be carefully chosen. In order to check the reliability of the analysis, a suitable set of estimators for the statistical moments of the device performance have to be introduced. It has been shown that the convergence of statistical moments estimators of the output variables represents a quite effective indicator of convergence in the approximation of PDF [123].

As already reported (see Section 2.3.2), in the case of the design of magnets for MRI, the main performance figure is the homogeneity of the magnetic field in the Volume of Interest (VOI). The axial-symmetric spherical harmonics expansion of the field (2.2) is here used. In Figure 8.8 the contour plot in ppm (part per million) of a typical field map in the high uniformity VOI region is shown.

The availability of analytical relationships allows to better verify the method convergence, preventing from undesirable effects due to the adoption of approximated formulae. As a matter of fact, from the numerical point of view the approximations or the truncation errors in evaluating the field homogeneity could act as a superimposed random noise which prevent from a correct interpretation of its statistical behaviour. Of course, once the statistical characterisation of the expansion coefficients has been performed, it is very easy to assess the statistical properties of the performance figure, namely the field homogeneity in the case of MRI magnets.

The moments obtained with the statistical analysis are powerful indices of the design robustness. In particular, the *mean value* indicates the most likely value of the performance, while the *variance* indicates the global robustness of the configuration. In addition, a number of effective information is also provided by the *cross correlation coefficients* among input (mechan-

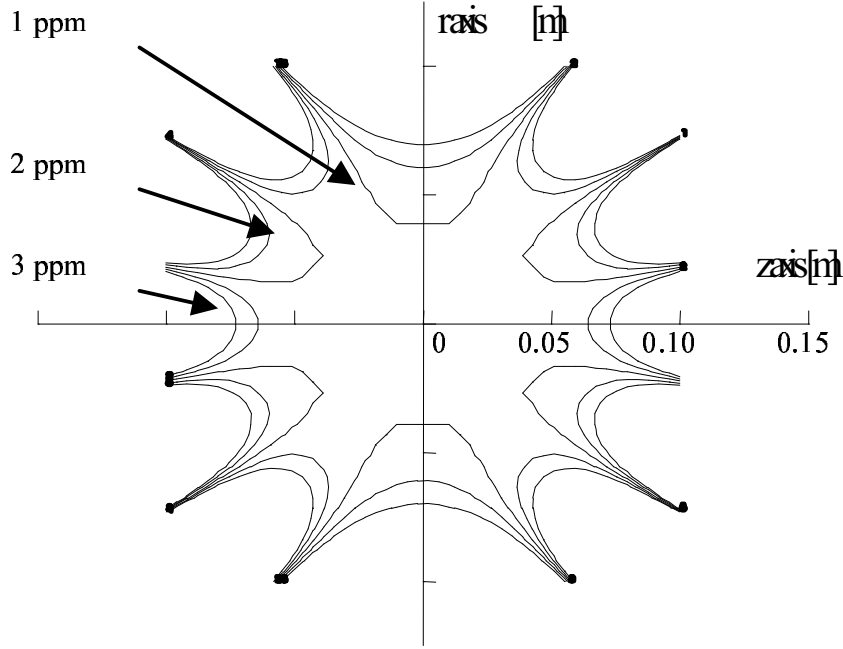


Figure 8.8: Typical MRI field contour plot in the VOI.

ical) parameters and output (performance figures) values. As a matter of fact, a cross correlation coefficient equal to 0 means that the two considered variables are uncorrelated, while a cross correlation coefficient equal to -1 or 1 means a linear dependence between the variables, which indicates that the impact of the considered input parameters on the device performance is very strong. Here the following estimator has been adopted for the cross correlation coefficients:

$$r_{hi} = \frac{\sum_{j=1}^N (p_{ij} - \bar{p}_i) (h_j - \bar{h})}{\sqrt{\sum_{j=1}^N (p_{ij} - \bar{p}_i)^2 \sum_{j=1}^N (h_j - \bar{h})^2}} \quad (8.6)$$

where  $i = 1, \dots, np$ , with  $np$  the number of input parameters,  $N$  is the number of MC runs,  $\bar{p}_i$  is the estimator of the mean of the  $i$ -th parameter,  $p_{i,j}$  is the value of  $i$ -th parameter at the  $j$ -th run,  $h_j$  is the  $j$ -th field homogeneity and  $\bar{h}$  the homogeneity mean.

Anyway, the cross correlation coefficients just indicate how close is the correlation among parameters, but do not give any indication about how large is the effect on the output parameters of variations of the input parameters.

On the other hand such a measure can be given by a non-normalised second order moment such as the variance, an estimator of which is defined as:

$$s_{hi} = \frac{1}{n-1} \sum_{j=1}^N (p_{ij} - \bar{p}_i) (h_j - \bar{h}) \quad (8.7)$$

with  $i = 1, \dots, np$ . These moments provide an indication about the most sensible parameters comparable to those provided by LM.

Moreover, the large number of cases needed to SM makes available a sampling of the relationship between the perturbed parameters and the performance figure. Therefore, as an additional fallout, it is possible to create a function interpolation of such a relationship in the complete tolerance domain. From this interpolation, which is not obliged to be linear, it is possible to estimate the complete "design sensitivity", in a way that can be considered a non-linear generalisation of the rationale behind the LM.

Thus, SM provide a much broader amount of information than LM but suffer from the serious drawback of requiring higher computation time to perform a reliable analysis. They appear to be particularly well suited for those cases in which the assessment of performance for a single test design can be accomplished with the use of analytical formulae.

### 8.3.2 Assessment of performance for the proposed algorithm

In this section, the analysis of a typical MRI magnet is performed by means of a statistical approach based on the MC method. In order to assess the achievement of the approach, while keeping the computational effort low, only those mechanical uncertainties which do not affect the coils axial-symmetry have been taken into account.

Such an analysis mainly provides the designer an easy and clear way to assess the performance of different configurations with respect to constructional issues. The most effective way to represent the performance of a configuration is therefore to use a number of charts providing the graphical description of the statistical behaviour of the input and output parameters.

On the other hand, synthetic information about the configuration robustness and sensitivity is given by the statistical moments of the input parameters and by the resulting moments of the field homogeneity (or, equivalently, the expansion coefficients  $A_{nm}$ ). In fact, for given statistical characteristics of the input parameters, the more similar is the mean field homogeneity to the nominal value and the lower is its variance, the more robust will be the configuration, while the higher is the covariance between a parameter and



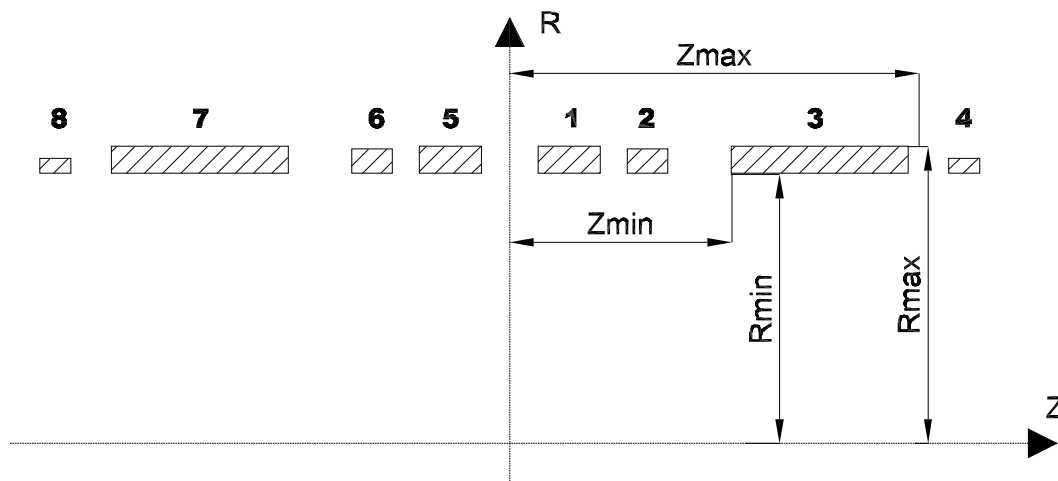


Figure 8.9: MRI magnet poloidal cross section with eight coils.

| Coil  | Zmin  | Zmax  | Rmin  | Rmax  |
|-------|-------|-------|-------|-------|
| 1 & 5 | 0.015 | 0.031 | 0.037 | 0.074 |
| 2 & 6 | 0.015 | 0.031 | 0.017 | 0.035 |
| 3 & 7 | 0.015 | 0.031 | 0.027 | 0.054 |
| 4 & 8 | 0.015 | 0.031 | 0.013 | 0.025 |

Table 8.8: MRI magnets: standard deviation of geometric tolerances in mm (mean=0).

the field homogeneity, the more sensible the configuration is with respect to that parameter.

In this example, the reference magnet configuration is composed by 8 superconducting coils: this design has been obtained by means of an optimised design method. In the nominal configuration, the device produces a central field of 3 T with a field homogeneity of 5 ppm over a 10 cm diameter VOI: the magnet poloidal cross section is sketched in Figure 8.9. The same figure also shows for one coil the geometrical parameters affected by the random uncertainties in the MC analysis. The mechanical tolerances have been modelled by using Gaussian distributions with variances chosen coherently with their confidence interval, as previously described. In Table 8.8, the standard deviations of the random uncertainties are reported, where the mean values are zero: the resulting total number of independent random variables is 32.

An important issue is the reliability of the MC simulation, which in turn depends on the number of runs in the statistical analysis. A possible way

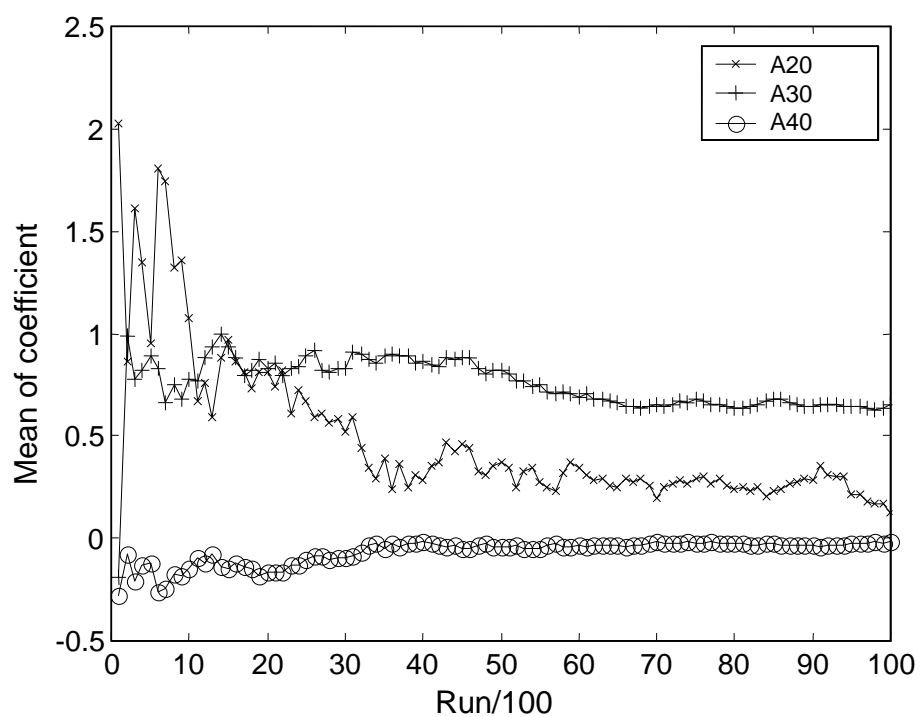


Figure 8.10: MC analysis of MRI magnets: the means of the first three field harmonic expansion coefficients against the number of runs.

to verify the convergence of the main performance figures towards meaningful statistical quantities is to check the stability of the statistical moments (*i.e.* mean, variance or even higher order statistics) versus the number of configurations. In Figure 8.10, it is reported the behaviour of the average of the coefficients  $A_{20}$ ,  $A_{30}$ ,  $A_{40}$  in ppm against the number of runs: in these tests, the convergence of the analysis was achieved after 10000 runs. In Figure 8.11, the PDF obtained for the  $A_{30}$  coefficient is plotted: the distribution has a mean of 0.7 and a standard deviation of 9.3. On the same graph, a normal (Gaussian) PDF with the same mean and standard deviation is also plotted.

Such information for each expansion coefficients is very useful to the design of a *shimming* corrective system, as the typical MRI magnet shimming system is composed by independent sets of coils, each specialised to counteract one of the terms  $A_{nm}$ . Therefore the knowledge of the coefficients PDF makes it possible to determine the geometrical and electrical parameters of the shim coils.

The PDF of the field homogeneity is non symmetric (Figure 8.12) with respect to the reference configuration value (equal to 5.723) and shows the following values: mean=41 ppm, standard deviation=24, maximum value=162 ppm, minimum value=5 ppm.

The Figure 8.13 reports the covariance coefficients among the field coefficient  $A_{30}$  and the input variables of the MC analysis. Such a plot can be useful to reveal the most sensible project parameters and it can also give useful information about the convergence of the simulation. In fact, homologous parameters of symmetric coils should show the same modulus of the covariance. For this purpose, in Figure 8.13 the covariance values have been clustered for each of the 8 coils using the same shading for corresponding parameters.

### 8.3.3 Section summary

A statistical method to assess the effects of manufacturing tolerances on the field homogeneity for an MRI magnet has been presented. The method is useful to evaluate the robustness of a design solution giving more information than a deterministic approach. Results of such methodology can provide a clear outline of the performances range of the actual device. The statistical behaviour of the field harmonic coefficient expansion, predicted by the presented approach, is also important for the designer to determine the shimming system, after a magnet configuration has been selected.

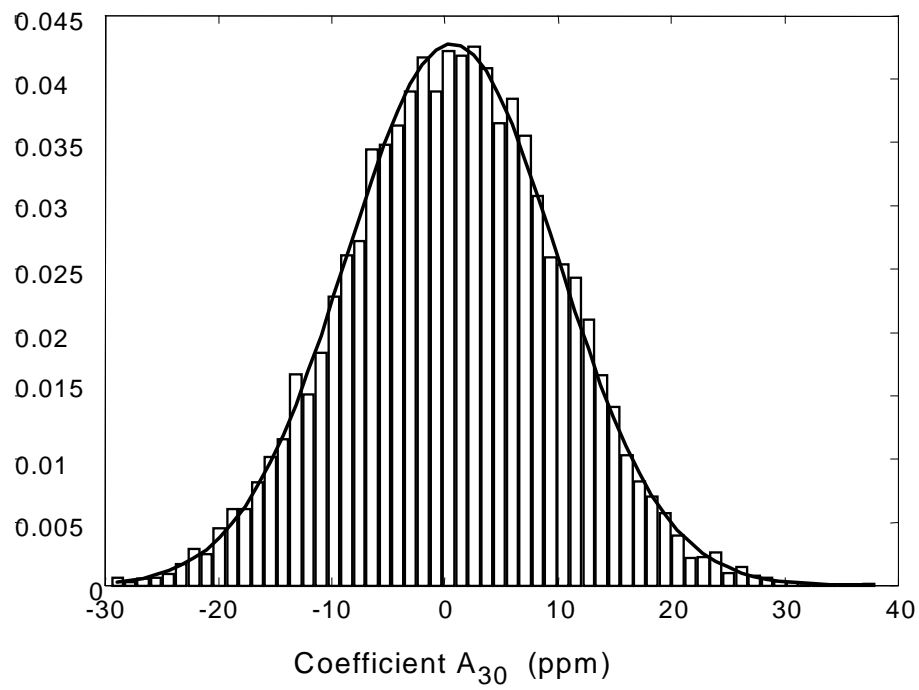


Figure 8.11: MC analysis of MRI magnets: PDF plot of coefficient  $A_{30}$  (mean=0.7, standard deviation=9.3) and the normal PDF with same mean and standard deviation, in continuous line.

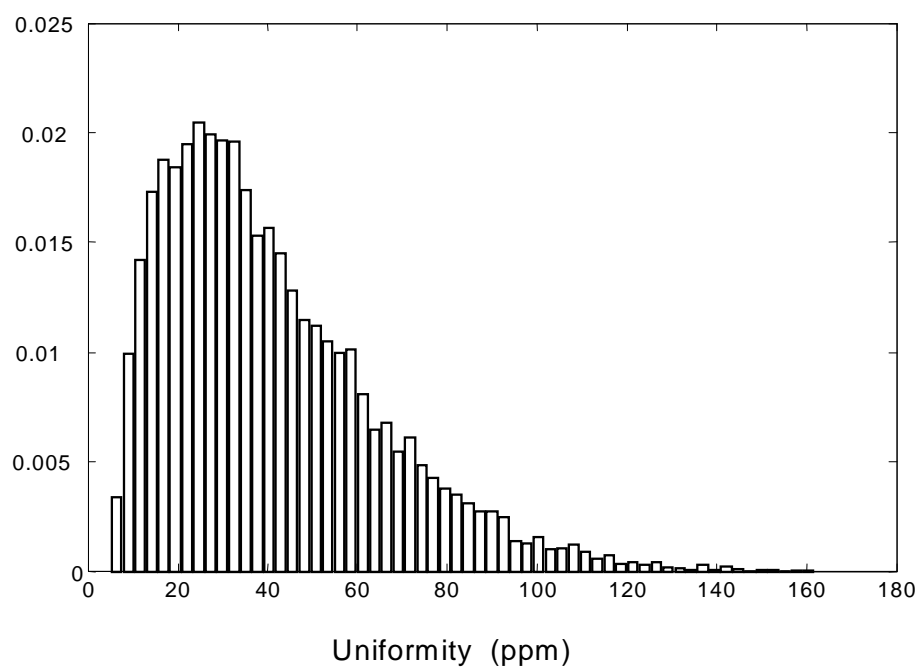


Figure 8.12: MC analysis of MRI magnets: PDF plot of uniformity in ppm: mean=41, standard deviation=24, maximum value=162, minimum value=5.

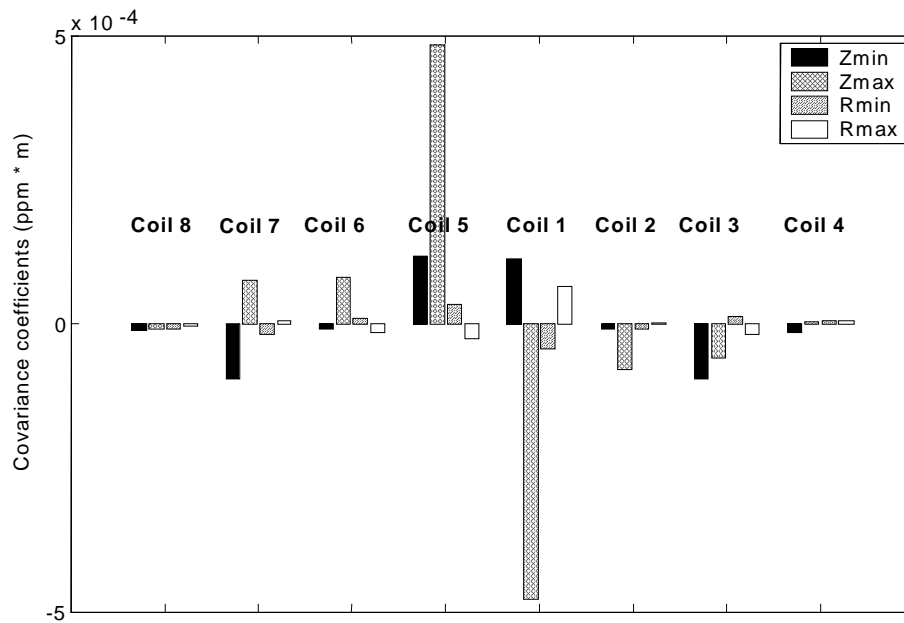


Figure 8.13: MC analysis of MRI magnets: histogram of covariance coefficients of input variables with  $A_{30}$  for each coil.

## 8.4 Marides: an industrial tool

The previous research results have been applied to the development of an industrial-oriented design tool. In the framework of the CREATE (Consorzio per la Ricerca e le Applicazioni Tecniche dell'Elettromagnetismo, Napoli) consortium, a research contract has been exploited for the Ansaldo CRIS (Consorzio Ricerche Innovative per il Sud): the main goal of the contract is to study and to implement methodologies for the optimal design of Magnetic Resonance Imaging (MRI) magnets and to develop a computer code able to help the designer for such a task.

Following the specifications of the industrial partner, a design environment has been implemented by using the Matlab language: the resulting code is named *Marides*, which stands for "Magnetic Resonance Imaging Design". *Marides* is characterised by an easy-to-use graphical interface (GUI) in such a way to be effectively used also by people not-expert in optimisation techniques. A typical GUI screen (see Figure 8.14) shows in the upper left corner a text windows listing input or results data; in the lower left corner a graphical window with the magnet coil sections, where in each coil section is sketched a map of the current density ratio with respect to the critical one; in the lower right corner, another graphical window plots the magnetic flux

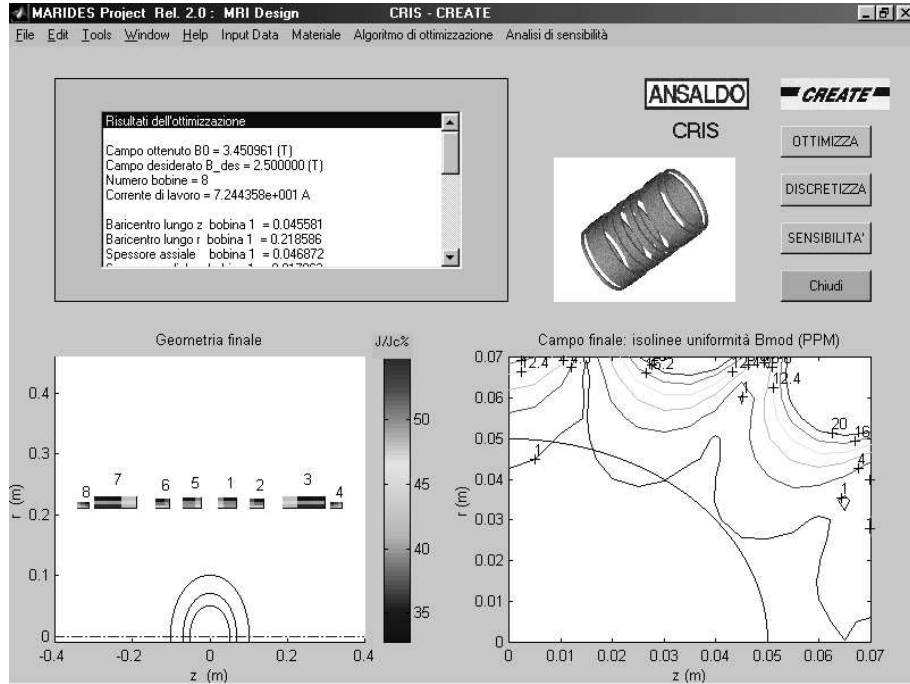


Figure 8.14: Marides GUI.

density field in the VOI region. The input data can be inserted by using pop-down menus commands or, for the expert user, by a text file.

The main topics about the MRI magnets design are already been presented in Section 2.3.2 and 8.3.1. The Marides code adopts two deterministic optimisation strategies: a quadratic quasi-Newton and a simplex algorithm [13]. As a general rule, the deterministic strategies are a much more "local search" approach than the stochastic ones, being strongly affected by the selection of the initial solution. But in an industrial design process, usually "good" initial designs are already available by the previous experiences and often the task is "just" to optimise them with respect to the customer specifications.

In a typical design session, the preliminary optimisation is performed by assuming the design geometrical variables can continuously vary. In the practical magnet construction, however, the coils are built by using superconducting wires which are wound in the caves of a drum: each coil is characterised by the two integer numbers of turns along the magnet axis and of superimposed radial layers. After the choice of a wire and of the assembling compactness factors (depending on the assembling procedure and tools), the optimal solution found has to be therefore discretised. The new solution is

usually somehow different from the optimal one and it has to be optimised again by keeping now the coils lengths and thicknesses fixed and letting the coils barycenter positions continuously move.

After the optimisation phase, with the Marides code it is possible to perform a Monte Carlo sensitivity analysis to evaluate the robustness of the proposed solution by the correlation indices among the coils geometrical variables and the field uniformity. In addition the MC analysis evaluates the (pseudo-)worst case configuration inside the parameters tolerances: this result is useful to properly design a possible *shimming* corrective coils system.

## 8.5 Solution robustness in optimal MRI magnets design

To evaluate the practical effectiveness of the method proposed in Section 4.5.3, the design of a MRI superconducting magnet has been considered [53]. As already reported, for the design of magnets for MRI, the main performance figure is the homogeneity of the magnetic field inside the VOI. The spherical harmonics expansion of the axialsymmetric field (2.2) is used and the lack of homogeneity  $Unif(\mathbf{x})$  for the magnet configuration  $\mathbf{x}$  is defined as in (2.3). The following  $OF$  has been used:

$$OF(\mathbf{x}) = w_1 Unif(\mathbf{x}) + w_2 Vol(\mathbf{x}) + w_3 Comp(\mathbf{x}) \quad (8.8)$$

where  $Vol(\mathbf{x})$  is the magnets volume, computed, with good approximation, as

$$Vol(\mathbf{x}) = \sum_{coils} 2\pi R_{min} \Delta Z \Delta R \quad (8.9)$$

and normalised by the maximum allowed coils volume, and  $Comp(\mathbf{x})$  is a measure of the compactness of the device, defined as the overall length of the magnet normalised by the maximum allowed length. The weights in (8.8) have been set to  $w_1 = 0.4$  and  $w_2 = w_3 = 1$ . It should be noticed that the volume of the magnets determines the total amount of used superconductor and therefore it provides an important figure of the device cost.

The main goal of the device is a central magnetic field of 3 T with a field homogeneity of 2 ppm over a 10 cm diameter spherical volume. The magnet configuration treated here is composed by 6 superconducting coils: a typical magnet poloidal cross section is sketched in Figure 8.15. In the same figure are also reported, for one coil, the geometrical parameters supposed to be affected by the random uncertainties, *i.e.* the coils inner radius  $R_{min}$ ,



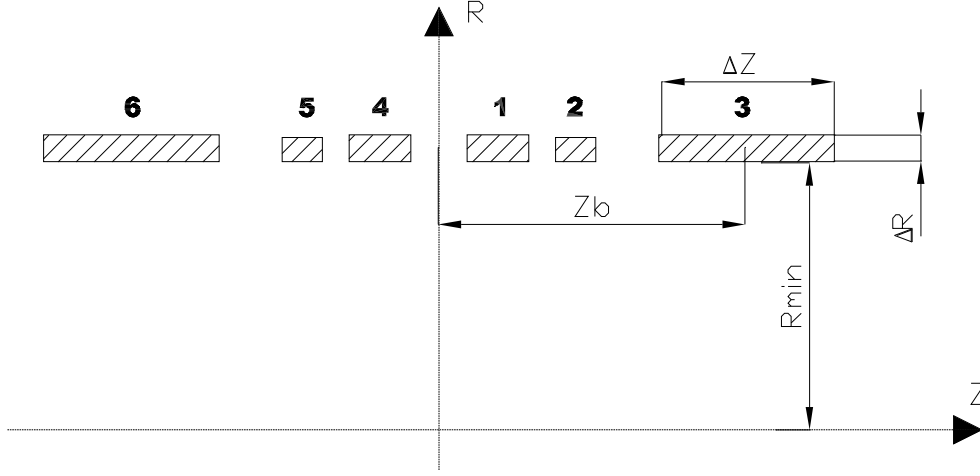


Figure 8.15: MRI magnet poloidal cross section with six coils.

the coils barycentre axial coordinates  $Z_b$ , the coil length  $\Delta Z$  and the coil thickness  $\Delta R$ . Due to technical reasons, the inner radii of all the coils are assumed to be the same. The coils are symmetric with respect to the  $z = 0$  plane: therefore the total number of independent variables is 10.

The mechanical tolerances has been modelled by using Gaussian distributions with variances chosen coherently with their confidence interval. The modified  $\overline{OF}$  is defined as in (4.16). The tolerances are assumed to be the same for all design geometrical parameters and equal to 0.1 mm. with a Gaussian PDF with  $\sigma = 3.8823 \times 10^{-5}$ . The normalised weights in (4.16) assume the values of  $P_1 = P_3 = 0.1922$  and  $P_2 = 0.6156$ .

A preliminary analysis by GA has provided a set of four different magnets layouts, each one corresponding to a local minimum of the  $OF$ . The geometrical parameters and the  $OF$  values are reported in Table 8.9 for the four magnets. The first three coils of the four solutions are sketched in Figure 8.16. We can see that the magnet A, C and D layouts are very similar: one of the difficulties of many engineering optimisation problem is that the local minima can be very close in the search space but often separated by regions of unfeasible solutions.

By ranking the magnets by the values of the  $OF$ , the best solution results the magnet A and the worst one is the magnet B. Even if, for this multidimensional space problem, it is not easy to visualize in some way the geometrical behavior of an  $OF$  in the search space, we can imagine that an attraction region is linked to each local minimum, in the same way as for the simple mono-dimensional previous test problem in Section 4.5.3.

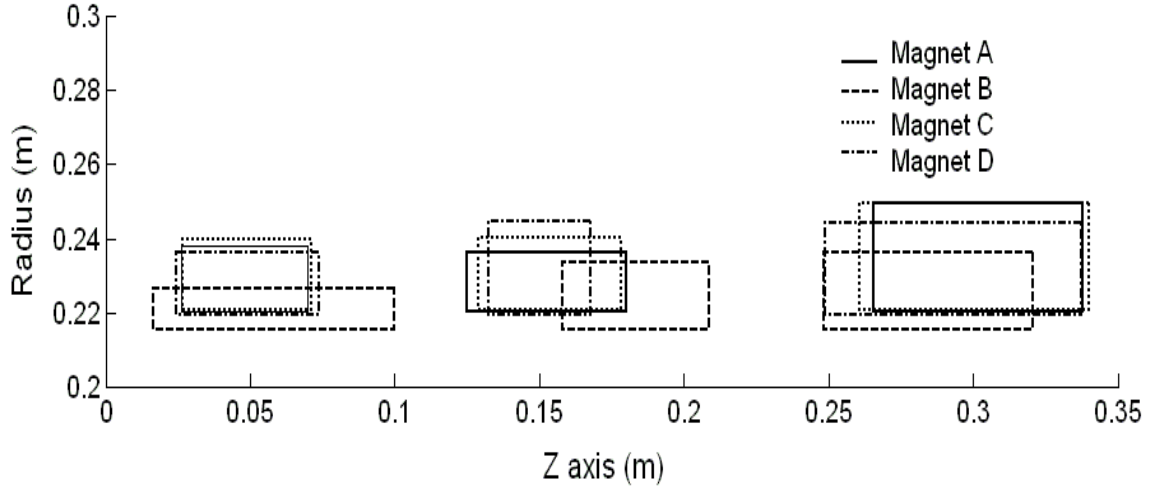


Figure 8.16: Different MRI magnet solution layouts: coils 1, 2 and 3.

|              | Magnet A | Magnet B | Magnet C | Magnet D |
|--------------|----------|----------|----------|----------|
| $R_{\min}$   | 0.2204   | 0.2155   | 0.2210   | 0.2198   |
| $Z_{b,1}$    | 0.0482   | 0.0582   | 0.0488   | 0.0491   |
| $\Delta Z_1$ | 0.0437   | 0.0835   | 0.0446   | 0.0495   |
| $\Delta R_1$ | 0.0179   | 0.0110   | 0.0190   | 0.0164   |
| $Z_{b,2}$    | 0.1527   | 0.1833   | 0.1536   | 0.1503   |
| $\Delta Z_2$ | 0.0551   | 0.0505   | 0.0490   | 0.0352   |
| $\Delta R_2$ | 0.0159   | 0.0183   | 0.0192   | 0.0251   |
| $Z_{b,3}$    | 0.3019   | 0.2845   | 0.3004   | 0.2932   |
| $\Delta Z_3$ | 0.0724   | 0.0723   | 0.0792   | 0.0888   |
| $\Delta R_3$ | 0.0293   | 0.0209   | 0.0285   | 0.0245   |
| $OF$         | 33.71    | 74.95    | 36.32    | 37.00    |

Table 8.9: MRI magnets: coils dimensions (in meters) for the different magnets and  $OF$  values.

|                 | Magnet A | Magnet B | Magnet C | Magnet D |
|-----------------|----------|----------|----------|----------|
| $OF$            | 33.71    | 74.95    | 36.32    | 37.00    |
| $\overline{OF}$ | 46.54    | 122.51   | 46.49    | 58.03    |

Table 8.10: MRI magnets: robustness for different magnets.

In order to compare the solutions also on the basis of the robustness, in Table 8.10 the values of the  $OF$  and of the modified  $\overline{OF}$  for each of the previous magnets are reported. By ranking the magnets by the values of the modified  $\overline{OF}$ , now the best solutions is the magnet C and the worst one is again the magnet B. The use of the modified  $\overline{OF}$  can be therefore used by the designer as a post-processing tool to add the robustness analysis to the optimisation phase.

In addition, the modified  $\overline{OF}$  expression has been directly inserted in the GA for the evaluation of the individuals fitness. By starting the evolution from the same initial populations used before, a new layout not similar to any of the previous magnets has been found as global minimum: this solution (magnet E, in Table 8.11) exhibits a modified  $\overline{OF}$  value of 45.71 and this is the lowest found value. The unmodified  $OF$  value of the new solution is a quite good 42.66, which is bigger than the best values of Table 8.10: therefore this solutions would be hardly selected by the optimisation process by using the standard  $OF$  expression. As shown for the demonstration example, the modification of the  $OF$  causes little movements of the minima in the search space: in this multidimensional search space problem, it is not easy to show if the new minima are in the same attraction regions than the previous solutions layouts.

## 8.6 Robust design and Biodiversity

The knowledge of the Pareto Front of the problem and the SA of the different Pareto optimal solutions proposed in Section 4.5.5, can be used for the choice of a possible solution for some particular design requirements, allowing the Decision Maker to take into account both the design robustness and the importance of different weighting of the various partial objectives.

To test the method proposed in Section 4.5.5, the TEAM 22 problem with three parameters has been selected: the IGA with different  $OF$ s has been used to find the Pareto optimal solutions. Multiple runs have been performed and nine non-dominated solutions have then been retained to provide an estimate of the Pareto Front. The resulting points of the Pareto Front are plotted in Figure 8.17, where the first objective  $F_1$  is the energy term in

|                 | Magnet E |
|-----------------|----------|
| $R_{min}$       | 0.2202   |
| $Z_{b,1}$       | 0.05064  |
| $\Delta Z_1$    | 0.0533   |
| $\Delta R_1$    | 0.01782  |
| $Z_{b,2}$       | 0.1578   |
| $\Delta Z_2$    | 0.06251  |
| $\Delta R_2$    | 0.01571  |
| $Z_{b,3}$       | 0.2968   |
| $\Delta Z_3$    | 0.09126  |
| $\Delta R_3$    | 0.02566  |
| $OF$            | 42.66    |
| $\overline{OF}$ | 45.71    |

Table 8.11: MRI magnets: most robust solution found.

(3.19) and the second objective  $F_2$  is the stray field term. For this "real case" problem, it is not possible to give indications about the Pareto Front to be connected or not, as made for the analytical case in Section 4.1.1.

Monte Carlo analysis has been then performed for a tolerance of 0.01 mm on the three design parameters, with 5000 runs for each point of the Pareto Front. A so narrow and non-realistic tolerance range is a consequence of the high sensibility of this benchmark problem to small variations of the design parameters. As examples, the PDF for the optimal point related to the weight  $w_1 = 0.2450$  is reported in Figure 8.18 for the objective  $F_1$  and in Figure 8.19 for the objective  $F_2$ . For each run of MC analysis, the mean values  $\mu$  and the standard deviations  $\sigma$  of the PDF for the  $F_1$  and  $F_2$  objectives are computed.

In Table 8.12 the values of the differences between the mean and the reference values for each point is reported together with the standard deviation. Note that the standard deviation for the second objective (the magnetic stray field) is at least three orders of magnitude less than the first objective (the stored energy) and therefore the magnetic stray field is statistically much less sensible to small design variations than the stored energy. The differences between the mean and the reference values of objectives show a non-uniform behaviour of the Pareto points, with some points (for instance see the rows 5, 7 and 8 in Table 8.12) subjected to statistical worsening of both objectives from small design changes: these can be indicated as points worse than the other ones.

From a "Decision Maker" point of view, such information is quite relevant, as it allows to select configurations with smallest energy sensitivity as the stray field is rather not sensitive to uncertainties.

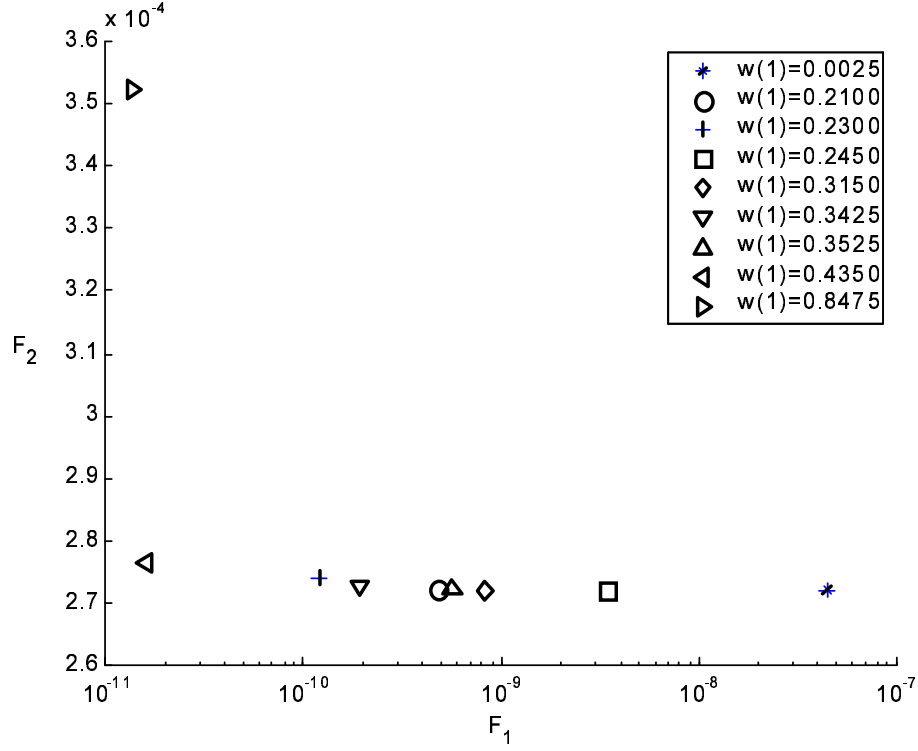


Figure 8.17: Pareto Front for the TEAM 22 problem.

|                               | $\mu(\mathbf{F}_1) - \mathbf{F}_1$ | $\mu(\mathbf{F}_2) - \mathbf{F}_2$ | $\sigma(\mathbf{F}_1) * 1\text{e} - 11$ | $\sigma(\mathbf{F}_2) * 1\text{e} - 14$ |
|-------------------------------|------------------------------------|------------------------------------|---|---|
| <b>w<sub>1</sub> = 0.0025</b> | -4.346e-8                          | 7.579e-11                          | 0.1030                                  | 0.1798                                  |
| <b>w<sub>1</sub> = 0.21</b>   | -3.588e-10                         | 1.802e-6                           | 0.0976                                  | 0.1844                                  |
| <b>w<sub>1</sub> = 0.23</b>   | 2.342e-8                           | -1.934e-6                          | 0.1016                                  | 0.1763                                  |
| <b>w<sub>1</sub> = 0.245</b>  | -1.307e-9                          | 1.759e-10                          | 0.1026                                  | 0.1812                                  |
| <b>w<sub>1</sub> = 0.315</b>  | 2.425e-8                           | 6.534e-7                           | 0.1069                                  | 0.1998                                  |
| <b>w<sub>1</sub> = 0.3425</b> | 1.6636e-8                          | -5.320e-7                          | 0.1011                                  | 0.1841                                  |
| <b>w<sub>1</sub> = 0.3525</b> | 1.933e-8                           | 4.167e-6                           | 0.0969                                  | 0.1832                                  |
| <b>w<sub>1</sub> = 0.435</b>  | 6.971e-10                          | 7.794e-5                           | 0.1120                                  | 0.2379                                  |
| <b>w<sub>1</sub> = 0.8475</b> | 2.697e-8                           | -8.010e-5                          | 0.1037                                  | 0.1628                                  |

Table 8.12: TEAM 22 problem: difference between mean value and reference one and standard deviation of partial objectives for different Pareto points.

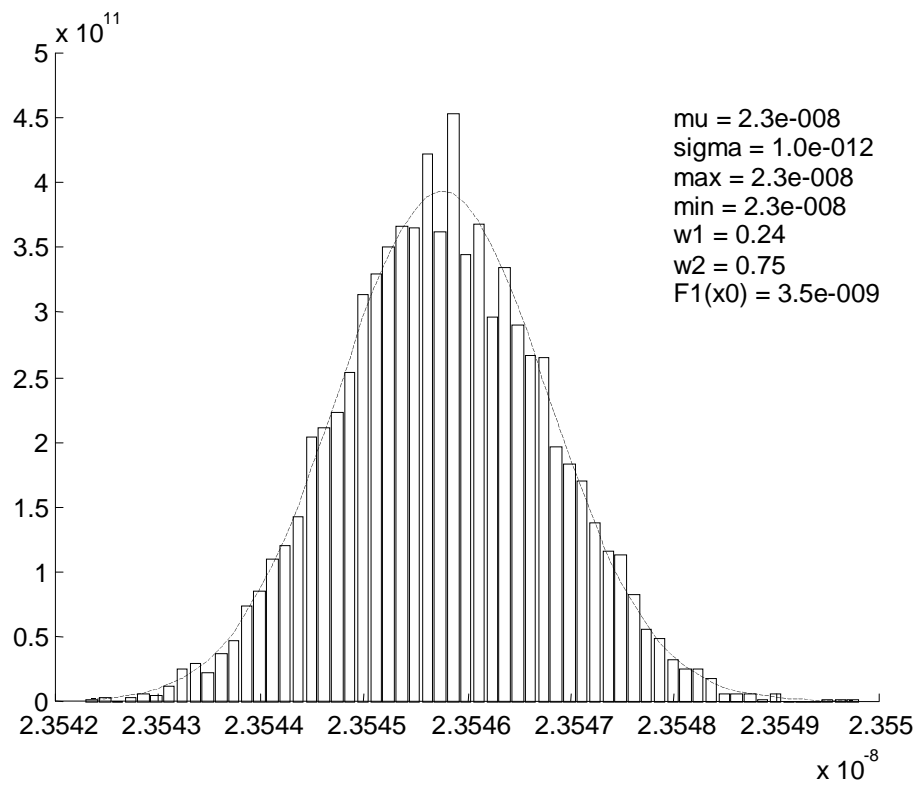


Figure 8.18: TEAM 22: PDF of objective  $F_1$  for  $w_1 = 0.245$  and the Gaussian distribution with the same mean and standard deviation (in dashed line).

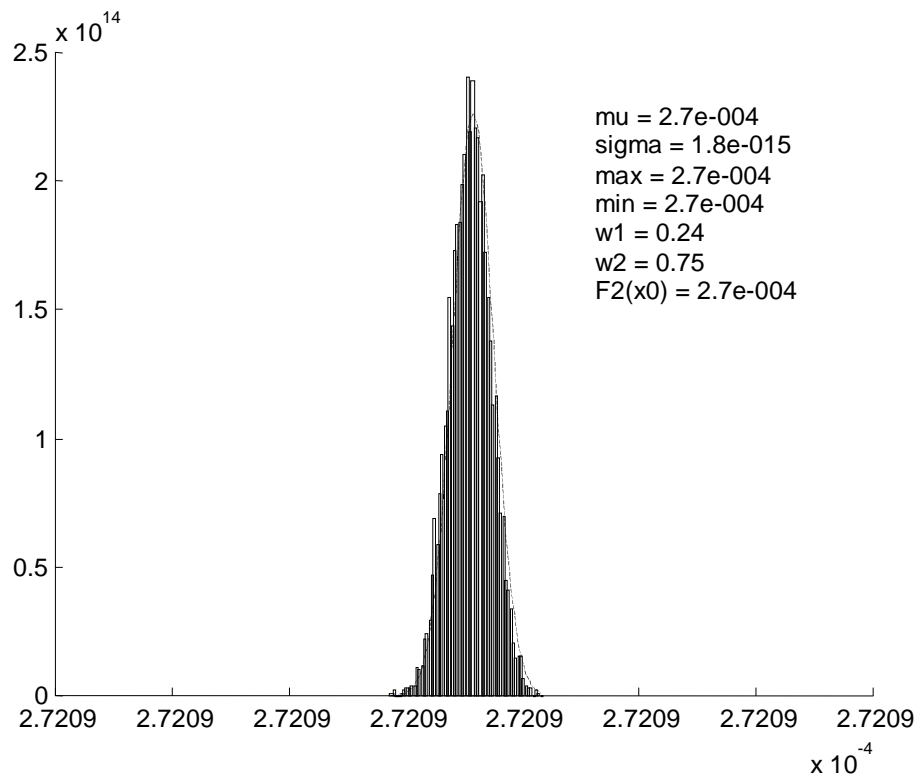


Figure 8.19: TEAM 22: PDF of objective  $F_2$  for  $w_1 = 0.245$  and the Gaussian distribution with the same mean and standard deviation (in dashed line).

### 8.6.1 Section summary

The effect of constructive parameters uncertainties on electromagnetic devices optimal design has been assessed by using Monte Carlo analysis. In order to analyse the impact of such uncertainties also in the case of multi-objective problems but not limiting the analysis to a particular selection of the relative importance of the different objectives, Pareto optimality has been adopted in the optimisation problem definition. Pareto Front has been generated by using multipopulation GA with biodiversity for the three parameters TEAM 22 benchmark problem, through a statistical analysis.

Different behaviour of the points has been evidenced with respect to the robustness of each design solution to construction tolerances. The proposed strategy can be used by the designer to rank and to compare the possible problem solutions, allowing to perform a robust design of electromagnetic devices.



# Chapter 9

## Conclusions

The design of superconducting magnets and other power devices can achieve a great benefit by the multi-objective optimisation techniques. The evolutionary models may efficiently be used for such a task: they are able to incorporate all objectives and constraints of real world design problems and to fulfill the high quality and robustness requirements today demanded by electric devices. There is a large research interest in these evolutionary optimisation models and new strategies and concepts are in the developing phase, often with a cross-fertilisation with other "soft computing" areas, such as fuzzy logic and neural networks.

In particular Genetic Algorithms have been extended to parallel computing area, gaining fast performances and acquiring new paradigms.

In this Thesis, all these topics have been introduced and discussed and new strategies have been proposed and applied to industrial relevant problems.

Two of the main results of this work are the two carried out "prototypes": the Marides code and the Beosun machine. They put in action many of the presented concepts.

Along the development phases of this Thesis, a number of scientific papers have been published or presented to conferences: they have been here already referenced [10], [51], [53], [80], [93], [103], [118], [121].

The research topics of this Thesis could be further developed in the following areas:

- Implementation of Pareto based evolutionary approaches with suitable definition of individuals ranking.
- Non-random generation of the initial populations: the use of concept of quasi-Monte Carlo strategy can improve the initial exploration of the search space.

- Linking of the optimisation codes with external "black boxes" programs, for problems where analytical solutions cannot be used. Real world electromagnetic problems are solved by using Finite Elements or Boundary Elements commercial codes: they can usually read input scripts and therefore can be inserted in an optimisation loop, as already done in Chapter 6 for the inverse problem resolution.

# Appendix A

## Code Fragments

### A.1 Weights for robust *OF*

```
function [w1,w2,w3,x1,x2,x3]=Compute_weights(DeltaX)
% -----
% Compute weights for
% Robust Optimisation with tolerance effect
%
% Tolerances = DeltaX
% Gaussian distribution
%
% See Section 4.5.3 for nomenclature
%
% by Dr. Marco Cioffi
% Department of Information Engineering
% Second University of Naples
% Aversa - Italy
%
% (15 November 2002)
%
ConfidenceRange = 0.99; % Same for all variables

% Evaluate sigma
k_sigma = fsolve('0.99-erf(x/sqrt(2))',1);
sigma = DeltaX/k_sigma;

Area_refus = cdf('Normal',-DeltaX,0,sigma); % Cut refused area
```

```
Area = 1-2*Area_refus; % Reduced area

a=-DeltaX/3;
b=+DeltaX/3;

% Points x1, x2, x3 : see Figure 4.4
x1 = -2*DeltaX/3;
x2 = 0;
x3 = +2*DeltaX/3;

w1=(cdf('Normal',a,0,sigma)-cdf('Normal',-DeltaX,0,sigma))/(a+DeltaX)/Area
w2 = (cdf('Normal',b,0,sigma)-cdf('Normal',a,0,sigma))/(b-a)/Area
w3 = w1

somma = w1+w2+w3

% Normalised weights
w1=w1/somma;
w2=w2/somma;
w3=w3/somma

% End of function
```

## A.2 IGA Aggression: create new MPI communicators

```

c Create new communicators
    Subroutine Create_SubComm_ECT(size_slave,
    &          process_ranks, nslave, isslave, nrank, my_COMM, my_rank,
    &          my_island, my_rank_subCOMM, size_subCOMM,
    &          size_island, slave_in_island)

c For 3 islands on 6 slaves
c isslave = 1 : it is a slave process of a multiple island where
c          nslave is the number of the island
c isslave = 255 for master
c process_ranks = list of the ranks for the new group
c nslave(i) = island of the process i
c nrank(i) = local master process of island i

c by Dr. Marco Cioffi
c Department of Information Engineering
c Second University of Naples
c Aversa - Italy
c
c (15 November 2002)

    implicit none
    include 'mpif.h'

    integer size, size_island, size_slave, slave_in_island

c Maximum number of slaves
    integer max_slaves
    parameter (max_slaves=20)

    integer process_ranks(0:max_slaves-1), nslave(0:max_slaves-1)
    integer proc, isslave(0:max_slaves-1), count1, nrank(0:max_slaves-1)
    integer my_rank_subCOMM, size_subCOMM, group_subCOMM(0:max_slaves-1)
    &          , subCOMM(0:max_slaves-1)
    integer i, j, my_COMM, my_rank, my_island, iisland,
    &          group_world, ierror, my_rank_world

```

```

integer ii, jj

call MPI_COMM_RANK(MPI_COMM_WORLD,my_rank_world,ierror)
call MPI_COMM_SIZE(MPI_COMM_WORLD,size,ierror)

c Number of islands: c 3 islands with groups of two/three
processes
    size_island = 3
    slave_in_island = size_slave/size_island

c Get the group underlying MPI_COMM_WORLD
    call MPI_COMM_GROUP(MPI_COMM_WORLD,group_world, ierror)

c Initialize isslave (also master)
    do i = 0, size_slave
        nslave(i) = 255
        isslave(i) = 255
    end do

c Loop on islands
    do ii = 1, size_island
        iisland = ii-1

c Create process map
        do jj=1, slave_in_island
            process_ranks(jj-1) = slave_in_island*(ii-1)+1
            nslave(slave_in_island*(ii-1)+1) = iisland
            isslave(slave_in_island*(ii-1)+1) = 1
        end do
        nrank(iisland) = slave_in_island*(ii-1)

c Create the new group group_subCOMM on the process_ranks
c list of ranks
        call MPI_GROUP_INCL(group_world, slave_in_island,
            & process_ranks, group_subCOMM(iisland), ierror)

c Create the new communicator subCOMM on the process_ranks
c list of ranks
        call MPI_COMM_CREATE(MPI_COMM_WORLD, group_subCOMM(iisland),

```

```
        &      subCOMM(iisland), ierror)

      end do
c End loop on islands

c Only in slaves (=subCOMM)
  if (isslave(my_rank_world) .ne. 255) then

c Assign island parameters
    my_island = nslave(my_rank_world)
    my_COMM = subCOMM(my_island)
    my_rank = my_rank_world

    call MPI_COMM_RANK(my_COMM,my_rank_subCOMM,ierror)
    call MPI_COMM_SIZE(my_COMM,size_subCOMM,ierror)

c End if: Only in slaves (=subCOMM)
  end if

  return
end
```

# Bibliography

- [1] Sen P. and Yang J.B. *Multiple Criteria Decision Support in Engineering Design*. Springer-Verlag, London, UK, 1998.
- [2] Pahl G. and Beitz W. *Engineering Design: A Systematic Approach*. Springer-Verlag, London, UK, II edition, 1996.
- [3] Cvetković Dragan. *Evolutionary Multi-Objective Decision Support Systems for Conceptual Design*. PhD Thesis, School of Computing, Faculty of Technology, University of Plymouth, July 2000.
- [4] Leyland Geoff. *Multi-objective optimisation applied to industrial energy problems*. PhD Thesis, Département de Génie Mécanique, École Polytechnique Fédérale de Lausanne, CH, 2002.
- [5] Andersson Johan. *Multiobjective Optimization in Engineering Design - Applications to Fluid Power Systems*. PhD Thesis, Linkping University, Sweden, 2001.
- [6] Feucht D.L. Design in Nature and the Nature of Design. *Origins & Design*, 19-2(37). Access Research Network, <http://www.arn.org/odesign/od192/od192.htm>.
- [7] Amir D. Aczel. *Probability 1*. Harcourt Brace, 1998.
- [8] Russenschuck S. Synthesis, inverse problems and optimisation in computational electromagnetics. *Int. Journal of Numerical Modeling*, 9:45–57, 1997.
- [9] Duchateau J-L., Spadoni M., Salpietro E., Ciazynski D., Ricci M., Libeyre P. and della Corte A. Development of high-current high-field conductors in Europe for fusion applications. *Superconductor Science and Technology*, 15(6):17–29, June 2002.



- [10] Cavaliere V., Cioffi M., Formisano A. and Martone R. Metodologie di progetto ottimo per magneti ad alto campo. In *Proc. of ET 2002 Riunione Nazionale dei Ricercatori di Elettrotecnica*. Udine, Italy, June 15-17 2000.
- [11] Cavaliere V., Formisano A., Martone R. and Primizia M. A genetic algorithm approach to the design of split coil magnets for MRI. *IEEE Trans. on Appl. Superconductivity*, 10(1):1376–1379, March 2000.
- [12] Garrett M.W. Axially Symmetric Systems for Generating and Measuring Magnetic Fields. Part I. *J. of Applied Physics*, 22(9):1091–1107, Sept. 1951.
- [13] Fletcher R. *Practical Methods of Optimization*. John Wiley & Sons, II Ed., 1987.
- [14] Sen P. Communicating preferences in multiple-criteria decision-making: the role of the designer. *J. Engineering Design*, 12(1):15–24, 2001.
- [15] Cohon J.L. *Multicriteria programming: brief review and application.*, pages 163–191. Design Optimization. J. S. Gero (Ed.) - Academic Press, Orlando, FL, USA, 1985.
- [16] Papoulis Athanasios. *Probability, random variables and stochastic processes*. Series in Electrical Engineering. McGraw - Hill, IV edition, Dec. 2001. ISBN: 0072817259.
- [17] Cvetković D. and Parmee I.C. Preferences and Their Application in Evolutionary Multiobjective Optimization. *IEEE Trans. on Evolutionary Computation*, 6(1):42–57, Febr. 2002.
- [18] Deb Kalyanmoy. *Optimization for engineering design: Algorithms and examples*. Prentice Hall, New Delhi, 1995.
- [19] Alotto P. *et al.* Multiobjective optimization in magnetostatics: A proposal for benchmark problems. *IEEE Trans. on Magnetism*, 32:1238–1241, 1996.
- [20] Grover F.W. *Inductance Calculation*. Dover Publications Inc., New York, 1946.
- [21] Urankar L. Vector potential and magnetic field of current-carrying finite arc segment in analytical form. Part III: exact computation for

- rectangular cross section. *IEEE Trans. on Magnetism*, 18:1860–1867, 1982.
- [22] Nash John F. Jr. Noncooperative games. *Annals Math.*, 54:289–295, 1951.
- [23] Coello Carlos Artemio Coello. *An empirical study of evolutionary techniques for multiobjective optimization in engineering design*. PhD thesis, Department of Computer Science of the Graduate School of Tulane University, New Orleans, Louisiana, USA, Apr. 1996.
- [24] Pareto Vilfredo. *Cours d'Economie Politique*, volume I-II. F. Rouge, Lausanne, 1896.
- [25] Schatzer Ch. and Binder A. Design optimization of a high-speed permanent magnet machine with the VEKOPT algorithm. In *Conference Record of the 2000 IEEE Industry Applications Conference, Vol. 1*, 2000.
- [26] Van Veldhuizen David A. *Multiobjective Evolutionary Algorithms: Classifications, Analyses, and New Innovations*. PhD Thesis, Department of Electrical and Computer Engineering. Graduate School of Engineering. Air Force Institute of Technology, Wright-Patterson AFB, Ohio, May 1999.
- [27] Van Veldhuizen D.A. and Lamont G.B. Multiobjective evolutionary algorithms: Analyzing the state-of-the-art. *Evolutionary Computation*, 8(2):125–147, 2000.
- [28] Zitzler E. *Evolutionary Algorithms for Multiobjective Optimization: Methods and Applications*. TIK-Schriftenreihe Nr. 30, Diss ETH No. 13398, Swiss Federal Institute of Technology (ETH), Zurich, CH, Dec. 1999. Shaker Verlag, Germany, ISBN 3-8265-6831-1.
- [29] Andersson Johan. A survey of multiobjective optimization in engineering design. Technical Report LiTH-IKP-R-1097, Department of Mechanical Engineering Linköping University, Linköping University, Sweden, 2000.
- [30] Min-Kyu K. Yong-Hwan OH, Tae-Kyung C. and Hyun-Kyo J. Optimal design of electric machine using genetic algorithms coupled with direct method. *IEEE Trans. on Magnetism*, 35(3):1742–1745, May 1999.

- [31] Hammersly J.M. and Handscomb D.C. *Monte Carlo Methods*. John Wiley & Sons, 1964.
- [32] Powell M.J.D. Direct search algorithms for optimization calculations. *Acta Numerica, Cambridge University Press*, 7:287–336, 1998.
- [33] Wright M.H. *Direct search methods: once scorned, now respectable*, pages 191–208. Proceedings of the 1995 Dundee Biennial Conference in Numerical Analysis. D. F. Griffiths and G. A. Watson (eds.), Addison Wesley Longman, Harlow, UK, 1996.
- [34] Rechenberg Ingo. *Evolutionstrategie: Optimierung technischer Systeme nach Prinzipien der biologischen Evolution*. Fromman-Holzboog Verlag, Stuttgart, Germany, 1973.
- [35] Holland J.H. *Adaption in Natural and Artificial Systems*. Univ. of Michigan Press, Ann Arbor, MI, USA, 1975.
- [36] Fraser A. Simulation of genetic systems by automatic digital computers I: introduction. *Australian J. of Biological Science*, 10:484–491, 1957.
- [37] De Jong Kenneth A. *An Analysis of the behavior of a class of Genetic Adaptive Systems*. Doctoral dissertation, Univ. of Michigan, Ann Arbor, MI, USA, 1975.
- [38] Goldberg David E. *Genetic Algorithms in Search, Optimization and Machine Learning*. Addison-Wesley Pub. Co., 1989. ISBN: 0201157675.
- [39] Michalewicz Zbigniew. Heuristic methods for evolutionary computation techniques. *Journal of Heuristics*, 1(2):177–206, 1995.
- [40] Michalewicz Zbigniew. *Genetic Algorithms + Data Structures = Evolution Programs*. Springer-Verlag, New York, 1996.
- [41] Fonseca C.M. and Fleming P.J. Multiobjective optimization and multiple constraint handling with evolutionary algorithms—Part I: A unified formulation. *IEEE Transactions on Systems, Man, and Cybernetics, Part A: Systems and Humans*, 28(1):26–37, 1998.
- [42] Hinterding R. and Michalewicz Z. Your brains and my beauty: parent matching for constrained optimisation. In *Proc. of the Fifth Intern. Confer. on Evolutionary Computations*, pages 810–815, Anchorage, Alaska, USA, 1998.

- [43] Rasheed Khaled. An adaptive penalty approach for constrained genetic-algorithm optimization. In John R. Koza *et al.*, editor, *Genetic Programming 1998: Proceedings of the Third Annual Conference*, pages 584–590, University of Wisconsin, Madison, Wisconsin, USA, 1998. Morgan Kaufmann.
- [44] Deb Kalyanmoy. An Efficient Constraint Handling Method for Genetic Algorithms. *Comput. Methods Appl. Mech. Engrg.*, 186:311–338, 2000.
- [45] Crossley W.A. and Williams E.A. A study of adaptive penalty functions for constrained genetic algorithm based optimization. In *Proc. of the AIAA 35th Aerospace Sciences Meeting and Exhibit*. Reno, NV, Jan. 6-9 1997. AIAA Paper 97-0083.
- [46] Cormier D., O’Grady P. and Sanii E. A constraint-based genetic algorithm for concurrent engineering. *International Journal of Production Research*, 36(6):1679–1697, 1998.
- [47] Vieira D.A.G., Adriano R.L.S., Vasconcelos J.A. and Krähenbühl L. New Approach with NPGA for Solving Constrained Multiobjective Optimisation Problems. In *Proc. of the 10th IEEE Conference on Electromagnetic Field Computation - CEFC 2002*, Perugia, Italy, June 16-19 2002.
- [48] Hill Raymond R. A Monte Carlo study of genetic algorithm initial population generation methods. In Farrington P.A. *et al.*, editor, *Proc. of the 1999 Winter Simulation Conference*, Phoenix, Arizona, USA. SIGSIM ACM.
- [49] Wolpert D.H. and Macready W.G. No free lunch theorems for optimization. *IEEE Trans. on Evolutionary Computation*, 1(1):67–82, April 1997.
- [50] Magyar G., Johnsson M. and Nevalainen O. An adaptive hybrid genetic algorithm for the three-matching problem. *IEEE Trans. on Evolutionary Computation*, 4(2):135–146, July 2000.
- [51] Cavaliere V., Cioffi M., Formisano A. and Martone R. Improvement of MRI magnets design through sensitivity analysis. *IEEE Trans. on Appl. Superconductivity*, 12(1):1413–1416, March 2002.
- [52] Yamamoto A. *et al.* Analysis of Mechanical Tolerances of a Low- $\beta$  Quadrupole Magnet for the LHC. *IEEE Trans. on Appl. Superconductivity*, 10(1):131–134, March 2000.

- [53] Cioffi M., Formisano A. and Martone R. Increasing Design Robustness in Evolutionary Optimisation. In *Proc. of PMAPS 2002*, Napoli, Italy, Sept. 22-26 2002.
- [54] Alotto P., Magele C., Pfluegl H., Steiner G. and Weber A. Robust Optimization in Electromagnetic Design. In *Proc. of the 10th IEEE Conference on Electromagnetic Field Computation - CEFC 2002*, Perugia, Italy, June 16-19 2002.
- [55] Alotto P., Magele C., Renhart W., Steiner G. and Weber A. Robust Target Functions in Electromagnetic Design. In *Proc. of the IGTE 2002*, Graz, Austria, September 16-18 2002.
- [56] Bellman R. *Dynamic Programming*. University Press, Princeton, USA, 1957.
- [57] Chipperfield A.J. and Fleming P.J. The MATLAB genetic algorithm toolbox. In *IEE Colloquium on Applied Control Techniques Using MATLAB*, Jan. 26 1995.
- [58] The University of Sheffield, Automatic Control & Systems Engineering Department. Genetic algorithm toolbox download page. <http://www.shef.ac.uk/gaipp/ga-toolbox/>.
- [59] Luenberger D.G. *Linear and Nonlinear Programming*. Addison-Wesley, 1984.
- [60] R.H.C. Takahashi, J.A. Ramirez, J.A. Vasconcelos, R.R. Saldanha. Sensitivity analysis for optimisation problems solved by stochastic methods. *IEEE Trans. on Magnetics*, 37(5):3566–3569, September 2001.
- [61] Vollaie C., Nicolas L. and Nicolas A. Parallel computing for electromagnetic field computation. *IEEE Trans. on Magnetics*, 34(5):3419–3422, September 1998.
- [62] Iwashita T. and Shimasaki M. Algebraic multicolor ordering for parallelized iccg solver in finite-element analyses. *IEEE Trans. on Magnetics*, 38(2-1):429–432, March 2002.
- [63] Ansorge R.E. and Shaw N.R. Genetic algorithms for MRI magnet design. *IEEE Trans. on Appl. Superconductivity*, 12(1):733–736, March 2002.

- [64] Van der Steen A.J. and Dongarra J.J. Overview of Recent Supercomputers. <http://www.top500.org/ORSC/2002>.
- [65] Ansorge R.E., Carpenter T.A., Hall L.D., Shaw N.R. and Williams G.B. Use of parallel supercomputing to design magnetic resonance systems. *IEEE Trans. on Magnetics*, 10(1):1368–1371, March 2000.
- [66] Hernandez J., Bosque J.L. and Canto J. Brain activity detection in functional magnetic resonance imaging on heterogeneous cluster. In *Proc. of the 2nd IEEE/ACM International Symposium on Cluster Computing and the Grid (CCGRID 2002)*, Berlin, Germany, May 2002. IEEE.
- [67] Trinitis C., Schulz M., Eberl M. and Karl W. SCI-based LINUX PC-Clusters as a platform for electromagnetic field calculations. In *Proc. of the Sixth International Conference on Parallel Computing Technologies (PaCT-2001)*, pages 510–513. Springer-Verlag, 2001.
- [68] Jacques T., Nicolas L. and Vollaire C. Le calcul de champs électromagnétiques sur architectures MIMD. *Revue Internationale de Genie Electrique*, 2(2):185–214, 1999.
- [69] Cantù-Paz E. and Goldberg D.E. Efficient parallel genetic algorithms: theory and practice. *Computer Methods in Applied Mechanics and Engineering*, 186:221–238, 2000.
- [70] Cantù-Paz E. A survey of parallel genetic algorithms. IlliGAL Report 97003, Illinois Genetic Algorithms Laboratory, University of Illinois at Urbana-Champaign, Urbana IL, May 1997.
- [71] Cantù-Paz E. *Designing Efficient and Accurate Parallel Genetic Algorithms*. PhD Thesis, University of Illinois at Urbana-Champaign, 1999.
- [72] Cantù-Paz E. *Efficient and Accurate Parallel Genetic Algorithms*, volume 1 of *Genetic Algorithms and Evolutionary Computation*. Kluwer Academic, 2000. ISBN: 0792372212.
- [73] Ioan D., Ciuprina G. and Dumitrescu C. Use of stochastic algorithms for distributed architectures in the optimisation of electromagnetic devices. *IEEE Trans. on Magnetics*, 34(5):43–63, Sep. 1998.
- [74] Fan Y., Jiang T. and Evans D.J. The parallel genetic algorithm for electromagnetic inverse scattering of a conductor. *Intern. J. Computer Math.*, 79(5):573–586, 2002.

- [75] Cantù-Paz E. Designing efficient master-slave parallel genetic algorithms. IlliGAL Report 97004, Illinois Genetic Algorithms Laboratory, University of Illinois at Urbana-Champaign, Urbana IL, 1997.
- [76] Belding T.C. The distributed genetic algorithm revisited. In L. (Ed.) Eschelman, editor, *Proc. the Sixth International Conference on Genetic Algorithms*, pages 114–121, San Francisco, CA, 1995. Morgan Kaufmann.
- [77] Matsumura T. A parallel and distributed genetic algorithm on loosely-coupled multiprocessor systems. Master th., Grad. School of Engineering, Electrical and Information Engin., University of the Ryukyus, Japan, 1998.
- [78] Sarma J. and De Jong K. *An analysis of the effects of neighborhood size and shape on local selection algorithms*, pages 236–244. Parallel Problem Solving from Nature IV. Springer-Verlag, Berlin, 1996.
- [79] Bianchini R. and Brown C.M. *Parallel genetic algorithms on distributed-memory architectures*, pages 67–82. Atkins S., & Wagner A. S. (Eds.).
- [80] Cioffi M., Formisano A. and Martone R. Resources allocation strategy for distributed genetic algorithms: the case of electromagnetic design. In *Proc. of SCI 2001 5th World Multiconference on Systemics, Cybernetics and Informatics*, Orlando FL, USA, July 22-25 2001.
- [81] Herrera F. and Lozano M. Gradual distributed real-coded genetic algorithms. *IEEE Trans. on Evolutionary Computation*, 4(1):43–63, April 2000.
- [82] Cantù-Paz E. Migration policies, selection pressure, and parallel evolutionary algorithms. *Journal of Heuristics*, 7(4):311–334, 2001.
- [83] Cohoon J.P., Martin W.N. and Richards D.S. *Genetic algorithms and punctuated equilibria in VLSI*, pages 134–144. Parallel Problem Solving from Nature IV. Springer-Verlag, Berlin, schwefel, h.p., manner, r. (eds.) edition, 1991.
- [84] Munetomo M., Takai Y. and Sato Y. An efficient migration scheme for subpopulation-based asynchronously parallel genetic algorithms. In Forrest S. (Ed.), editor, *Proc. the Fifth International Conference on Genetic Algorithms*, page 649, San Mateo, CA, USA, 1993. Morgan Kaufmann.

- [85] Lin S.C., Punch W. and Goodman E. Coarse-grain parallel genetic algorithms: Categorization and new approach. In *Sixth IEEE Symposium on Parallel and Distributed Processing*, Los Alamitos, CA, USA, October 1994. IEEE Computer Society Press.
- [86] Martin W.N., Lienig J. and Cohoon J.P. *Island (migration) models: evolutionary algorithms based on punctuated equilibria*, chapter 6.3. Handbook of Evolutionary Computation. IOP Publishing Ltd, 1997.
- [87] Marin F.J., Trelles-Salazar O. and Sandoval F. *Genetic algorithms on LAN-message passing architectures using PVM: Application to the routing problem*, pages 534–543. Parallel Problem Solving from Nature III. Springer-Verlag, Berlin, Davidor Y., Schwefel, H.P., Manner, R. (Eds.) edition, 1994.
- [88] MPI standard. <http://www.mpi-forum.org/>.
- [89] Levine D. Users guide to PGAPack parallel genetic algorithm library. Technical Report ANL-95/18, Argonne National Laboratory, Argonne, IL, USA, January 1996.
- [90] Wikramaratna Roy. Pseudo-random Number Generation for Parallel Monte Carlo: A Splitting Approach. SIAM News Online, November 2000. <http://www.siam.org/siamnews/11-00/splitting.pdf>.
- [91] Fachat A. and Hoffmann K.H. Blocking vs. non-blocking communication under MPI on a master-worker problem. SFB393 Preprint 98-18, Inst. fur Physik, Technische Universitt Chemnitz, Germany, May 1998.
- [92] Cantù-Paz E. and Goldberg D.E. On the scalability of parallel genetic algorithms. *Evolutionary Computation*, 7(4):429–449, 1999.
- [93] Cavaliere V., Cioffi M., Formisano A. and Martone R. Robust design of High Field Magnets through Monte Carlo Analysis. In *Proc. of IGTE 2002 Conference*. Graz, Austria, Sept. 16-18 2002.
- [94] Dawkins Richard. *The Blind Watchmaker: Why the Evidence of Evolution Reveals a Universe Without Design*. Penguin Books Paperback, 1990.
- [95] Bowler John R. Inversion of eddy current data to reconstruct flaws by an optimisation process. *Inter. J. of Applied Electromagnetics in Materials*, 4:277–284, 1994.



- [96] Bowler John R. Review of eddy-current inversion with applications to non-destructive evaluation. *Inter. J. of Applied Electromagnetics in Materials*, 8(1):3–16, 1997.
- [97] Schiller D., Meier T. and Bical D. Improvement of the Reliability of Fatigue Crack Detection on Holes of Typical Aircraft Structures by using Multi-Frequency EC-Technique. In *ATA NDT Forum*. Albuquerque, New Mexico, USA, Sept. 27 - Oct. 1, 1998.
- [98] Glorieux C., Moulder J., Basart J. and Thoen J. The determination of electrical conductivity profiles using neural network inversion of multi-frequency eddy-current data. *J. Phys. D: Appl. Phys.*, 32(5):616–622, March 1999.
- [99] Albanese R., Formisano A., Martone R., Morabito C., Rubinacci G. and Villone F. Analysis of metallic tubes with ECT and neuro-fuzzy processing. *Int. J. Applied Electromagnetics and Mechanics*, 9(3):325–338, 1998.
- [100] Kreutzbruck M.v., Allweins K., Rhl T., Mck M., Heiden C., Krause H.J. and Hohmann R. Defect detection and classification using a SQUID based multiple frequency eddy current nde system. *IEEE Trans. on Appl. Superconductivity*, 11(1):1032–1037, 2001.
- [101] Chady T., Enokizono M. and Sikora R. Signal restoration using dynamic neural network model for eddy current nondestructive testing. *IEEE Trans. on Magnetics*, 37(5):3737–3740, 2001.
- [102] Grman J., Ravas R. and Syrovà L. Application of Neural Networks in Multifrequency Eddy-Current Testing. *Measurement Science Review*, 1(1):25–28, 2001.
- [103] Cioffi M., Formisano A. and Martone R. Analysis of Concurrent Multi-Frequency Eddy Current Testing Data. In *Proc. of ENDE 2002*, Saarbruchen, Germany, June 13-14 2002.
- [104] *Electromagnetic Nondestructive Evaluation (ENDE)*, volume VI of *Studies in Applied Electromagnetics and Mechanics*. Editor F. Kojima, IOS Press, 2000.
- [105] *Electromagnetic Nondestructive Evaluation (ENDE)*, volume III of *Studies in Applied Electromagnetics and Mechanics*. Eds: T. Takagi, J. Bowler, N. Nakagawa, J. Pavo, IOS Press, May 7 1997.

- [106] Albanese R. and Rubinacci G. *Finite Element Methods for the Solution of 3D Eddy Current Problems*, volume 102 of *Advances in Imaging and Electron Physics*. Academic Press, 1998.
- [107] Cioffi M., Rubinacci G., Tamburrino A. and Ventre S. A distributed object-oriented approach to electromagnetic nondestructive testing. <http://www.epcc.ed.ac.uk/tracs/Cioffitug99.html>, Sept. 22 1999.
- [108] Albanese R., Rubinacci G. and Villone F. An integral computational model for crack simulation and detection via eddy currents. *J. of Comp. Physics*, 152:736–755, 1999.
- [109] Albanese R., Rubinacci G., Tamburrino A. and Villone F. Phenomenological approaches based on an integral formulation for forward and inverse problems in eddy current testing. *Int. J. Applied Electromagnetics and Mechanics*, 12(3-4):115–137, 2000.
- [110] Yusa N., Uchimoto T., Chen Z. and Miya K. Application of genetic algorithm to ECT inversion problems. In *Proc. of the Fourth Japan-Central Europe Joint Workshop*, pages 114–117, 2001.
- [111] Berthiau G., de Barmon B., Benoist B. and Masia A. *Inversion Process Driven by Global Optimization Heuristics Coupled with MESSINE, a Fast-Running forward Model*, volume IV of *Electromagnetic Nondestructive Evaluation*, pages 175–180. S.S. Upda et al. (Eds.), IOS Press, Amsterdam, 2000.
- [112] Popper Karl R. *Meccanismi contro l'invenzione creativa: brevi considerazioni su un problema aperto*, pages 7–18. L'automa spirituale. Menti, cervelli e computer. Laterza, Roma, 1991.
- [113] Becker D.J., Sterling T., Savarese D., Dorband J.E., Ranawak U.A. and Packer C.V. Beowulf: a parallel workstation for scientific computation. In *Proc. of the International Conference on Parallel Processing*, 1995.
- [114] High Availability Linux project. <http://www.linux-ha.org/>.
- [115] Beowulf at NASA Goddard. <http://beowulf.gsfc.nasa.gov>.
- [116] *How to Build a Beowulf: A Guide to the Implementation and Application of PC Clusters*. Edited by T. Sterling, J. Salmon, D. J. Becker and D. F. Savarese, MIT Press, 1999.
- [117] Fernández J. Performance of message-passing MATLAB toolboxes. In *Proc. of VecPar'02*, Porto, Portugal, June 26-28 2002.

- [118] Cioffi M., Formisano A. and Martone R. Distributed niching concept for electromagnetic shape optimization by genetic algorithm. In *Proc. of PARELEC 2000*, Trois Riviere, Quebec, Canada, August 27-30 2000.
- [119] Sneary A.B., Friend C.M., Richens P. and Jones H. Development of High Temperature Superconducting Coils Using Bi-2223/Ag Tapes. *IEEE Trans. on Appl. Superconductivity*, 9(2):936–939, 1999.
- [120] Snitchler G., Kalsi s.s., Manlief M., Schwall R.E., Sidi-Yekhlef A., Ige S., Medeiros R., Francavilla T.L. and Gubser D.U. High field warm-bore HTS conduction cooled magnet. *IEEE Trans. on Appl. Superconductivity*, 9(2):553–558, 1991.
- [121] Cavaliere V., Cioffi M., Formisano A. and Martone R. Shape Optimisation of High  $T_c$  Superconducting Magnets. *IEEE Trans. on Magnetism*, 38(2, Part 1):1129–1132, March 2002.
- [122] Block A. *La Legge di Murphy, e altri motivi per cui le cose vanno a rovescio*. Longanesi, Milano, 1988.
- [123] Gao J., Chase K.W. and Magleby S.P. Comparison of Assembly Tolerance Analysis by the Direct Linearization and Modified Monte Carlo Simulation Methods. In ASME, editor, *Proc. of ASME Design Engineering Technical Conferences*, volume 1 of *DE-Vol. 82*, pages 353–360, Boston, MA, USA, Sept. 17-20 1995.

# List of Quotations

|                         | Bibliography | page |
|-------------------------|--------------|------|
| <i>John F. Nash Jr.</i> | [22]         | 26   |
| <i>Richard Dawkins</i>  |              | 55   |
|                         | [94]         | 70   |
| <i>Karl R. Popper</i>   | [112]        | 81   |
| <i>The Murphy's Law</i> | [122]        | 98   |

# Index

- Central Limit Theorem, 17
- Confidence interval, 17, 44
- Deterministic methods, 30
- Error function *erf*, 44
- Evolutionary Strategies, 34
- Generational finite increment, 42, 59
- GUI, 86
- ITER, 8
- Linearisation Methods, 101
- Migration policy, 60
- Minmax formulation, 28
- Monte Carlo methods, 32, 47, 49, 101, 116
- MPI, 62, 63, 85
- No Free Lunch Theorem, 41
- OF landscape, 26, 68, 78
- Parallel Matlab, 86
- Pareto Front, 15
- Pareto Set, 15
- PDF, 16
- Penalty functions, 19, 38
- PGAPack, 62, 85
- PMF, 16, 45
- Random number generator, 62
- Rastrigin function, 20, 49
- Scalar Objective Function, 18, 27
- Singular Value Decomposition (SVD), 49
- Standard normal PDF, 17
- Statistical Methods, 101
- This index, 141
- Tokamak, 8